

การพิสูจน์เอกลักษณ์ของหมึกปากกาลูกคลื่นด้วยเอทีอาร์เอฟทีไออาร์ไมโครสเปกโทรสโกปี

นางสาวปิยวรรณ แคนยุกต์

วิทยานิพนธ์นี้เป็นส่วนหนึ่งของการศึกษาตามหลักสูตรปริญญาวิทยาศาสตรมหาบัณฑิต

สาขาวิชาปิโตรเคมีและวิทยาศาสตร์พอลิเมอร์

คณะวิทยาศาสตร์ จุฬาลงกรณ์มหาวิทยาลัย

ปีการศึกษา 2551

ลิขสิทธิ์ของจุฬาลงกรณ์มหาวิทยาลัย

CHARACTERIZATION OF BALLPOINT PEN INKS BY ATR FT-IR  
MICROSPECTROSCOPY

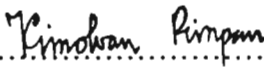
Miss Piyawan Canyouk

A Thesis Submitted in Partial Fulfillment of the Requirements  
for the Degree of Master of Science Program in Petrochemistry and Polymer Science  
Faculty of Science  
Chulalongkorn University  
Academic Year 2008  
Copyright of Chulalongkorn University

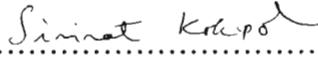
Thesis Title                      CHARACTERIZATION OF BALLPOINT PEN INKS BY  
ATR FT-IR MICROSPECTROSCOPY  
By                                      Miss Piyawan Canyouk  
Field of Study                      Petrochemistry and Polymer Science  
Thesis Principal Advisor      Associate Professor Sanong Ekgasit, Ph.D.


---


Accepted by the Faculty of Science, Chulalongkorn University in Partial  
Fulfillment of the Requirements for the Master's Degree


..........Deputy Dean for Administrative affairs,  
Acting dean, The faculty of Science  
(Associate Professor Vimolvann Pimpan, Ph.D.)

#### THESIS COMMITTEE

..........Chairman  
(Associate Professor Sirirat Kokpol, Ph.D.)


..........Thesis Principal Advisor  
(Associate Professor Sanong Ekgasit, Ph.D.)

..........Member  
(Assistant Professor Varawut Tangpasuthadol, Ph.D.)

..........External Member  
(Assistant Professor Toemsak Srihirin, Ph.D.)

ปิยวรรณ แคนยุกต์: การพิสูจน์เอกลักษณ์ของหมึกปากกาถูกสิ้นด้วยเอทีอาร์เอฟทีไออาร์ไมโครสเปกโทรสโกปี (CHARACTERIZATION OF BALLPOINT PEN INKS BY ATR FT-IR MICROSPECTROSCOPY) อ. ที่ปรึกษาวิทยานิพนธ์หลัก: รศ. ดร. สนอง เอกสิทธิ์, 89 หน้า.

อุปกรณ์ไมโครไออาร์อีชนิดใหม่แบบสไลด์ที่มีเจอร์มาเนียมเป็นหัวตรวจวัดถูกนำมาใช้ร่วมกับกล้องจุลทรรศน์อินฟราเรดเพื่อพิสูจน์การปลอมแปลงเอกสาร เนื่องจากไมโครไออาร์อีชนิดใหม่มีพื้นที่ในการตรวจวิเคราะห์ขนาดเล็กจึงสามารถใช้ในการศึกษาคราบหมึกที่ปรากฏบนกระดาษได้ แถบการดูดกลืนที่ได้จากเทคนิคนี้มีความสัมพันธ์โดยตรงกับองค์ประกอบเชิงเคมีของหมึก จึงสามารถใช้แถบการดูดกลืนที่ได้ไปใช้พิสูจน์แหล่งที่มาของหมึก เนื่องจากหมึกปากกามีองค์ประกอบเฉพาะตัวขึ้นกับการเลือกใช้วัตถุดิบของผู้ผลิต ทำให้แถบการดูดกลืนแสงของหมึกแสดงเอกลักษณ์เฉพาะด้วย แม้ว่าแถบการดูดกลืนแสงของหมึกที่ถูกเขียนบนกระดาษถูกรบกวนด้วยองค์ประกอบที่อยู่ในกระดาษก็สามารถใช้ช่วงการดูดกลืนแสงที่แสดงเฉพาะเอกลักษณ์ของหมึกในการจำแนกหมึกได้ สามารถติดตามการปลอมแปลงหมึกที่ถูกขีดทับด้วยหมึกจากปากกาด้ามอื่นได้ด้วยวิธีการวิเคราะห์แบบจุดต่อจุด เทคนิคนี้สามารถวิเคราะห์โดยไม่ทำลายและไม่ต้องเตรียมตัวอย่าง จึงสามารถนำไปใช้ในการหมึกบนเอกสารที่ถูกปลอมแปลงและหลักฐานทางนิติวิทยาศาสตร์อื่นๆ ได้

สาขาวิชา ..... ปิโตรเคมีและวิทยาศาสตร์พอลิเมอร์ .....ลายมือชื่อนิสิต.....ปิยวรรณ แคนยุกต์  
ปีการศึกษา.....2551.....ลายมือชื่ออาจารย์ที่ปรึกษาวิทยานิพนธ์หลัก.....

# # 4972383123: MAJOR PETROCHEMISTRY AND POLYMER SCIENCE

KEYWORD: FORENSIC ANALYSIS / INK CHARACTERIZATION / ATR FT-IR  
MICROSPECTROSCOPY

PIYAWAN CANYOUK: CHARACTERIZATION OF BALLPOINT PEN INK  
BY ATR FT-IR MICROSPECTROSCOPY. THESIS PRINCIPAL ADVISOR:  
ASSOC. PROF. SANONG EKGASIT, Ph.D, 89 pp.

A homemade slide-on Ge  $\mu$ IRE for ATR FT-IR spectral acquisition with an infrared microscope is employed for ballpoint pen inks characterization. Due to the small sampling area of the IRE, a trace of written ink on a paper can be analyzed. Direct correlation between the molecular information and their infrared absorption enable the identification of inks. Since inks have their own unique formula depending on manufacturer recipe, their spectra demonstrate their unique characteristic. Although the spectra of ink written on paper have interference from paper, the wavenumber region which display unique ink characteristic can be identified and employed for the ink identification. Moreover, a line-crossing of ink which is forged with other pen inks is investigated by linear point-by-point measurement. The operations are non-destructive and can be performed without an additional sample preparation. The technique suitable for document examination in as well as other forensic evidences based on unique chemical signature of ink.

Field of student ..... Petrochemistry and Polymer Science ..... Student's signature..... *Sanong Ekgasit*  
Academic year ..... 2008 ..... Principal advisor's signature..... *Sanong Ekgasit*

## ACKNOWLEDGEMENTS

I would like to express my sincere gratitude to Associate Professor Dr. Sirirat Kokpol, Assistant Professor Dr. Varawut Tangpasuthadol, and Assistant Professor Dr. Toemsak Srihirin for the insightful suggestions and contribution as thesis committee. Thanks to the National Center of Excellence for Petroleum, Petrochemicals, and Advance Materials, NCE-PPAM, for partial financial supports.

Gratefully thanks Associate Professor Dr. Sanong Ekgasit, my thesis advisor and Associate Professor Chuchaat Thammacharoen for the invaluable guidance, comments, and suggestions.

Finally, thanks my friends and colleagues at the Sensor Research Unit, Department of Chemistry, Faculty of Science, Chulalongkorn University for the everlasting friendship and spiritual supports throughout the time of study.

Above all, I am profoundly grateful to my parents and the endearing family for their patient love, perpetual encouragement, and overwhelming supports.

# CONTENTS

	Page
ABSTRACT (IN THAI).....	iv
ABSTRACT (IN ENGLISH).....	v
ACKNOWLEDGEMENTS.....	vi
CONTENTS.....	vii
LIST OF FIGURES.....	x
LIST OF TABLES.....	xvi
LIST OF ABBREVIATIONS.....	xvi
LIST OF SYMBOLES.....	xvii
CHAPTER I INTRODUCTION.....	1
1.1 Ink chemistry.....	1
1.2 Forensic document examination.....	3
1.3 Ink characterization.....	3
1.4 Fourier transform infrared (FT-IR) spectroscopy.....	5
1.4.1 Attenuated total reflection Fourier transform infrared (ATR FT-IR) spectroscopy.....	6
1.4.2 ATR FT-IR microspectroscopy.....	6
1.5 The objectives of this research.....	7
1.6 The scopes of this research.....	7
CHAPTER II THEORETICAL BACKGROUND.....	8
2.1 Fundamentals of light spectroscopy.....	9
2.1.1 Electromagnetic radiation.....	9
2.1.2 Interaction of light and matters.....	10
2.1.3 Infrared spectroscopy.....	11

2.2 Attenuated total reflection Fourier transform infrared (ATR FT-IR) spectroscopy.....	13
2.2.1 Principles of light reflection and refraction.....	13
2.2.2 Internal reflection element (IRE).....	15
2.2.3 ATR spectral intensity.....	17
2.2.4 Depth profiling using ATR FT-IR spectroscopy.....	20
2.2.5 Limitations of ATR FT-IR spectroscopy.....	21
2.3 ATR FT-IR microspectroscopy.....	22
2.3.1 Infrared microscope.....	22
2.3.2 Principle of light entering the Ge $\mu$ IRE.....	24
 CHAPTER III EXPERIMENTAL SECTION.....	 26
3.1 Materials and equipments.....	26
3.1.1 Ballpoint pen ink samples.....	26
3.1.2 White smooth A4 paper samples.....	27
3.1.3 Instruments.....	28
3.2 Default spectral acquisition.....	28
3.3 Homemade slide-on Ge $\mu$ ATR accessory.....	29
3.4 Experimental procedure for dried ink characterization.....	34
3.5 Experimental procedure for paper characterization .....	34
3.5.1 Experimental procedure for depth dependent of paper characterization .....	34
3.5.2 Experimental procedure for characterization of paper.....	35
3.6 Characterization of ink written on paper .....	35
3.6.1 Sample preparation.....	36
3.6.2 Experimental procedure for depth dependence of ink on paper characterization.....	36
3.6.3 Experimental procedure for ink on paper characterization... ..	36
3.6.4 Experimental procedure for time dependence of ink on paper characterization.....	36



	Page
CHAPTER IV RESULTS AND DISCUSSION.....	37
4.1 Characterization of inks.....	37
4.1.1 Spectral assignments of ballpoint pen ink.....	37
4.1.2 Spectral comparison of the same model ballpoint pen ink.....	44
4.1.3 Spectral comparison of various brands of ballpoint pen inks.....	46
4.1.4 Spectral comparison of various models of the same brand ballpoint pen inks.....	48
4.2 Characterization of paper.....	51
4.2.1 Spectral assignment of paper.....	53
4.2.2 Spectral comparison of various paper brands and gsms.....	56
4.3 Characterization of ink on paper.....	58
4.3.1 Depth dependent of ink written on paper.....	58
4.3.2 Spectral assignment of ink written on paper.....	60
4.3.3 Spectral comparison of various brands ballpoint pen inks written on paper.....	67
4.3.4 Spectral comparison of various models of the same brand ballpoint pen ink written on paper.....	69
4.3.5 Spectral comparison of ageing of ink written on paper.....	72
4.4 Characterization of line-crossing ink on paper.....	75
CHAPTER V CONCLUSIONS.....	84
REFERENCES.....	85
CURRICULUM VITAE.....	89

## LIST OF FIGURES

Figure	Page
2.1 Propagation of a linearly polarized electromagnetic wave in the direction of propagation. Electric (E) and magnetic (H) vector are always perpendicular to each other and to the direction of propagation.	8
2.2 The electromagnetic spectrum.....	9
2.3 Interactions of light with matter.....	10
2.4 Illustration of various $-CH_2-$ vibrational modes.....	12
2.5 Reflection and refraction of a plane wave at a dielectric based on Snell's Law.....	14
2.6 Condition under which total internal reflection occurs. Light travels from an optically denser medium and impinges at the surface of the optically rarer medium ( $n_1 > n_2$ ) with angle of incidence equal the critical angle.....	15
2.7 IRE configurations: (a) Single reflection hemispherical crystal, and (b) Multiple reflections.....	16
2.8 The MSEF at various experimental condition (A, A') and its decay characteristic (B, B'). The simulation parameters are $n_0 = 4.00$ for Ge, $n_0 = 2.40$ for ZnSe, $\nu = 1000 \text{ cm}^{-1}$ , $n_1(\nu) = 1.50$ , $k_1(\nu) = 0.0, 0.1, 0.2, 0.3, 0.4$ and $0.5$ , respectively.....	19
2.9 The evanescent field at the boundary between the IRE and the sample..	21
2.10 Optical diagram of an infrared microscope.....	23
2.11 The infrared radiation tracing with in the objective of infrared microscope.....	24
2.12 Schematic illustration of ray tracing within the infrared objective focused radiation traveling within the Ge $\mu$ IRE.....	25
3.1 The slide-on housing and compositions of the homemade Germanium $\mu$ ATR accessory.....	30
3.2 Detailed drawing of the homemade miniature ATR accessory with Germanium $\mu$ IRE. (A) the housing attached to the objective, (B) the slide-on set with the Ge $\mu$ IRE, and (C) the complete accessory.....	31

Figure	Page
3.3 Example of procedures for spectral acquisition (A) Continuum infrared microscope attached to the Nicolet 6700 FT-IR spectrometer, (B) slide-on Ge $\mu$ IRE is fixed on the position of slide-on housing on the 15X Schwarzschild-Cassegrain infrared objective, and (C) the complete homemade $\mu$ ATR accessory ready for a spectral acquisition..	32
3.4 Schematic illustration of ray tracing within the 15X Schwarzschild-Cassegrain infrared objective (A), focused radiation traveling within the Ge $\mu$ IRE (B), and image of the tip of Ge $\mu$ IRE under the visible light illumination (C).....	33
4.1 ATR FT-IR spectra of 20 commercial dried black ballpoint pen inks acquired by the “contact and collect” operation: (a) Faber-Castel <sup>®</sup> (Grip Ball 1424), (b) Faber-Castel <sup>®</sup> (Click Ball 1422), (c) Faber-Castel <sup>®</sup> (Super Tech Point 1420), (d) Faber-Castel <sup>®</sup> (Ball Pen 1423), (e) Lancer <sup>®</sup> (Spiral 825), (f) Lancer <sup>®</sup> (Click 878), (g) Lancer <sup>®</sup> (Pro-Riter), (h) Lancer <sup>®</sup> (Cadet), (i) Horse <sup>®</sup> (Ball Pen H-402), (j) Reynolds <sup>®</sup> (Fine Carbure), (k) Reynolds <sup>®</sup> (800), (l) Standard <sup>®</sup> (g’Soft), (m) Standard <sup>®</sup> (Fizz Hi Grip), (n) Stabilo <sup>®</sup> (Marathon 318), (o) Stabilo <sup>®</sup> (F), (p) Quantum <sup>®</sup> (GeloBal 007), (q) Quantum <sup>®</sup> (GeloBal QCGB 1230), (r) Pilot <sup>®</sup> (Super Grip), (s) Pentel <sup>®</sup> (Star V), and (t) Staedler <sup>®</sup> (Noris Stick 434 F).....	39
4.2 ATR FT-IR spectra of 20 commercial dried blue ballpoint pen inks acquired by the “contact and collect” operation: (a) Faber-Castel <sup>®</sup> (Grip Ball 1424), (b) Faber-Castel <sup>®</sup> (Click Ball 1422), (c) Faber-Castel <sup>®</sup> (Super Tech Point 1420), (d) Faber-Castel <sup>®</sup> (Ball Pen 1423), (e) Lancer <sup>®</sup> (Spiral 825), (f) Lancer <sup>®</sup> (Click 878), (g) Lancer <sup>®</sup> (Pro-Riter), (h) Lancer <sup>®</sup> (Cadet), (i) Horse <sup>®</sup> (Ball Pen H-402), (j) Reynolds <sup>®</sup> (Fine Carbure), (k) Reynolds <sup>®</sup> (800), (l) Standard <sup>®</sup> (g’Soft), (m) Standard <sup>®</sup> (Fizz Hi Grip), (n) Stabilo <sup>®</sup> (Marathon 318), (o) Stabilo <sup>®</sup> (F), (p) Quantum <sup>®</sup> (GeloBal 007), (q) Quantum <sup>®</sup> (GeloBal QCGB 1230), (r) Pilot <sup>®</sup> (Super Grip), (s) Pentel <sup>®</sup> (Star V), and (t) Staedler <sup>®</sup> (Noris Stick 434 F).....	40

Figure	Page
4.3 ATR FT-IR spectra of (A) wet ink, (B) dry ink obtained from holding the sample for an hour, (C) wet ink spectrum subtracted by dry ink one, (D) 2-phenoxyethanol from library, (D) dry ink spectrum subtracted by wet ink one, and (E) crystal violet from library.....	42
4.4 Chemical structures of some triarymethane dyes: (A) crystal violet, (B) methyl violet, (C) tetramethyl para-rosaniline, and (D) victoria blue.....	43
4.5 ATR FT-IR spectra of FABER-CASTEL (Grip Ball 1424) blue ink at various manufactured date: (A) 31/ 05/ 2007, (B) 11/ 08/ 2007, and (C) 08/ 09/ 2007.....	44
4.6 ATR FT-IR spectra of FABER-CASTEL (Grip Ball) blue ink at various manufactured date: (a) 08/ 09/ 2007 and (b) 31/ 05/ 2007.....	46
4.7 ATR FT-IR spectra of (A) black and (B) blue ballpoint pen inks: (a) Faber-Castel <sup>®</sup> (Grip Ball 1424), (b) Quantum <sup>®</sup> (GeloBal 007), (c) Lancer <sup>®</sup> (Spiral 0.5 825), (d) Standard <sup>®</sup> (g' soft), (e) Staedrler <sup>®</sup> (Noris stick 434 F), (f) Horse <sup>®</sup> (Ball Pen H-402), (g) Reynolds <sup>®</sup> (Fine Carbure), (h) Pilot <sup>®</sup> (Super Grip), (i) Pentel <sup>®</sup> (Star V), and (j) The One <sup>®</sup> (GPB-3001).....	47
4.8 ATR FT-IR spectra of (A) black and (B) blue Faber-Castel <sup>®</sup> brand ballpoint pens ink.....	48
4.9 ATR FT-IR spectra of (A) black and (B) blue Lancer <sup>®</sup> brand ballpoint pens ink.....	49
4.10 ATR FT-IR spectra of different points of the same paper sheet.....	52
4.11 SEM image of the paper surface.....	54
4.12 ATR FT-IR spectra of paper at the same point with different degree of contact with the slide-on homemade Germanium $\mu$ IRE.....	55
4.13 ATR FT-IR spectra of different paper brands and gsms: (A) Double A <sup>®</sup> (80 gsm), (B) Shih-Szu <sup>®</sup> (80 gsm), (C) Quality (80 gsm), (D) Eagle <sup>®</sup> (80 gsm), (E) Valuesave <sup>®</sup> (80 gsm), and (F) Quality <sup>®</sup> (70 gsm).....	57

Figure	Page
4.14 ATR FT-IR spectra of black Lancer <sup>®</sup> (Click 878) ink written on paper at the same point with various extent of contact with the homemade slide-on Ge $\mu$ IRE.....	59
4.15 ATR FT-IR spectra of different points of Faber-Castel <sup>®</sup> (Grip Ball 1424) black ink of the same continuous line on paper.....	62
4.16 The ATR FT-IR spectra taken from Figure 4.16 classified by the highest peak intensity of calcium carbonate character (at 1498 $\text{cm}^{-1}$ ) can be divided into 4 groups (A, B, C, and D in order of increasing peak intensity).....	64
4.17 ATR FT-IR spectra of 20 commercial black ballpoint pen inks written on paper: (a) Faber-Castel <sup>®</sup> (Grip Ball 1424), (b) Faber-Castel <sup>®</sup> (Click Ball 1422), (c) Faber-Castel <sup>®</sup> (Super Tech Point 1420), (d) Faber-Castel <sup>®</sup> (Ball Pen 1423), (e) Lancer <sup>®</sup> (Spiral 825), (f) Lancer <sup>®</sup> (Click 878), (g) Lancer <sup>®</sup> (Pro-Riter), (h) Lancer <sup>®</sup> (Cadet), (i) Horse <sup>®</sup> (Ball Pen H-402), (j) Reynolds <sup>®</sup> (Fine Carbure), (k) Reynolds <sup>®</sup> (800), (l) Standard <sup>®</sup> (g'Soft), (m) Standard <sup>®</sup> (Fizz Hi Grip), (n) Stabilo <sup>®</sup> (Marathon 318), (o) Stabilo <sup>®</sup> (F), (p) Quantum <sup>®</sup> (GeloBal 007), (q) Quantum <sup>®</sup> (GeloBal QCGB 1230), (r) Pilot <sup>®</sup> (Super Grip), (s) Pentel <sup>®</sup> (Star V), and (t) Staedler <sup>®</sup> (Noris Stick 434 F).....	65
4.18 ATR FT-IR spectra of 20 commercial blue ballpoint pen inks written on paper: (a) Faber-Castel <sup>®</sup> (Grip Ball 1424), (b) Faber-Castel <sup>®</sup> (Click Ball 1422), (c) Faber-Castel <sup>®</sup> (Super Tech Point 1420), (d) Faber-Castel <sup>®</sup> (Ball Pen 1423), (e) Lancer <sup>®</sup> (Spiral 825), (f) Lancer <sup>®</sup> (Click 878), (g) Lancer <sup>®</sup> (Pro-Riter), (h) Lancer <sup>®</sup> (Cadet), (i) Horse <sup>®</sup> (Ball Pen H-402), (j) Reynolds <sup>®</sup> (Fine Carbure), (k) Reynolds <sup>®</sup> (800), (l) Standard <sup>®</sup> (g'Soft), (m) Standard <sup>®</sup> (Fizz Hi Grip), (n) Stabilo <sup>®</sup> (Marathon 318), (o) Stabilo <sup>®</sup> (F), (p) Quantum <sup>®</sup> (GeloBal 007), (q) Quantum <sup>®</sup> (GeloBal QCGB 1230), (r) Pilot <sup>®</sup> (Super Grip), (s) Pentel <sup>®</sup> (Star V), and (t) Staedler <sup>®</sup> (Noris Stick 434 F).....	66
4.19 ATR FT-IR spectra of (A) black and (B) blue ballpoint pen inks: (a) Faber-Castel <sup>®</sup> (Grip Ball 1424), (b) Quantum <sup>®</sup> (GeloBal 007), (c)	

Figure	Page
Lancer <sup>®</sup> (Spiral 0.5 825), (d) Standard <sup>®</sup> (g' soft), (e) Staedrler <sup>®</sup> (Noris stick 434 F), (f) Horse <sup>®</sup> (Ball Pen H-402), (g) Reynolds <sup>®</sup> (Fine Carbure), (h) Pilot <sup>®</sup> (Super Grip), (i) Pentel <sup>®</sup> (Star V), and (j) The One <sup>®</sup> (GPB-3001).....	68
4.20 ATR FT-IR spectra of Faber-Castel <sup>®</sup> ballpoint pen inks: (A) black, (B) blue ballpoint pen ink on paper: (a) Faber-Castel <sup>®</sup> (Grip Ball 1424), (b) Faber-Castel <sup>®</sup> (Click Ball 1422), (c) Faber-Castel <sup>®</sup> (Super Tech Point 1420), and (d) Faber-Castel <sup>®</sup> (Ball Pen 1423).....	69
4.21 ATR FT-IR spectra of Lancer <sup>®</sup> ballpoint pen inks: (A) black, (B) blue ballpoint pen ink on paper: (a) Lancer <sup>®</sup> (Spiral 825), (b) Lancer <sup>®</sup> (Click 878), (c) Lancer <sup>®</sup> (Pro-Riter), and (d) Lancer <sup>®</sup> (Cadet).....	70
4.22 ATR FT-IR spectra of ink on paper: (A) Lancer <sup>®</sup> (Spiral 825), (B) Quantum <sup>®</sup> (GeloBal 007), (C) Pentel <sup>®</sup> (Star V), and (D) The One <sup>®</sup> (GPB-3001) detected every 3 days.....	73
4.23 ATR FT-IR spectra of ink on paper: (a) Lancer <sup>®</sup> (Spiral 825), (B) Quantum <sup>®</sup> (GeloBal 007), (C) Pentel <sup>®</sup> (Star V), and (D) The One <sup>®</sup> (GPB-3001) after kept 21 days.....	74
4.24 ATR FT-IR spectra of crossing ink between Faber-Castel <sup>®</sup> (Ball pen) ink top with Pentel <sup>®</sup> (Star V) on paper at the same point with various extent of contact with the homemade $\mu$ IRE: (A) Pentel <sup>®</sup> ink added immediately and (B) added after 7 days.....	76
4.25 ATR spectra of (A) blue Faber-Castel <sup>®</sup> (Ball pen) and (B) blue Horse <sup>®</sup> (H 042) ink top on Reynolds <sup>®</sup> (Fine carbure).....	78
4.26 ATR spectra of blue Faber-Castel <sup>®</sup> (Ball pen) ink top with Standard <sup>®</sup> (Hi soft) ink: (A) horizontal and (B) vertical analysis.....	80
4.27 ATR spectra of crossing ink of blue Faber-Castel <sup>®</sup> (Ball pen) ink.....	81
4.28 ATR spectra of blue Reynolds <sup>®</sup> (Fine carbure) ink top with Faber-Castel <sup>®</sup> (Ball pen) ink: (A) stored for 1 hour and (B) stored for 45 days.....	82

## LIST OF TABLES

Table	Page
1.1 Composition of ink.....	2
2.1 Properties of material used for internal reflection elements.....	16
3.1 Ballpoint pen ink samples.....	26
3.2 A4 paper samples.....	27
4.1 Peak assignments of functional groups in ballpoint pen ink.....	38
4.2 Peak assignments of cellulose fiber.....	53
4.3 Peak assignments of calcium carbonate.....	53
4.4 Peak assignments of ink written on paper.....	61

## LIST OF ABBREVIATIONS

ATR	: Attenuated total internal reflection
FT-IR	: Fourier transform infrared
Ge	: Germanium
IR	: Infrared
IRE	: internal reflection element
KBr	: Potassium bromide
MCT	: mercury-cadmium-telluride
MSEF	: mean square electric field
MSEvF	: mean square evanescent field
$\mu\text{m}$	: micron
S/N	: signal-to -noise ratio
TIR	: Total internal relection



## LIST OF SYMBOLS

$n_1$	: Refractive index of the dense medium (IRE)
$n_2$	: Refractive index of the sample
$I$	: Light intensity
$I_0$	: Intensity of incident beam
$I_R$	: Intensity of reflected beam
$I_S$	: Intensity of scattered beam
$I_T$	: Intensity of transmitted beam
$I_A$	: Intensity of absorbed beam
$\alpha_1$	: Angle of incidence
$\alpha_2$	: Angle of reflection
$\theta$	: Angle of incidence
$\theta_c$	: Critical angle
$A$	: Absorbance
$R$	: Reflectance
$\varepsilon$	: Absorption coefficient
$\nu$	: Wavenumber
$R$	: Reflectance
$d_p$	: Penetration depth
$\lambda$	: Wavelength

# CHAPTER I

## INTRODUCTION

### 1.1 Ink chemistry

Ink is complex mixture of colorants, vehicles, and additives which are adjusted in composition to produce the writing characteristic. Some general categories and examples of material used in inks are showed in Table 1.1. The colorant is the most important part of the ink because it is only part that observable. There are two types of colorant, pigments and dyes. Pigments are insoluble in water whereas dyes are soluble in water or other solvents. Ballpoint pen ink contains 40-50 percent dye [1]. Most of analytical methods focus on colorant determination because ink formations tend to have unique organic dyes or pigments [2].

Vehicles or carrier are solvents that make the ink flow and carry the colorants to material surface. Hydrocarbon resins have become an important ingredient in ink due to low molecular weight polymer [3]. Molecular weigh affect to ink viscosity. Normally, pigments are only soluble in hydrocarbon solvents but some types can be modified to make them water soluble or dispersible [4].

Additives can be added for ink properties improvement, such as flow modifiers, surface activator, solubility enhancers, and preservatives. One of the main functions of polymer in ink is dispersants. Other functions are aiding film formation and improving the mechanical and specific properties of ink, such as abrasion resistance [5]. Detection of those additive compounds can be beneficial to forensic examiner because the compounds can be manufacturer-specific.

Table 1.1 Components of ink [6].

Ink compositions		Characteristics	Properties affected
Coloring material	Dyes	Classified as acidic, basic, solvent, etc., depending on characteristic and soluble in vehicle.	Appearance
	Pigment	Consist of finely ground multimolecular granules and insoluble in vehicle.	
Vehicle	Oils	Linseed, soy, mineral or other type of oil. Classified as drying, non-drying, or combination, depending on degree of unsaturation of oil.	Flow and drying characteristics
	Solvents	Any of several organic solvents or water.	
	Resins	Non-crystalline material of high molecular weight.	
Other additives	Driers	Catalyzed oxidation of drying oils. Many are inorganic salts.	Drying characteristic
	Plasticizers	Reduces brittles of ink. Consist of solvents with low volatility.	Stability of ink film
	Surfactants	Changes surface tension of ink. Typically consist of soaps or detergents.	Wetting ability
	Waxes	Increase flexibility and reduce brittleness. May be hydrocarbon waxes, greases such as petroleum jelly.	Hardness/ flexibility

## 1.2 Forensic document examination

The work of forensic document examination is answer questions about a disputed document with a variety of scientific processes and methods. There are occasions when documents are either altered or created for specifically purpose. Almost all of the questioned documents have financial signification such as tax return, wills, and insurance claims [7].

## 1.3 Ink characterization

Forensic document examiners are mainly interested in the identification of signatures and handwriting, but they are also interested in writing materials and printing equipment [8]. To identification and interpretation of alteration, a study of the chemical composition of ink used on documents may confirm two documents are written using the same pen that believed to have the same author or not.

One way of comparing inks by microspectrophotometry (MSP) in reflection mode and filtered light examination (FLE) using the image capture to following the optical properties of ink [9]. Viewing the ink writing under infrared luminescence also show difference in the inks [10]. Chemical imaging has been used for comparison of ink samples [11]. The digital processing methods such as *lab color mode* (available in Adobe® Photoshop®) are used to differentiate writing instrument inks by separate the brightness information from the color within an image [12]. The flaw of optical techniques is its limited ability to differentiate the visually similar ballpoint pen ink.

Thin-layer chromatography (TLC) analysis with various solvent systems is used for ink discrimination [6, 13]. TLC can be used to give high discriminating power and blend with other technique for additional information, for example FT-IR [14]. High performance thin-layer chromatography (HPTLC) has replaced the older technique of ink analysis due to the better quality of separation [15]. High performance liquid chromatography (HPLC) offers the detailed information regarding the concentration of different components of inks [16-18]. Solid-phase microextraction is an adsorption/desorption technique to identification the evaporation

of ink volatilization components [19-20]. Limited of sample destruction and carefully sample preparation are foibles of this technique.

Mass spectrometry has been used in the analysis of ink. The methods involve gas chromatograph coupled with a mass spectrometer (GC-MS) for study of drying ink [21]. Laser desorption mass spectrometry (LDMS) has been used for the analysis of dye molecule on paper [22]. Laser desorption/ionization mass spectrometry (LDI-MS) is non-destructive and rapid technique for analysis of dye [15, 23]. Matrix assisted laser desorption/ionization mass spectrometry (MALDI-MS) improves the sensitivity of LDI-MS used for dyes on paper study [24]. Direct analysis in real time (DART) which is sampling at interface has been reported for differentiating writing ink [25]. Although, several methods of mass spectrometry have been used in the ink analysis, these methods require cutting sample material from a questioned document.

The determination of the order of crossing lines occurred in case of questioned document has been altered at later dated by adding a part of it. The most widely used technique in the analysis of line crossing is microscope. The optical microscope (OM) is primary tool used but they have problem in case of two inks are similar in color. Because of its destructive nature (conductive coating), scanning electron microscope (SEM) method are used after the optical observations [26]. With the problem of determination of sequence of crossing line made by the same type of ink, scanning probe microscopy (SPM) has been used to line crossing study by incorporating height analysis [27]. Atomic force microscopy (AFM) can characterize the surface of line crossing base on topographical feature without sample modification [28]. However, these techniques have the disadvantage of destruction by cutting off the sample for characterization. In case of forensic analysis, it is the essences to preserve the original sample.

Although various techniques are employed for forensic examination of inks, most methods used large sample and are destructive. These methods are not suitable for routine analysis of forensic investigation and comparison the trace of ink written on paper. The destructive technique such as solvent extraction or cutting a part of document for hold the sample in the analysis instruments must be lastly used in order to keep their original sample for further analysis. Fourier Transform Infrared (FT-IR)

spectroscopy is one of techniques providing the chemical information with unique characteristic depending on their components. This technique can be applied for forensic analysis of inks and inks written on substrate.

#### **1.4 Fourier transform infrared (FT-IR) spectroscopy**

Fourier transform infrared (FT-IR) spectroscopy is the well-known molecular spectroscopic technique. It is performed by irradiating a sample with an infrared beam. Some of the radiation is absorbed by the functional groups present in matter so that the identification of compounds is often possible from the functional group. This technique has been applied as an analytical technique in various fields such as, food industry, material science, and many others.

Traditionally, FT-IR spectroscopy is one of the techniques for ink analysis with various modes, i.e., transmission with KBr plates [14, 29-30]. It has been suggested that infrared spectroscopy can determine the main dye components in ink and compare of with others inks for ink classification. In transmission mode leads to the destruction of the document because the ink must be extracted from the paper.

Synchrotron radiation Fourier transform infrared (SR-FT-IR) spectroscopy has been used for directly ink on paper characterization [31-32]. The technique can be used for the direct analyses of ink on paper without mechanically damaging the ink and paper or having to chemically extract or separate the ink. However, this method does not widespread due to the limitation of using synchrotron radiation as light source.

Limitations of the analysis by conventional FT-IR spectroscopy include the destructives sample, complicated sample preparation, and large amounts of sampling area for analysis for obtain good spectra. These problems can be overcome by the use of an attenuated total reflection (ATR) spectroscopy.

#### **1.4.1 Attenuated Total Reflection Fourier transform infrared (ATR FT-IR) spectroscopy**

Attenuated total reflection Fourier transform infrared (ATR FT-IR) spectroscopy is a spectroscopic technique utilizing a uniquely internal reflection phenomenon. That occurs when light traveling in an internal reflection element (IRE) impinges on surface of a rarer medium with an incident angle greater than the critical angle. Therefore, ATR spectroscopy is a surface-sensitive characterization of materials that contact with an IRE. This technique has been used in the application including qualitative, quantitative analysis, surface analysis and depth profiling.

The technique possesses several advantages of being non-destructive sample, fast operation, and having little or no sample preparation. Due to non-destructive nature, this technique is suitable for analysis of ink written on paper and other forensic evidences.

Conventional ATR spectroscopy is desirable to achieve contact over the entire IRE surface. This requirement is easily achieved a good contact with liquid samples but obtaining good contact with solid samples is difficult. It should be preventing a damage of the brittle surface of the IRE due to an excessive force as solid sample is pressed against the IRE.

A conventional ATR accessory (Seagull<sup>TM</sup>, Harrick Scientific, USA) with a hemispherical Ge IRE (diameter of 25 mm) has been employed for ATR FT-IR spectral acquisitions of ink [33]. It should be noted that in the sample preparation, the small squares piece of paper with completely coverage of paper by the ink. Due to the large sampling area, the line of ink written on paper with single stroke cannot be analyzed.

#### **1.4.2 ATR FT-IR Microspectroscopy**

Infrared microspectroscopy is the union of microscopy and spectroscopy for microanalysis. That has been developed in order to reveal the sample in both transmission and reflection modes. By coupling the focused radiation into the

designed IRE made of high reflective index materials. Microscopy reveals a pivotal role in selecting samples for analysis, observing the microstructure of sample and defining the microscope area for analysis.

Due the conventional IRE has limitations, the homemade  $\mu$ IRE accessory (slide-on Ge  $\mu$ IRE) is developed. The advantage of the accessory is small contact area of cone-shape  $\mu$ IRE and small inks trace on paper can be analyzed. Additionally, ATR FT-IR spectroscopy with the  $\mu$ IRE accessory requires short time for spectral acquisition due to no sample preparation of ink from the paper substrate. The operation is non-destructive and can be preformed without an additional sample preparation.

In this research, commercial ballpoint pen inks from various manufacturers are characterized. The nature of ATR FT-IR technique is the non-destructive tool for identifying ink trace. These potential application has significant impact on forensic science.

### **1.5 The objectives of this research**

The objectives of this research are to develop ATR FT-IR microspectroscopic technique for characterization of ballpoint pen inks and ink written on paper and apply for forensic analysis.

### **1.6 Scopes of the research**

1. To characterize dried ballpoint pen inks with different brands and model using ATR FT-IR microspectroscopy with the homemade  $\mu$ IRE accessory.
2. To characterize white photocopy paper with ATR FT-IR microspectroscopy with the homemade  $\mu$ IRE accessory.
3. To characterize the ink and line-crossing ink written on paper by ATR FT-IR microspectroscopy with the homemade  $\mu$ IRE accessory.



## CHAPTER II

### THEORETICAL BACKGROUND

#### 2.1 Fundamental of Infrared Spectroscopy

Infrared spectroscopy is particularly spectroscopic technique used to study the interaction of infrared radiation with the sample. Because of the high information content of the spectrum, such technique has become most of analytical methods.

##### 2.1.1 Electromagnetic Radiation

Electromagnetic radiation is an energy wave composed of an electric and magnetic field component. These are perpendicular to each other and the direction of propagation of the wave as shown in Figure 2.1. For producing electromagnetic radiation, some type of energy has to be various type of radiation (e.g. light, heat) which regarding to wavelength or frequency. The wavelength range of the electromagnetic spectrum consists of wide scale ranging from radio-waves to gamma-rays as shown in Figure 2.2.

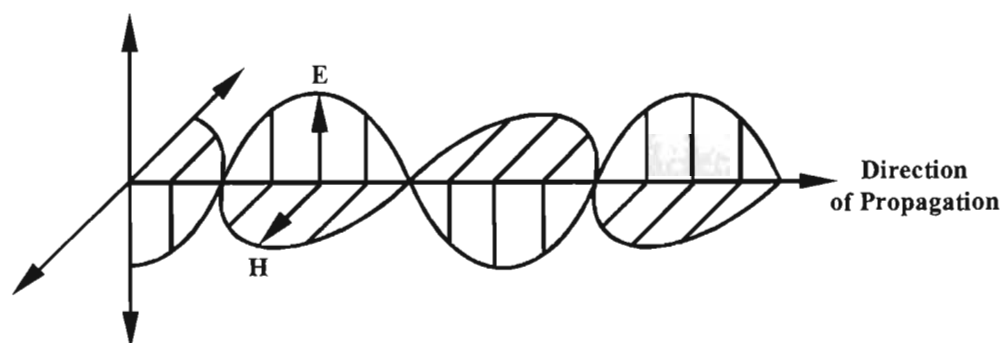


Figure 2.1 Propagation of a linearly polarized electromagnetic wave in the direction of propagation. Electric (E) and magnetic (H) vector are always perpendicular to each other and to the direction of propagation.

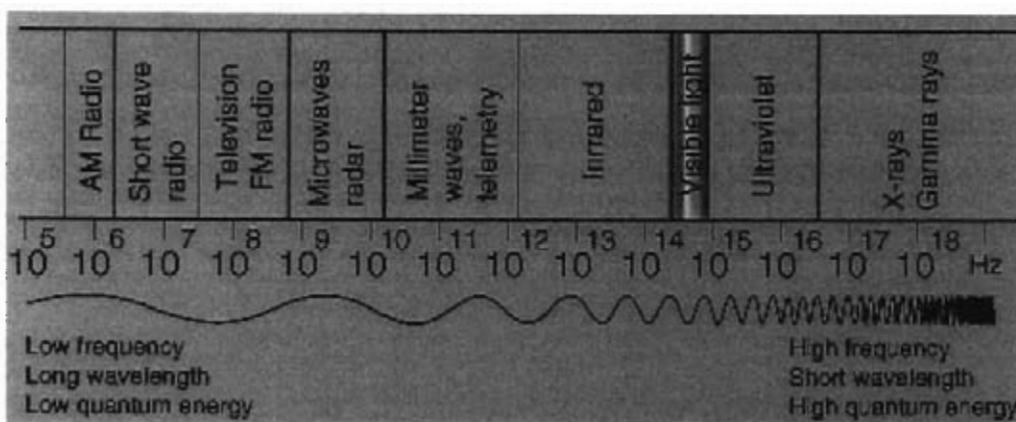


Figure 2.2 The electromagnetic spectrum.

Generally, electromagnetic radiation can be classified by wavelength into radio waves, microwave, terahertz radiation, infrared radiation, visible light, ultraviolet radiation, X-rays, and gamma rays frequency, respectively.

### 2.1.2 Interaction of light and matters

Spectroscopy is the science that associates with the interaction of electromagnetic radiation with matter. Many of those implicate transitions between specific energy states of chemical species and observed by following the absorption or emission of electromagnetic radiation. There are several types of interaction of electromagnetic radiation and matters, such as reflection, refraction, diffraction, and scattering that do not involve transitions between energy stages but rather cause the change of the optical properties of radiation (e.g. direction and polarization). Those interactions are often related to bulk properties of sample rather than to specific chemical species [34].

When an electromagnetic radiation impinges on a material, infrared rays of the incident radiation may be reflected, scattered, transmitted, or absorbed which depend on the experimental design. The total number of incident energy is the sum of reflected, scattered, transmitted, and absorbed light. A schematic illustration for an interaction between light and matter is shown in Figure 2.2. This process can be expressed by the following relationship [35]:

$$I_0 = I_R + I_S + I_T + I_A \quad (2.1)$$

where  $I_0$  is the intensity of the incident radiation and  $I_R$ ,  $I_S$ , and  $I_T$  are the reflected, scattered, and transmitted radiations, respectively.  $I_A$  is the radiation absorbed by matter. The intensity of each radiation depends on the intensity and wavelength of the incident radiation. Moreover, the optical properties of the matter, the concentrations of species, and the geometry of the experimental setup are considered.

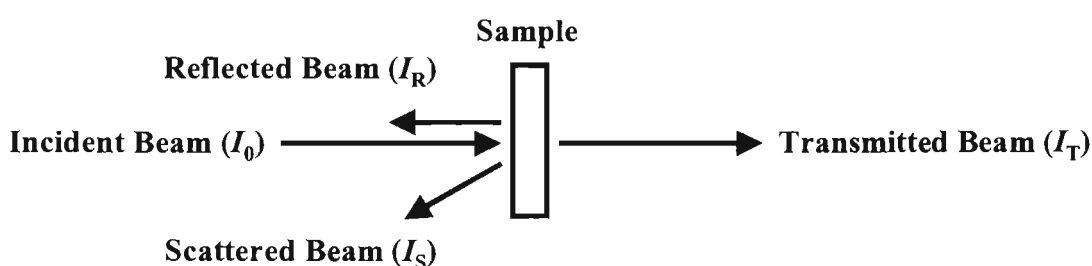


Figure 2.3 Interactions of light with matter.

Considering the electromagnetic radiation when the sample is inserted between a light source and a detector as shown in Figure 2.3, the sample absorbs a fraction of the incident radiation. For measurement the amount of light being absorbed by the sample, the ratio of the simple attenuated ( $I$ ) and nonattenuated ( $I_0$ ) intensities of the radiation are measured. The ratio is proportional to the transmittance of the sample. This relationship of proportional light can be quantitatively related to the chemical composition of the sample by the *Beer-Lambert law* as [35]:

:

$$\frac{I}{I_0} = e^{-A(\bar{\nu})} = e^{-c_2 \varepsilon(\bar{\nu}) l} \quad (2.2)$$

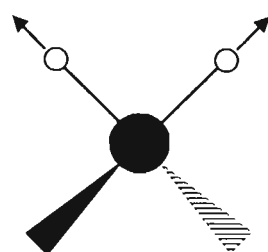
where  $A(\bar{\nu})$  is the absorbance of the sample at a given wavenumber  $\bar{\nu}$ ,  $c_2$  is the concentration of the absorbing functional group,  $\varepsilon(\bar{\nu})$  is the wavenumber-dependent absorption coefficient, and  $l$  is the film thickness for the infrared beam at a normal incidence to the sample surface.

### 2.1.3 Infrared spectroscopy

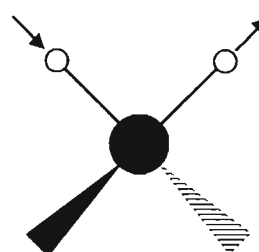
Infrared spectroscopy is one of the most common spectroscopic techniques. The infrared spectroscopic analysis is the method to determine the chemical functional groups in the sample. Owing to various sampling accessories, this technique can analyze wide range of sample types such as gases, liquids and solids. Therefore, infrared spectroscopy is an important and popular technique for structural elucidation and compound identification.

The infrared region of the electromagnetic spectrum is presented from 14,000-10  $\text{cm}^{-1}$  that can be divided into three regions (near, mid, and far infrared). The region of most interest for chemical analysis is the mid-infrared region (4,000-400  $\text{cm}^{-1}$ ). The physical properties measured in this technique are the ability of molecules absorbs infrared radiation. Since the atoms in molecules are not static, they vibrate with specific frequency which depends on the mass of the atom and the length and the strength of the bond [36]. Molecular vibrations are activated by bonds absorbing radiation of the same frequency as their nature vibrational frequency, usually in the infrared region.

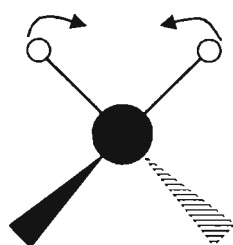
The major types of molecular vibrations are stretching and bending. The various types of vibrations are illustrated in Figure 2.4. All vibrations within a molecule have not result in an absorption band in the infrared region. Those vibrations have to result in the change of dipole moment during the vibration called infrared active. This means that for homonuclear diatomic molecule such as hydrogen ( $\text{H}_2$ ), nitrogen ( $\text{N}_2$ ), and oxygen ( $\text{O}_2$ ) is not observed the infrared absorption and these molecules have zero dipole moment as well as bond stretching. For heteronuclear diatomic molecules such carbon monoxide ( $\text{CO}$ ) and hydrogen chloride ( $\text{HCl}$ ) which have a permanent dipole moment, infrared activity occurs because stretching of this bond leads to the change in dipole moment.



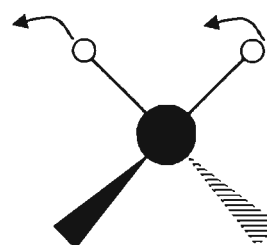
Symmetrical stretching



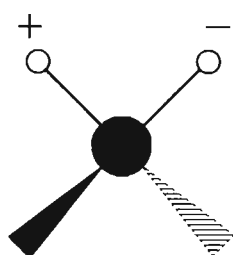
Asymmetrical stretching



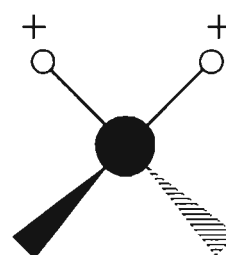
Bending, or scissoring



Rocking, or in plane bending



Twisting, or out-of-plane bending



Wagging, or out-of-plane bending

Figure 2.4 Illustration of various  $-\text{CH}_2-$  vibrational modes.

## 2.2 Attenuated total reflection Fourier transform infrared (ATR FT-IR) spectroscopy

Conventional infrared spectrometers are double beam instrument. This means that there are two radiation beams, one passing through the sample and the other passing through the reference. A monochromator is used to collect radiation of only one frequency at a time to pass through the sample and the reference. A detector compares the radiation transmitted by the sample with the radiation that is passing through the reference and the spectrum is plotted. While Fourier transform infrared spectroscopy (FT-IR) use only one beam and all frequencies pass through the instrument at once. It is called FT-IR spectroscopy because a mathematical treatment Fourier transformation is used to interpret the data and produce a spectrum [36].

ATR FT-IR spectroscopy is characterization technique based on internal reflection principle. Due to the requirement of non-destructive analysis, this technique is developed for obtained the infrared spectrum of the surface of material or the spectrum of materials either too thick to be analyzed by transmission spectroscopy. In this technique, the sample is placed in contact with the internal reflection element (IRE), the light is totally reflected and the sample interacts with the *evanescent wave* which resulting in the absorption of radiation by the sample.

### 2.2.1 Principles of light reflection and refraction

Reflection of light or radiant energy is the abrupt change in the direction of propagation when the radiation is incident on an interface. An optical interface is created whenever there is a discrete change in optical properties; namely the refractive index and/or absorption index. When electromagnetic radiation strikes a boundary between two media with different refractive indices, refraction and reflection occur. The law that governs the reflection process requires that the angle of incidence be equal to the angle of reflection. In this case, reflection is specular. If electromagnetic radiation passes from one medium to another that has a different refractive index, a sudden change of beam direction is detected because of the difference in propagation velocity through two media. If light propagates through a medium with refractive

index  $n_1$  and enters a medium with refractive index  $n_2$  (Figure 2.5), the light path will change, the extent of refraction is given by the following relationship [35]:

$$\frac{\sin \alpha_1}{\sin \alpha_2} = \frac{n_2(\bar{\nu})}{n_1(\bar{\nu})} \quad (2.3)$$

where  $\alpha_1$  and  $\alpha_2$  are the angle of incidence and refraction, respectively.

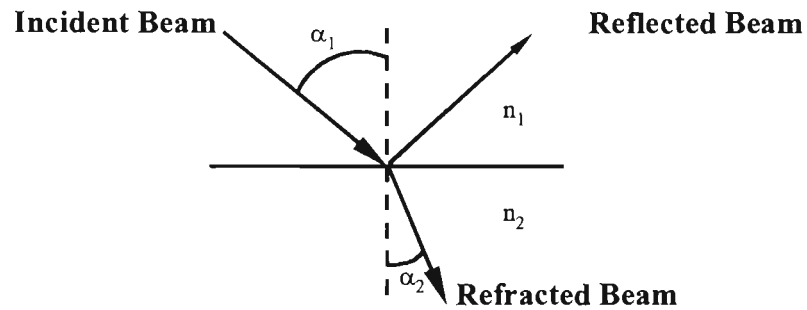


Figure 2.5 Reflection and refraction of a plane wave at a dielectric based on Snell's Law.

Total internal reflection occurs when light (or radiant energy) traveling through a medium of high refractive index is incident on the interface with a lower index (i.e.,  $n_1 > n_2$ ) with an incident angle greater than the critical angle. The critical angle can be derived from Snell's law and given by Equation 2.4 [37].

$$\theta_c = \sin^{-1}(n_2(\bar{\nu}) / n_1(\bar{\nu})). \quad (2.4)$$

According to Figure 2.6, when the angle of incidence equals the critical angle,  $\theta_c$ , the refracted angle equals  $90^\circ$ . This implies that the phenomenon is under a

total internal reflection there is no light from the optically denser medium travels across the interface into the optically rarer medium. If the rarer medium is non-absorbing, then all incident radiation (*i.e.*, at angles greater than the critical angle) are internally reflected. If the rarer medium absorbs radiation at a specific wavelength, the intensity of the reflected radiation is reduced at that particular wavelength. In other words, the internal reflection is attenuated. This attenuation of the total reflection produces ATR spectra.

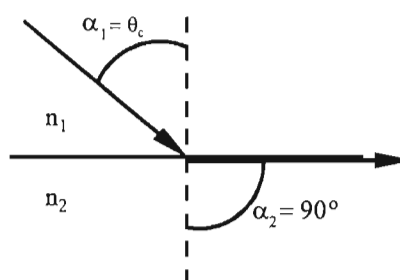


Figure 2.6 Condition under which total internal reflection occurs. Light travels from an optically denser medium and impinges at the surface of the optically rarer medium ( $n_1 > n_2$ ) with angle of incidence equal the critical angle.

Total internal reflection spectroscopy is, therefore, the technique of recording the optical spectrum of a sample material that is in contact with an optically denser medium. The wavelength dependence of the reflectivity of this interface is measured by introducing light into the denser medium. In this technique the reflectivity is a measure of the interaction of the electric field with the material and the resulting spectrum is also a characteristic of the material.

### 2.2.2 Internal reflection element (IRE)

The internal reflection element (IRE), also referred as ATR crystal, is made of a material with a high reflective index and be transparent throughout the mid-infrared spectral region [36]. Typical IREs are zinc selenide (ZnSe), silicon (Si), germanium (Ge), and diamond as shown the details in Table 2.1.



Table 2.1 Properties of material used for internal reflection elements.

Material	Reflective index at $1000\text{ cm}^{-1}$	ATR spectral range ( $\text{cm}^{-1}$ )	Hardness ( $\text{kg mm}^{-2}$ )	Depth of penetration ( $\mu\text{m}$ ) (at $45^\circ, 1000\text{ cm}^{-1}$ )
Germanium	4.0	5500-675	550	0.66
Silicon	3.4	8900-1500, 360-120	1150	0.85
Zinc selenide	2.4	15000-650	120	2.01
Diamond	2.4	25000-100	5700	2.01

The IRE can divide into two groups, single-reflection and multiple-reflection IRE as shown in Figure 2.7. The single-reflection IRE can be used to record spectra of materials which absorption is adequate strong or contrast. On the other hand, the multiple-reflection can be employed to enhance the contrast that cannot be obtained with single-reflection [37]. A large variety of IRE shapes have been developed such as hemicylinder, microhemicylinder, and hemisphere depending on designing to simplify instrumentation and nature of samples. The ease of obtaining an internal reflection spectrum and the information obtained from the spectrum are determined by characteristics of the IRE, for example, reflective index, hardness and shape of IRE.

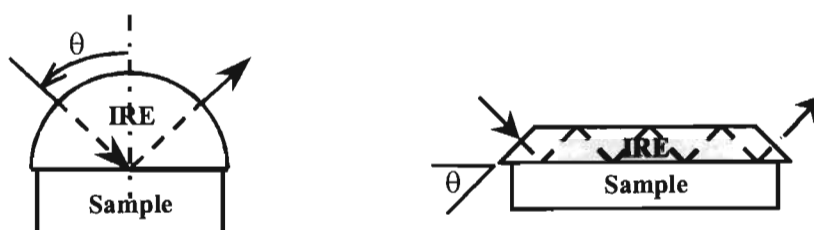


Figure 2.7 IRE configurations: (a) Single reflection hemispherical crystal, and (b) Multiple reflections.

### 2.2.3 ATR spectral intensity

According to the Snell's law, the critical angle equal to  $\sin^{-1}(n_2(\nu)/n_1(\nu))$ , where  $n_1(\nu)$  and  $n_2(\nu)$  are the real portion of complex refractive index of high refractive index medium (i.e., IRE), and lower refractive index medium (i.e., sample),  $n_1(\nu) > n_2(\nu)$ , at frequency  $\nu$ . The complex refractive index of a medium is defined as [39]:

$$\hat{n}(\nu) = n(\nu) + ik(\nu) \quad (2.5)$$

Where  $i$  is equal to  $\sqrt{-1}$ ,  $\hat{n}(\nu)$  is the complex refractive index,  $n(\nu)$  is the refractive index, and  $k(\nu)$  is the absorption index at frequency  $\nu$ .

For ATR technique, incident light travels from IRE, and impinges at the interface between the IRE and sample with incident angle is greater than the critical angle. Under non-absorbing condition (i.e.,  $k_2(\nu) = 0$ ), no light travel across the interface and no reflection losses due to absorption. The incident light is totally reflected at the interface and this phenomenon is defined as ***total reflection phenomenon***.

If the lower refractive index medium is absorbing (i.e.,  $k_2(\nu) > 0$ ), total internal reflection no longer occurs and the infrared beam is attenuated as a result of absorption by the medium. This phenomenon is called the ***attenuated total reflection (ATR) phenomenon***. Since no light travels across the boundary, there is a strong electric field at the interface of absorbing medium. Interaction between the electric field and the absorbing medium is the cause of reflection loss in ATR experiment. The magnitudes of the interaction between light and the sample can be expressed in term of absorbance. The relationship between absorbed and reflected intensity in an ATR spectrum is given by:

$$A(\theta, \nu) = 1 - R(\theta, \nu) \quad (2.6)$$

where  $A(\theta, \nu)$  and  $R(\theta, \nu)$  are absorptance and reflectance, respectively.

Generally, absorptance in ATR can be expressed in terms of experimental parameters and material characteristic by the following expression [40-41]:

$$A_l(\theta, \nu) = \frac{4\pi\nu}{n_1 \cos\theta} \int_0^\infty n_2(\nu)k_2(\nu) \langle E_{zl}^2(\theta, \nu) \rangle dz \quad (2.7)$$

where  $A(\theta, \nu)$  is absorptance and  $l$  indicates the polarization of the incident beam.  $\langle E_{zl}^2(\theta, \nu) \rangle$  is the mean square electric field (MSEF) at depth  $z$ ,  $n_1$  is the refractive index of the IRE,  $n_2(\nu)$  and  $k_2(\nu)$  are the refractive index and absorption index of the sample, respectively.

The MSEF is a function of both the material properties (e.g., refractive index of the two media) and the experimental parameters (e.g., angle of incidence, frequency, and polarization of the incident beam). Given the nature of the MSEF in the absorbing medium, the sample layer which closest to the interface has a much higher per thickness conduct to the total absorptance than the layer found further into the bulk which decrease exponentially as a function of depth. The strength and decay characteristic of the MSEF vary with the absorption strength are shown in Figure 2.8

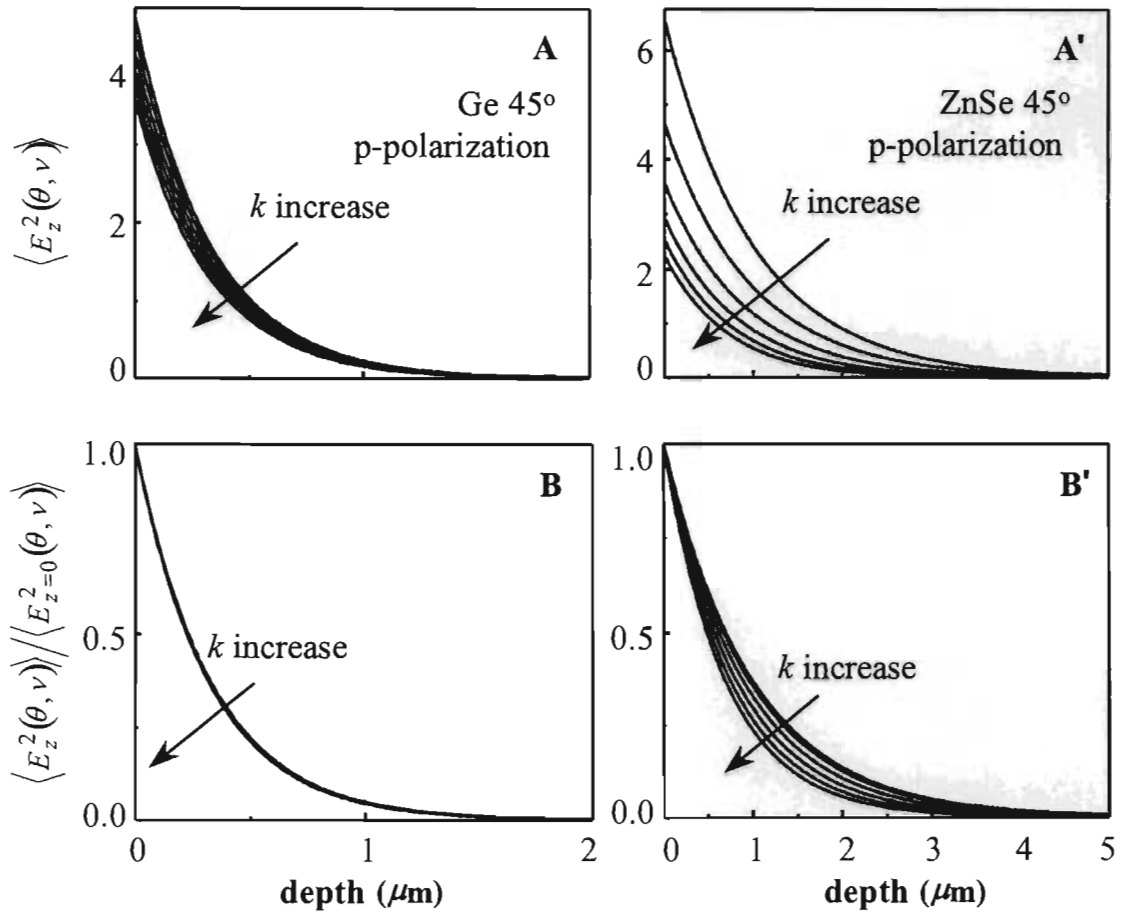


Figure 2.8 The MSEF at various experimental condition (A, A') and its decay characteristic (B, B'). The simulation parameters are  $n_0 = 4.00$  for Ge,  $n_0 = 2.40$  for ZnSe,  $\nu = 1000 \text{ cm}^{-1}$ ,  $n_1(\nu) = 1.50$ ,  $k_1(\nu) = 0.0, 0.1, 0.2, 0.3, 0.4$  and  $0.5$ , respectively.

### 2.2.4 Depth profiling using ATR FT-IR spectroscopy

ATR FT-IR spectroscopy is known as a depth profiling and surface characterization technique. The important factor that makes this technique appropriate for depth profiling application is MSEF under total internal reflection condition. The MSEF is very powerful at the interface and exponentially decays as a function of distance from the interface of IRE and sample. The decay pattern of MSEF can be expressed in terms of the distance from IRE and sample interface by following expression [41]:

$$\langle E_z^2(\theta, \nu) \rangle = \langle E_0^2(\theta, \nu) \rangle e^{-2z/d_p(\theta, \nu)} \quad (2.8)$$

where  $d_p(\theta, \nu)$  is the penetration depth.  $\langle E_0^2(\theta, \nu) \rangle$  and  $\langle E_z^2(\theta, \nu) \rangle$  are the MSEF at the interface and the depth  $z$ , respectively. The evanescent field characteristic at the boundary between the IRE, and the sample is shown in Figure 2.11 [35].

The penetration depth is described as the distance into the sample where the MSEF decay to  $1/e^2$  of its value at the interface of IRE and sample. The penetration depth is given in terms of material characterization and experimental parameters by:

$$d_p(\theta, \nu) = \frac{1}{2\pi\nu n_1 (\sin^2 \theta - (n_2/n_1)^2)^{1/2}} \quad (2.9)$$

where  $d_p(\theta, \nu)$  is the penetration depth,  $n_1$  and  $n_2$  are the refractive index of the IRE and sample, respectively.

From the equation 2.9, the depth of penetration can be varied by changing the angle of incidence, type of IRE, and frequency. Penetration depth can be decreased by means of an IRE with much greater than refractive index than that of the rarer one, a large angle of incidence, or a high frequency of incident radiation.

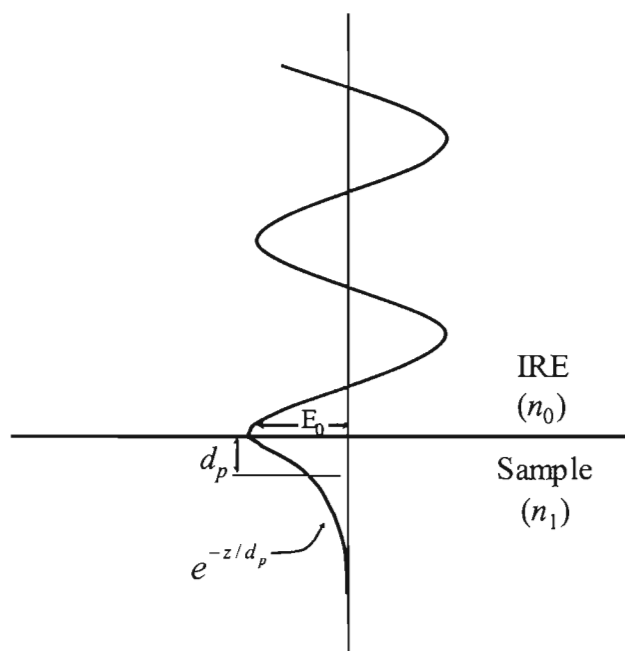


Figure 2.9 The evanescent field at the boundary between the IRE and the sample.

### 2.2.1 Limitations of ATR FT-IR spectroscopy

For ATR analysis, any sample that comes into contact with the IRE can be analyzed. Therefore, the uniform sample-IRE contact is of a greater concern. With traditional ATR spectroscopy (macro methods), it is desirable to achieve contact over the entire IRE surface (approximately  $5 \times 5 \text{ mm}^2$ ). While this requirement is easily achieved with liquid samples, obtaining good contact with solid samples will be difficult. Moreover, a large contact area also results in an average molecular information over a large sampling area. The change of molecular information in small area cannot investigate.

## 2.3 ATR FT-IR microspectroscopy

### 2.3.1 Infrared microscope

FT-IR microspectroscopy defines as the combination of a microscope to an infrared spectrometer. An infrared microscope has been developed in order to analyze the small samples that take an advantage of normal infrared spectrometer. Uses of this technique include general characterization of particulate matter, polymer characterization, semiconductor measurements, the identification of contaminants, forensic evidences, biological, and pharmaceutical applications [42]. The optical diagram of an infrared microscope is shown in Figure 2.10.

A ray tracing within the 15X Schwarzschild Cassegrain infrared objective is shown in Figure 2.11. The concave primary mirror and the convex secondary mirror of the objective focus radiation onto the reflecting plane with angles of incidence ranging from  $15.6^\circ$  to  $35.5^\circ$ . ATR spectra are always collected with the reflection mode based on the phenomenon known as total internal reflection by coupling the focused radiation into specially designed  $\mu$ IRE made of high reflective index materials and by making the angle of incidence at the sampling surface greater than the critical angle.

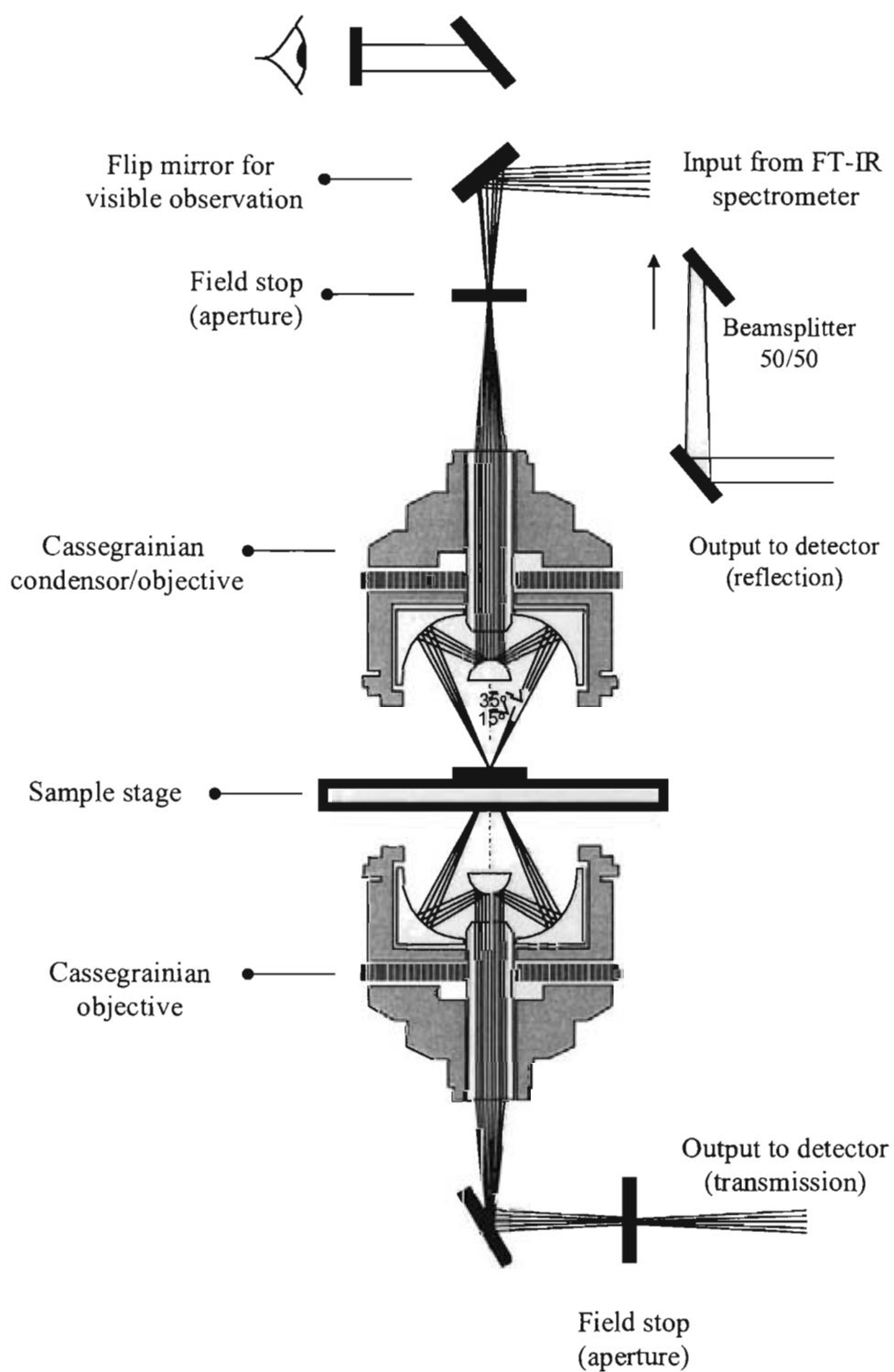


Figure 2.10 Optical diagram of an infrared microscope.



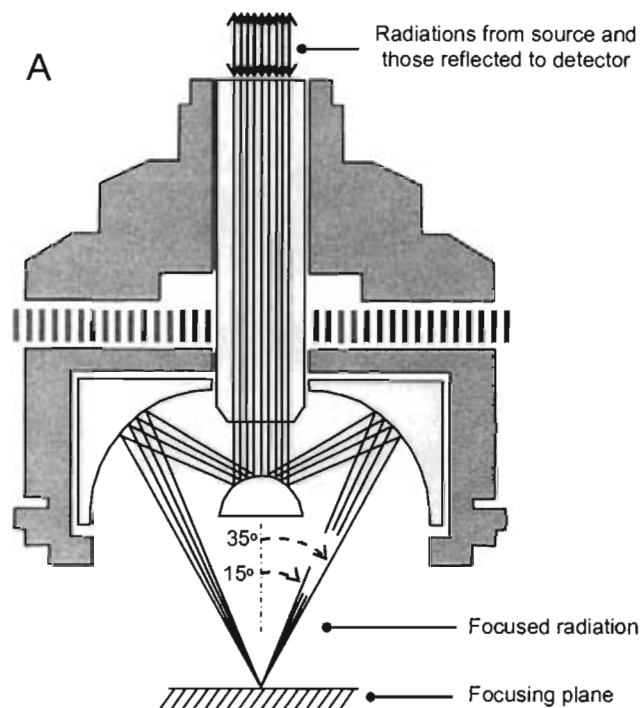


Figure 2.11 The infrared radiation tracing with in the objective of infrared microscope.

### 2.3.2 Principle of light entering the Ge $\mu$ IRE

The optical design of the objective, the focused radiation contains rays with angles of incidence ranging from  $15^\circ$  to  $35^\circ$ . By coupling this focused radiation into specially designed IREs made of high refractive index materials and by making the angle of incidence at the sampling surface greater than the critical angle, a spectral acquisition under the ATR FT-IR condition can be realized [35].

The hemispherical dome of the miniature cone-shaped Ge IRE facilitates the coupling of the focused radiation traveling into the IRE by minimizes the reflection loss at the air/Ge interface. If a nearly perfect coupling is assumed, the radiation transmitted through the air/Ge interface of the dome and impinged the Ge/air interface of the tip without a significant change in the angle of incidence [43]. To ensure a good contact, the circular tip of the IRE is made a hemispherical surface. Since the contact area is small ( $\sim 100 \mu\text{m}$  or less than in diameter), a good contact was achieved with a minimal force exert on the tip. For the Ge  $\mu$ IRE ( $n_{\text{Ge}} = 4.0$ ), the critical angle for the

total internal reflection (TIR) at the interface with air ( $n_{\text{air}} = 1.0$ ) and an organic medium ( $n_{\text{organic}} = 1.5$ ), respectively, are  $14.48^\circ$  and  $22.02^\circ$ . As a result, parts of the coupled radiation can be employed for ATR FT-IR investigation of a material having an optical contact with the tip of the miniature IRE. To eliminate interference from the internal reflection associated with the radiation having an angle of incidence smaller than the critical angle, an opaque circular adhesive tape is placed on the center of the hemispherical dome. Due to an effective condensation of the coupled radiation and an efficient light-matter interaction under the ATR condition at the tip of the IRE, ATR FT-IR spectra of a small specimen or a small area can be acquired with superb spectral quality.

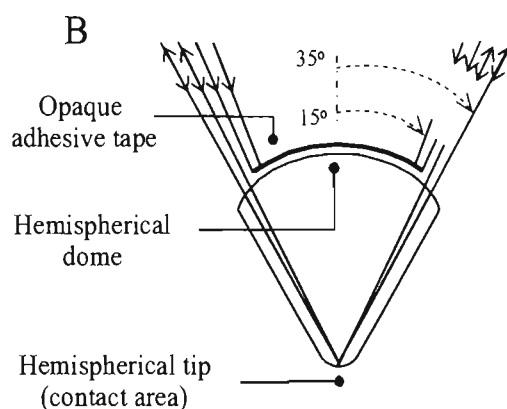


Figure 2.12 Schematic illustration of ray tracing within the infrared objective focused radiation traveling within the Ge  $\mu$ IRE.

## CHAPTER III

### EXPERIMENTAL SECTION

Owing to the analysis of ballpoint pen inks on paper employed for forensic documented examination, ink marks obtained from the pen had a width of line depending on the diameter of pen tip. Generally, a size of pen tip is about 0.38-1.0 mm but the contact area of conventional IRE as a hemispherical Ge IRE is  $5 \times 5 \text{ mm}^2$  which is larger than those of the ink marks. Therefore, the homemade Ge  $\mu$ IRE is developed for small contact area ( $50 \times 50 \text{ }\mu\text{m}^2$ ) which is suitable for analysis of ink.

#### 3.1 Materials and Equipments

##### 3.1.1 Ballpoint pen ink samples

Commercial ballpoint pen from various brands and models were collected. All employed samples are shown in Table 3.1.

Table 3.1 Ballpoint pen ink samples

Sample	Brand	Model	Colors	
			Black	Blue
1	Faber-Castel <sup>®</sup>	Grip Ball 1424	√	√
2	Faber-Castel <sup>®</sup>	Click Ball 1422	√	√
3	Faber-Castel <sup>®</sup>	Super Tech Point 1420	√	√
4	Faber-Castel <sup>®</sup>	Ball Pen 1423	√	√
5	Lancer <sup>®</sup>	Spiral 825	√	√
6	Lancer <sup>®</sup>	Click 878	√	√
7	Lancer <sup>®</sup>	Pro-Riter	√	√
8	Lancer <sup>®</sup>	Cadet 818	√	√

Table 3.1 (continue)

Sample	Brand	Model	Colors	
			Black	Blue
9	Horse <sup>®</sup>	Ball Pen H-402	√	√
10	Reynolds <sup>®</sup>	Fine Carbure	√	√
11	Reynolds <sup>®</sup>	800	√	√
12	Standard <sup>®</sup>	G soft	√	√
13	Standard <sup>®</sup>	Fizz Hi Grip	√	√
14	Stabilo <sup>®</sup>	Marathon 318	√	√
15	Stabilo <sup>®</sup>	F	√	√
16	Quantum <sup>®</sup>	GeloBal 007	√	√
17	Quantum <sup>®</sup>	GeloBal 1230	√	√
18	Pilot <sup>®</sup>	Super grip	√	√
19	Pentel <sup>®</sup>	Star V	√	√
20	Staedtler <sup>®</sup>	Noris Stick 434 F	√	√
21	The One <sup>®</sup>	GPB-3001	√	√

### 3.1.2 White Smooth A4 Paper Samples

Commercial A4 papers from various bands and gsm's that were made in Thailand were collected. All employed samples are shown in Table 3.2.

Table 3.2 A4 Paper samples

Sample	Brand	Weight (Grams per square meter, gsm)
1	Double A <sup>®</sup>	80
2	Shih-Tzu <sup>®</sup>	80
3	Eagle <sup>®</sup>	80
4	Valuesave <sup>®</sup>	80
5	Quality <sup>®</sup>	80
6	Quality <sup>®</sup>	70

### 3.1.3 Instruments

1. Nicolet 6700 FT-IR spectrometer (Thermo Electron Corporation, Madison, WI, USA) equipped with a mercury-cadmium-telluride (MCT) detector.
2. Continuum™ infrared microscope with a built-in 15X Schwarzschild-Cassegrain infrared objective and a 10X glass objective.
3. Homemade slide-on Ge  $\mu$ ATR accessory with a cone-shaped Ge as IRE.

## 3.2 Default Spectral Acquisition

### Nicolet 6700 FT-IR Spectrometer

#### Instrumental Setup

Source	Standard Global™ Infrared Light Source
Detector	MCT/A
Beam splitter	Ge-coated KBr

#### Acquisition Parameters

Spectral resolution	4 $\text{cm}^{-1}$
Number of scans	128 scans
Spectral format	Absorbance
Mid-infrared range	4000-650 $\text{cm}^{-1}$

#### Advanced Parameters

Zero filing	none
Apodization	Happ-Genzel
Phase correction standard	Mertz

### Continuum Infrared Microscope

#### Instrumental Setup

Objective	15X Schwarzschild-Cassegrain
Aperture size	150 $\times$ 150 $\mu\text{m}^2$

### 3.3 Homemade Slide-on Germanium $\mu$ ATR Accessory

The homemade slide-on Germanium  $\mu$ ATR accessory equipped with a cone-shaped Ge  $\mu$ IRE. This has a large number of advantages. For example, there is a small sampling area ( $50 \times 50 \mu\text{m}^2$ ). Moreover, samples can be analyzed without additional sample preparation.

The homemade slide-on Ge  $\mu$ ATR accessory consists of two parts as shown in Figures 3.1. Detailed drawing of the homemade miniature ATR accessory with Ge  $\mu$ IRE are shown in Figure 3.2. The first component is the slide-on housing which is designed for placing the slide-on Ge  $\mu$ IRE into the Continuum infrared microscope. The second component is the slide-on Ge  $\mu$ IRE which is designed for alignment adjusted to obtain high energy throughput. In Figure 3.3, the slide-on Ge  $\mu$ IRE is slid into the position and locked by knob of the slide-on housing which is located on the built in 15x Schwarzschild-Cassegrain infrared objective that connected to Nicolet 6700 FT-IR Spectrometer. The incident radiation from the infrared microscope is coupled into the dome-shaped Ge  $\mu$ IRE and impinged on the tip while total internal reflection occurred at the Ge tip. Ray tracing within infrared microscope and the infrared radiation traveling into Ge  $\mu$ IRE are shown in Figure 3.4. The couple radiation can be employed for ATR FT-IR spectra acquisition as the tip of the Ge  $\mu$ IRE contact the ink sample.

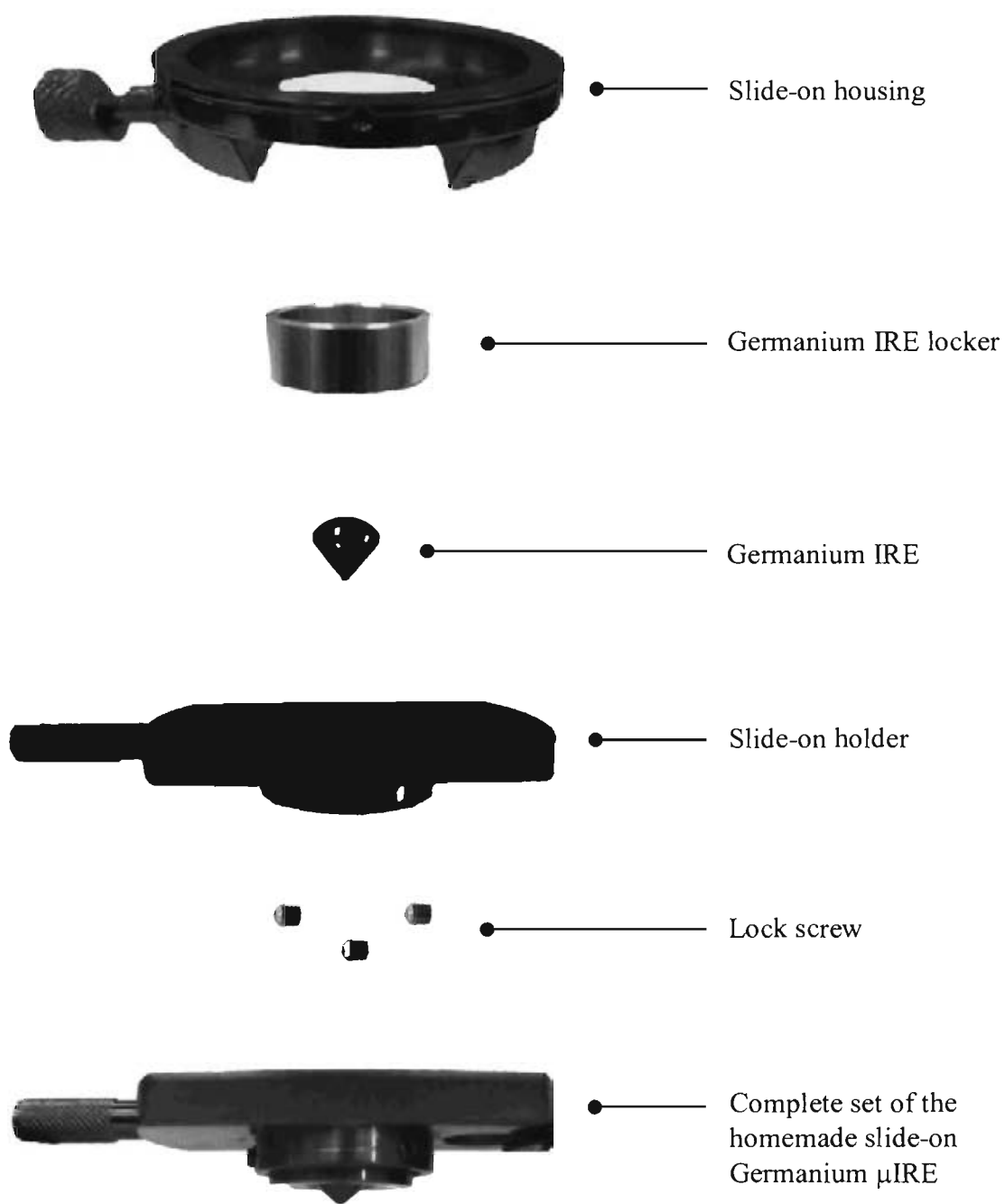


Figure 3.1 The slide-on housing and compositions of the homemade Germanium  $\mu$ ATR accessory.

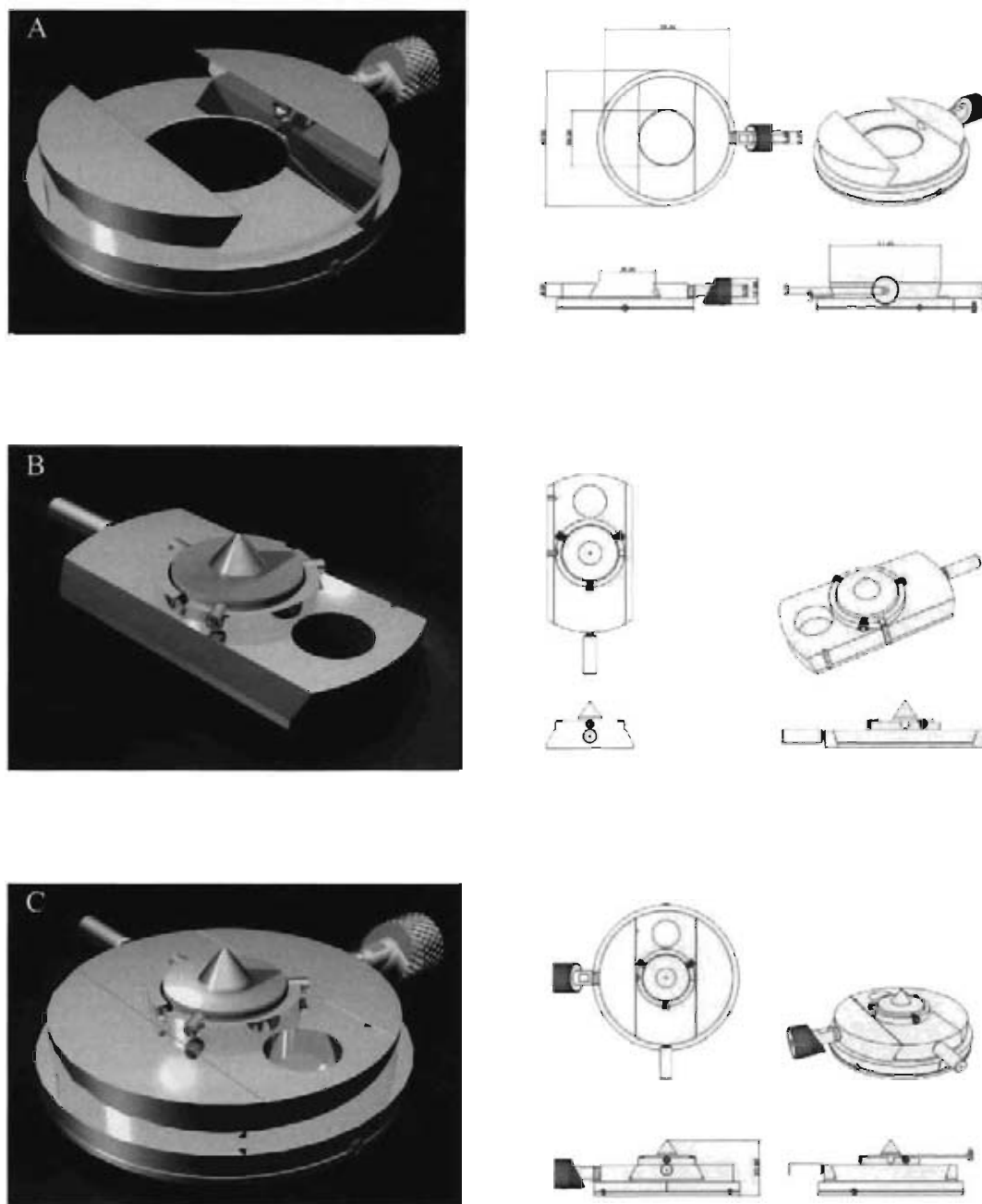


Figure 3.2 Detailed drawing of the homemade miniature ATR accessory with Germanium  $\mu$ IRE. (A) the housing attached to the objective, (B) the slide-on set with the Ge  $\mu$ IRE, and (C) the complete accessory.





Figure 3.3 Example of procedures for spectral acquisition (A) Continuum infrared microscope attached to an infrared spectrometer, (B) slide-on Ge  $\mu$ IRE is fixed on the position of slide-on housing attached to the 15X Schwarzschild-Cassegrain infrared objective, and (C) the complete homemade  $\mu$ ATR accessory ready for a spectral acquisition.

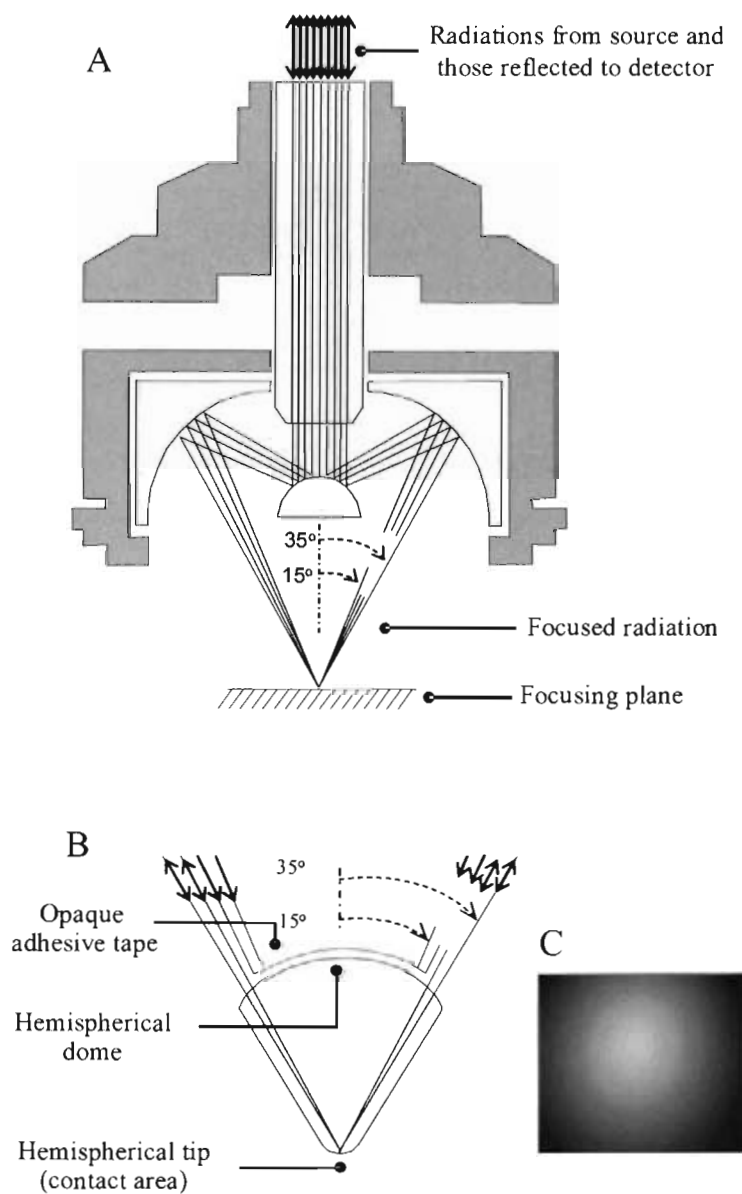


Figure 3.4 Schematic illustration of ray tracing within the 15X Schwarzschild-Cassegrain infrared objective (A), focused radiation traveling within the Ge  $\mu$ IRE (B), and image of the tip of Ge  $\mu$ IRE under the visible light illumination (C).

### 3.4 Characterization of dried ink

All spectra were collected by using a Continuum<sup>TM</sup> infrared microscope equipped with a mercury-cadmium-telluride (MCT) detector. The microscope was attached to the Nicolet 6700 FT-IR Spectrometer (Thermo Electron Corporation, Madison, WI USA). Spectra in the mid-infrared region (4000-650  $\text{cm}^{-1}$ ) at spectral resolution of 4  $\text{cm}^{-1}$  were collected with 128 co-addition scans. The aperture size of infrared radiation was set at 150x150  $\mu\text{m}^2$ . To analyze ink, the samples were placed on the microscope stage. The position of analyzed samples was selected through a built-in objective. The slide-on Germanium  $\mu\text{IRE}$  was slid into the position of the slide-on housing which was aligned to the focal point of the built-in infrared objective.

To analyze ink samples, the analyzed pen ink was smeared on the glass slide and was placed on the microscope stage. After that, the stage was moved up in order to develop the ink onto the tip of the Ge  $\mu\text{IRE}$  by “*contact and collect*” operation. When the ink trace was brought into an optical contact with the  $\mu\text{IRE}$ , some of ink traces stuck with the  $\mu\text{IRE}$  after the substrate was removed. The spectra of ink trace on the  $\mu\text{IRE}$  were collected under the ATR mode without any interference of the substrate.

### 3.5 Experimental procedure for paper

#### 3.5.1 Experimental procedure for depth dependence of paper characterization

Continuum<sup>TM</sup> infrared microscope attached to the Nicolet 6700 FT-IR Spectrometer (Thermo Electron Corporation, Madison, WI USA) was used for all ATR spectra acquisition. A homemade slide-on Ge  $\mu\text{IRE}$  was slid into the position of slide-on housing and locked at the focal point where set through the built-in infrared objective. The aperture size of infrared radiation was set at 150x150  $\mu\text{m}^2$ . All spectra acquired with 128 co-addition scans and spectral resolution of 4  $\text{cm}^{-1}$  condition in mid-infrared region (4000-650  $\text{cm}^{-1}$ ). The single beam obtained from spectral

acquisition of the homemade slide-on Germanium  $\mu$ IRE with no sample contacting was used as a background spectrum.

In the measurement, a point which was analyzed on paper surface was selected randomly. The degree of contact was controlled by the z-stage controller with a step-size in range of 30-40  $\mu\text{m}$ . The spectrum was collected at the start point that did not show any peak in sample spectrum. Afterward, the stage was gradually raised and a spectrum acquisition collected continuously. When the intensities of all peaks in the spectrum did not change after raising the microscope stage, the measurement finished.

### **3.5.2 Experimental procedure for characterization of paper**

To take the spectra of samples, the samples on microscope stage were moved up to contact the tip of the  $\mu$ IRE (at sampling position). The spectral point by point of the sample was detected in strength line with a step-size of 100  $\mu\text{m}$  which controlled by X-Y stage controller. The degree of contact was controlled by the contact alert sensor plate installed on the microscope stage.

### **3.6 Experimental procedure for ink written on paper characterization**

All ATR spectra were collected with Continuum<sup>TM</sup> infrared microscope equipped with a mercury-cadmium-telluride (MCT) detector. The microscope was attached to the Nicolet 6700 FT-IR Spectrometer (Thermo Electron Corporation, Madison, WI USA). Spectra in mid-infrared region (4000-650  $\text{cm}^{-1}$ ) at spectral resolution of 4  $\text{cm}^{-1}$  were collected with 128 co-addition scans. A homemade ATR accessory with a slide-on miniature Ge  $\mu$ IRE was employed for all spectral acquisitions. A background spectrum was collected though the Ge  $\mu$ IRE when it did not contact to a sample.

### **3.6.1 Sample preparation**

Ink sample were applied directly to paper from the pen. For ink sample, a straight line was drawn with a single stroke on paper and leaved for 24 hours. For sample preparation for time dependent characterization, the samples were kept in a cupboard.

In case of line-crossing study, the first ink was pasted directly from the pen onto the paper and leaved for an hour. After that, the second ink was applied in opposite direction of the first ink and leaved for 24 hours for spectrum acquisition.

### **3.6.2 Experimental procedure of depth dependence of inks written on papers characterization**

ATR spectra of ink deposited on paper were collected with the same procedure as those in Section 3.5.1

### **3.6.3 Experimental procedure of ink written on paper characterization**

The ink deposited on paper spectra were measured every 2 days. The experimental procedure was the same procedure as those in Section 3.5.2.

### **3.6.4 Experimental procedure of time dependence of ink on paper characterization**

The ink deposited on paper spectra were measured every 3 days. The experimental procedure was the same procedure as those in Section 3.5.2.

## CHAPTER IV

### RESULTS AND DISCUSSION

ATR FT-IR microspectroscopy is well-known for its spectral information related to molecular structure and chemical composition. Thanks to the homemade slide-on Ge  $\mu$ IRE, the observed spectra provide the chemical signatures or components of ink and ink written on paper without a destructive sample preparation. The chemical information of ink and ink written on paper are characterized and compared to other inks for applying to questioned document.

#### 4.1 Characterization of inks

##### 4.1.1 Spectral assignments of ballpoint pen ink

Written inks mainly consist of colorants (dyes and/or pigments) and vehicles (solvents and resins). There is also a wide range of other ingredients, such as antioxidants, preservatives, and trace elements, but these are form a small fraction of the overall ink composition. The detailed recipes are patented so it is very difficult to know all ink compositions [30]. Although there are several components in ink, the chemical compositions in ink of each manufacturer are unique depending on their materials [44]. ATR FT-IR spectra of some black and blue ballpoint pen inks from various manufacturers are shown in Figure 4.1 and 4.2, respectively. The ink spectra can be divided into two regions. First, the broad absorption band at 3450-3160  $\text{cm}^{-1}$  belongs to O-H stretching vibration and the sharp peaks in 3061-2845  $\text{cm}^{-1}$  are assigned to C-H stretching vibration. Another region is the fingerprint region at 1600-750  $\text{cm}^{-1}$  as different molecular arrangement gives different absorption patterns at these frequencies [45]. Moreover, there had no strong peak shown in the range of 2000-1600  $\text{cm}^{-1}$  which is the characteristic of carbonyl (C=O) stretching vibration. It means that such ink does not have aliphatic acid or ester group in their components, as mentioned by J. Wang [29]. Some spectra show weak absorption band of non-conjugated alkene, C=C stretching, in the region 1680-1620  $\text{cm}^{-1}$  which is absent for

symmetrical molecules [46]. The band assignments of ink associated with the functional group of various components in ballpoint pen ink are summarized in Table 4.1.

Table 4.1 Peak assignments of functional groups observed in ballpoint pen ink [46-47]

Wavenumber (cm <sup>-1</sup> )	Peak Assignments
3450-3160	O-H stretching vibration
3061-3000	Aromatic =C-H stretching vibration
3010-2905	Asymmetric C-H stretching vibration
2945-2845	Symmetric C-H stretching vibration
1600-1580	Conjugated -C=C- stretching vibration
1470-1440	Asymmetric C-H deformation vibration
1380-1350	Symmetric C-H deformation vibration
1280-1220	Symmetric C-O stretching vibration
1250-1150	Asymmetric C-O stretching vibration
1190-1130	C-N stretching vibration
1100-1000	C-OH stretching vibration
1000-650	Out-of plane C-H deformation vibration

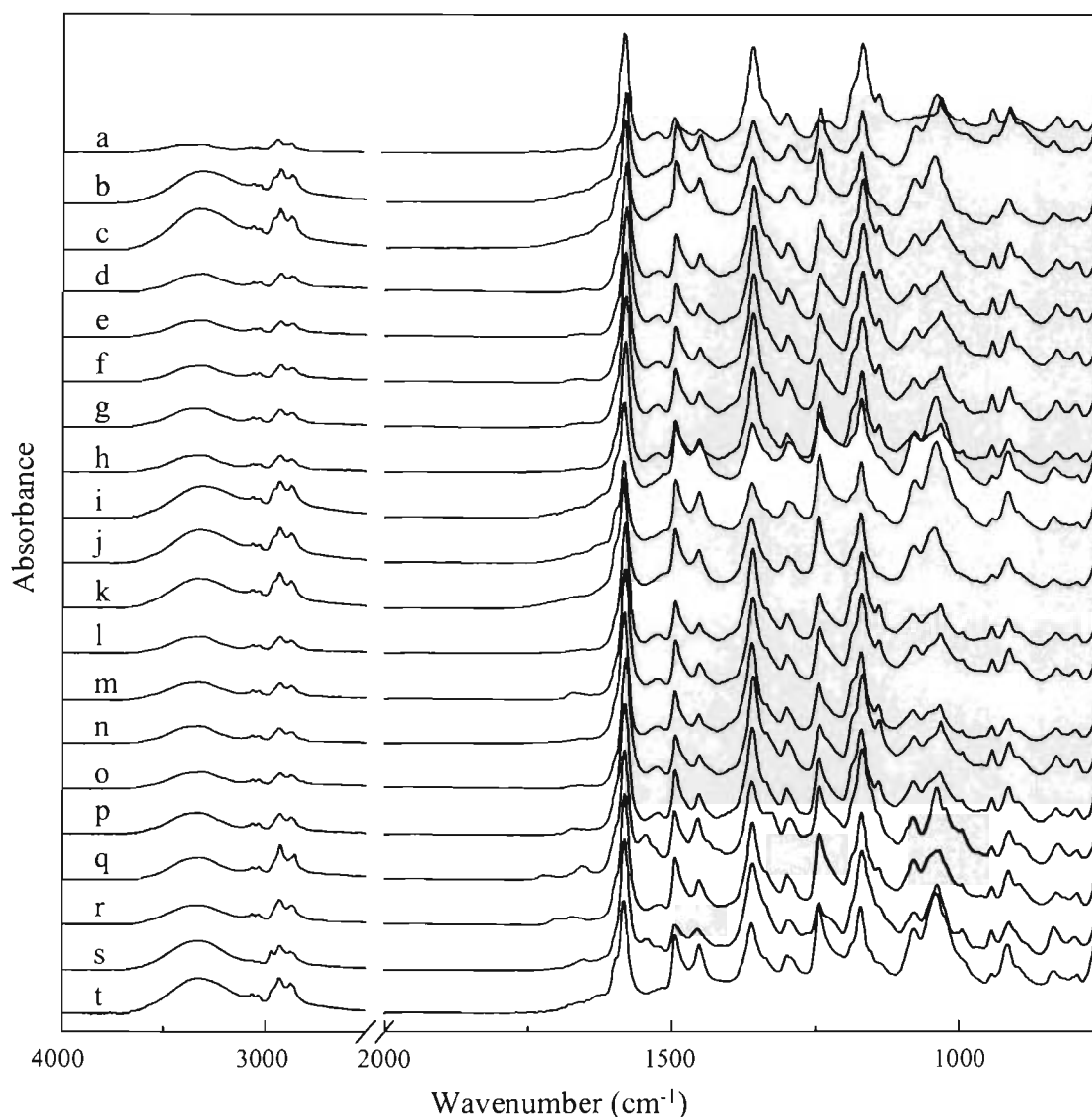


Figure 4.1 ATR FT-IR spectra of 20 commercial dried black ballpoint pen inks acquired by the “contact and collect” operation: (a) Faber-Castel<sup>®</sup> (Grip Ball 1424), (b) Faber-Castel<sup>®</sup> (Click Ball 1422), (c) Faber-Castel<sup>®</sup> (Super Tech Point 1420), (d) Faber-Castel<sup>®</sup> (Ball Pen 1423), (e) Lancer<sup>®</sup> (Spiral 825), (f) Lancer<sup>®</sup> (Click 878), (g) Lancer<sup>®</sup> (Pro-Riter), (h) Lancer<sup>®</sup> (Cadet), (i) Horse<sup>®</sup> (Ball Pen H-402), (j) Reynolds<sup>®</sup> (Fine Carbure), (k) Reynolds<sup>®</sup> (800), (l) Standard<sup>®</sup> (g’Soft), (m) Standard<sup>®</sup> (Fizz Hi Grip), (n) Stabilo<sup>®</sup> (Marathon 318), (o) Stabilo<sup>®</sup> (F), (p) Quantum<sup>®</sup> (GeloBal 007), (q) Quantum<sup>®</sup> (GeloBal QCGB 1230), (r) Pilot<sup>®</sup> (Super Grip), (s) Pentel<sup>®</sup> (Star V), and (t) Staedler<sup>®</sup> (Noris Stick 434 F).



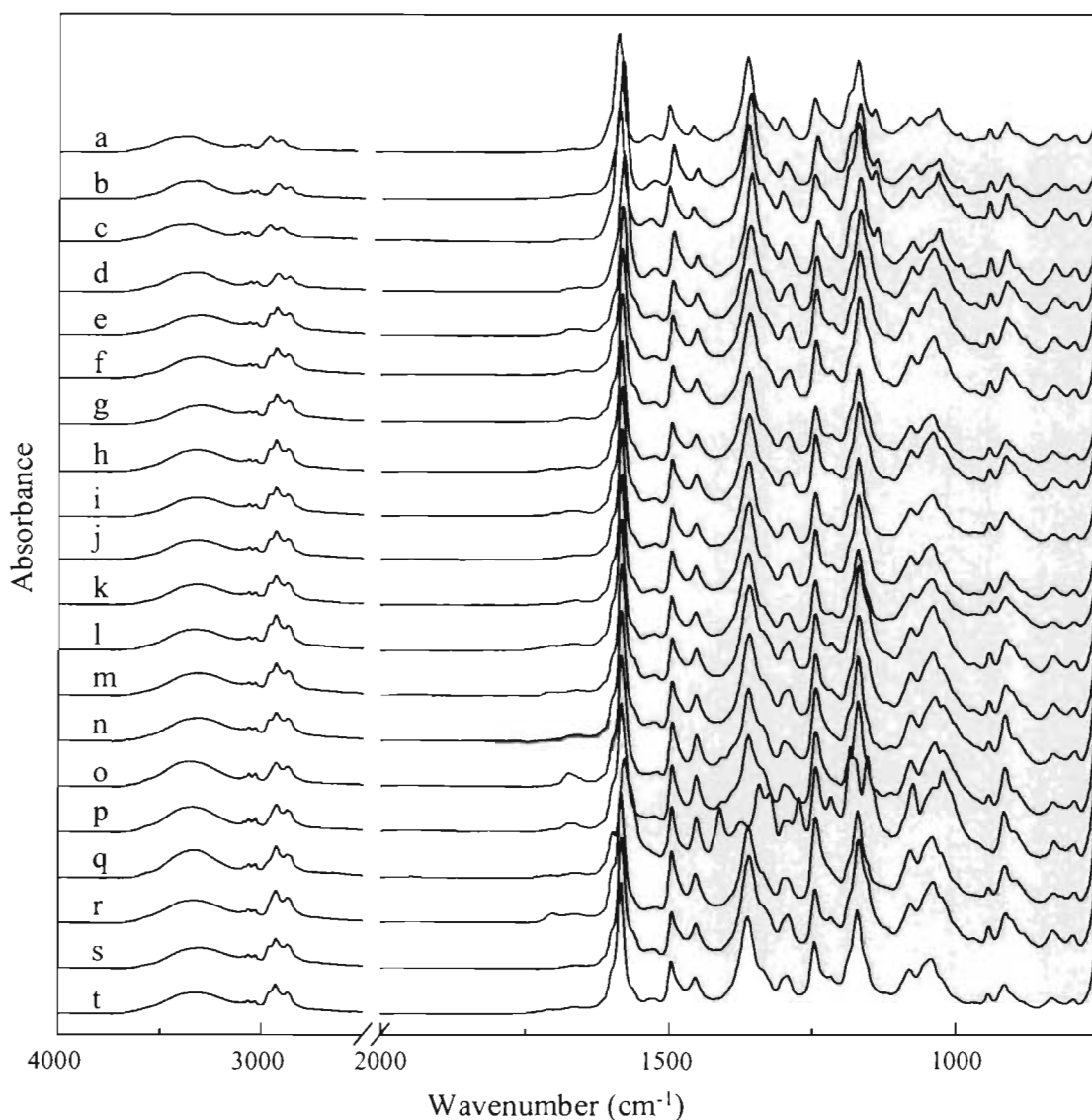


Figure 4.2 ATR FT-IR spectra of 20 commercial dried blue ballpoint pen inks acquired by the “contact and collect” operation: (a) Faber-Castel<sup>®</sup> (Grip Ball 1424), (b) Faber-Castel<sup>®</sup> (Click Ball 1422), (c) Faber-Castel<sup>®</sup> (Super Tech Point 1420), (d) Faber-Castel<sup>®</sup> (Ball Pen 1423), (e) Lancer<sup>®</sup> (Spiral 825), (f) Lancer<sup>®</sup> (Click 878), (g) Lancer<sup>®</sup> (Pro-Riter), (h) Lancer<sup>®</sup> (Cadet), (i) Horse<sup>®</sup> (Ball Pen H-402), (j) Reynolds<sup>®</sup> (Fine Carbure), (k) Reynolds<sup>®</sup> (800), (l) Standard<sup>®</sup> (g’Soft), (m) Standard<sup>®</sup> (Fizz Hi Grip), (n) Stabilo<sup>®</sup> (Marathon 318), (o) Stabilo<sup>®</sup> (F), (p) Quantum<sup>®</sup> (GeloBal 007), (q) Quantum<sup>®</sup> (GeloBal QCGB 1230), (r) Pilot<sup>®</sup> (Super Grip), (s) Pentel<sup>®</sup> (Star V), and (t) Staedler<sup>®</sup> (Noris Stick 434 F).

Since ink contains the volatile compounds used as solvents, the compositions of ink can change with the time. To determine these components, the blue Pentel<sup>®</sup> (Star V) ink trace was pasted on the glass slide and was quickly transferred onto the  $\mu$ IRE tip. We defined it as wet ink. To proof that the volatile compound disappears with the time, the sample was analyzed after storage for an hour which called dried ink. The dried ink trace is the residual consisted of dyes or pigments and nonvolatile compounds. The ATR FT-IR spectra of wet and dried ink are shown in Figure 4.3 (A) and (B), respectively. Spectral subtraction is used for the determination of volatile compounds that disappear with time. The subtraction result of wet ink spectrum by dried ink one is shown in Figure 4.3 (C). The spectral search shows matching of 2-phenoxyethanol from the HR Aldrich FT-IR Collection Edition II Library, as shown in Figure 4.3 (D). This indicated that the volatile compound used in this sample is probably 2-phenoxyethanol. The conclusion coincide with those reported in literatures, the volatiles found in the ballpoint pen ink are usually 2-phenoxyethanol, benzyl alcohol, propylene glycol, and 1-methyl-2-pyrrolidinone [19, 25, 48].

On the other hand, the dried ink spectrum subtracted by the wet ink spectrum as shown the result in Figure 4.3 (E) matched the Crystal violet spectrum as listed in the same library. The crystal violet is classified in triarylmethane dyes, a group of dyes of which molecular structure has a central carbon atom connected to three aromatic rings. The chemical structure of some triarylmethane dyes i.e., crystal violet, methyl violet, tetramethyl para-rosaniline, and victoria blue are shown in Figure 4.4. The difference between those dyes is a number of methyl group or carbon atoms bonded to the three nitrogen atoms. Moreover, combination of crystal violet and methyl violet has been found in blue-colored ballpoint pen ink [16, 23, 49-50].

Although inks have various compositions, analysis of ink by ATR FT-IR microspectroscopy with homemade accessory can provide the ink chemical compositions like as other analytical techniques. This technique does not require an additional sample preparation that makes easy to analyze sample in short time. Moreover, the spectral signature of the volatile compound can be extracted via the subtractive operation.

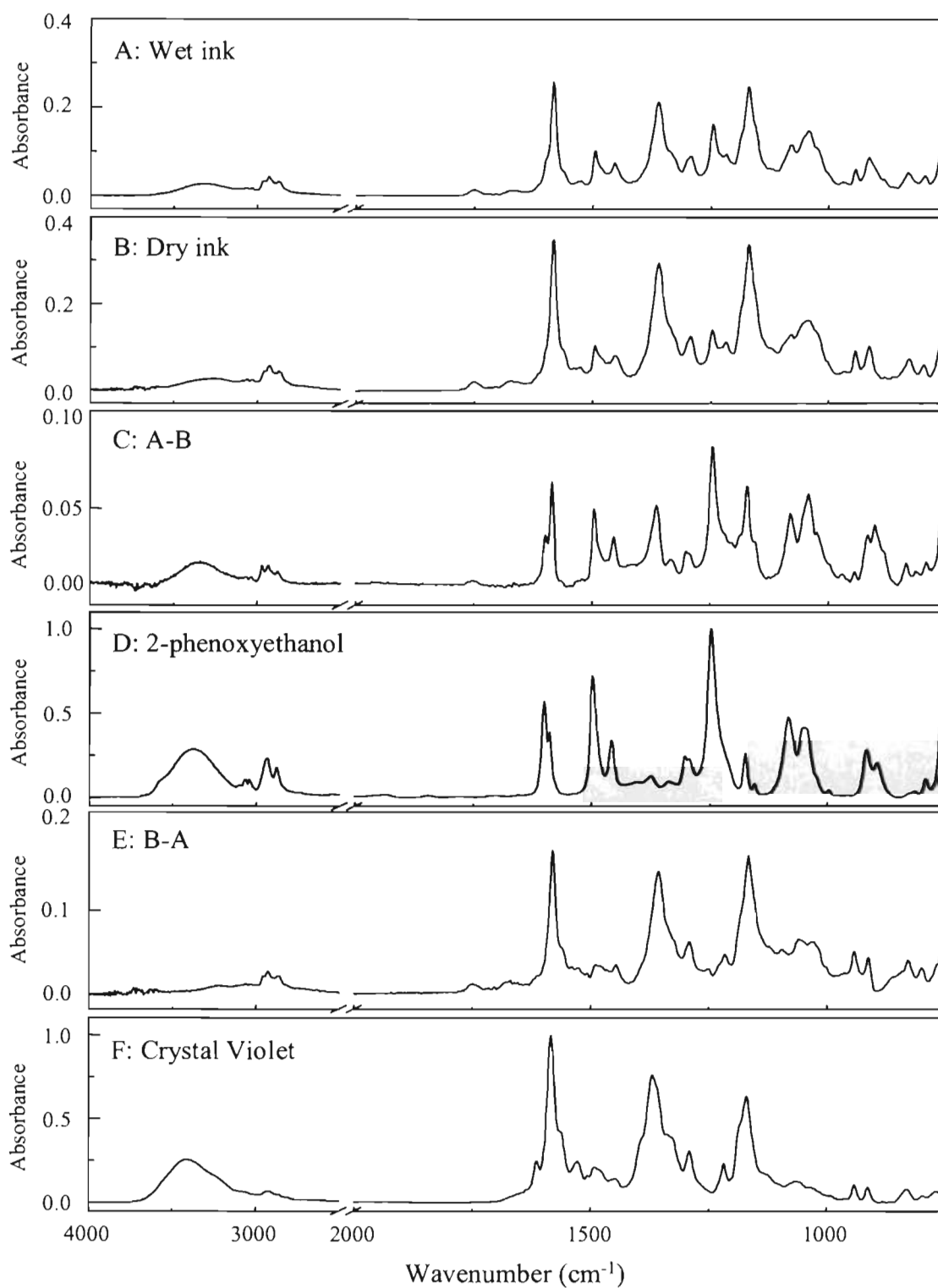
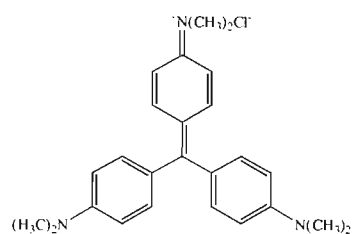
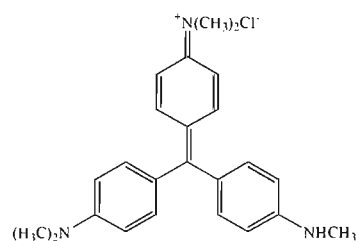


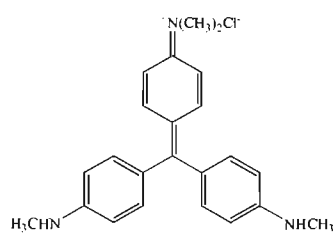
Figure 4.3 ATR FT-IR spectra of (A) wet ink, (B) dry ink obtained from holding the sample for an hour, (C) wet ink spectrum subtracted by dry ink one, (D) 2-phenoxyethanol from library, (E) dry ink spectrum subtracted by wet ink one, and (F) crystal violet from library.



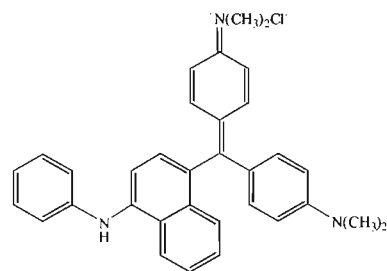
A: Crystal Violet



B: Methyl Violet



C: Tetramethyl Para Rosaniline



D: Victoria Blue

Figure 4.4 Chemical structures of some triarymethane dyes: (A) crystal violet, (B) methyl violet, (C) tetramethyl para-rosaniline, and (D) victoria blue [16].

#### 4.1.2 Spectral comparison of the same model ballpoint pen ink

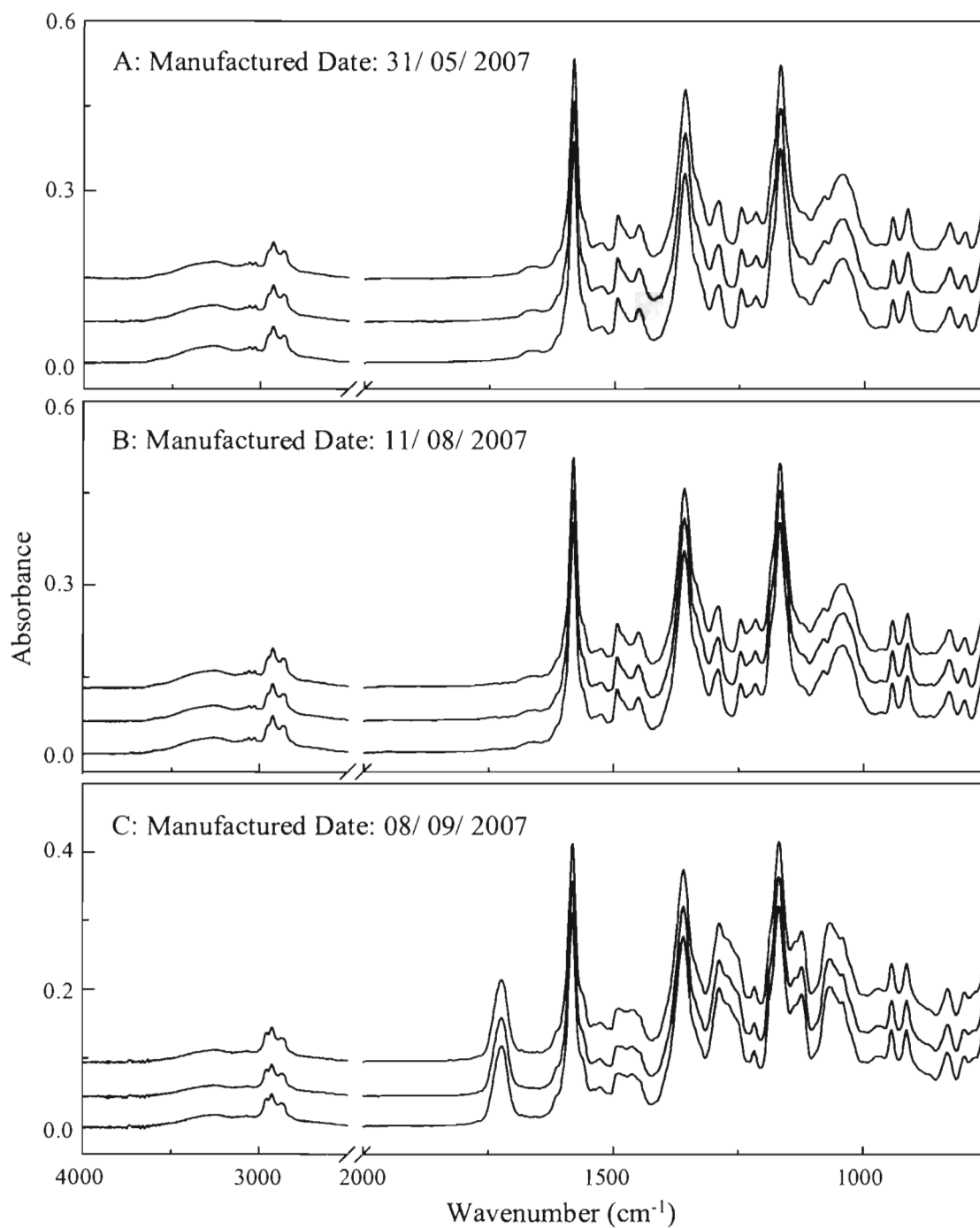


Figure 4.5 ATR FT-IR spectra of FABER-CASTEL (Grip Ball 1424) blue ink at various manufactured date: (A) 31/ 05/ 2007, (B) 11/ 08/ 2007, and (C) 08/ 09/ 2007.

All spectra of FABER-CASTELL (Grip Ball 1424) blue ballpoint pen inks produced at various manufacturing date are shown in Figure 4.5. It can be seen obviously that each ink from the same pen gives the same spectral pattern. For example, all spectra in Figure 4.6 (A) having all peak positions and intensities that can be superimposed perfectly. This means that ink in the same pen tube have the same compositions and is well-blended. From the observed spectra, the strong absorption band at  $1581\text{ cm}^{-1}$  belongs to the characteristic of skeletal vibration of triarymethane dye. In addition, the peaks at  $1359$  and  $1168\text{ cm}^{-1}$  can be assigned to the C-H deformation and C-N stretching vibration of triarylmethane dyes, respectively [29]. Moreover, some differences in spectral pattern can imply that ink from different pens with the same ink spectral pattern cannot confirm whether those ink traces came from the same pen.

According to the discussion above, all spectra in Figure 4.5 (A) and (B) show the same spectral pattern. Therefore, the inks from both pens have similarity in chemical compositions. On the contrary, the observed spectra in Figure 4.5 (C) differ from both spectra in Figure 4.5 (A) and (B). The comparison of both spectra in Figure 4.5 (B) and (C) are shown in Figure 4.6. Such spectra in Figure 4.6 demonstrate the different chemical information of ink clearly. For example, the absorption band at  $1723\text{ cm}^{-1}$  assigned to carbonyl absorption, the absorption band at  $1285$ ,  $1283$ , and  $1128\text{ cm}^{-1}$  are not present in Figure 4.7 (b). This indicates that the main composition of this ink is alkyd resin but the absorption band of triarylmethane dyes are also conspicuous [29].

This might be an implication of the changing ingredients of a formulation due to cost savings, market factors, and consumer demand. Thanks to the ink information relating to formulation changes, a database of inks can be used to discriminate and identify the ink entries forensically [44].

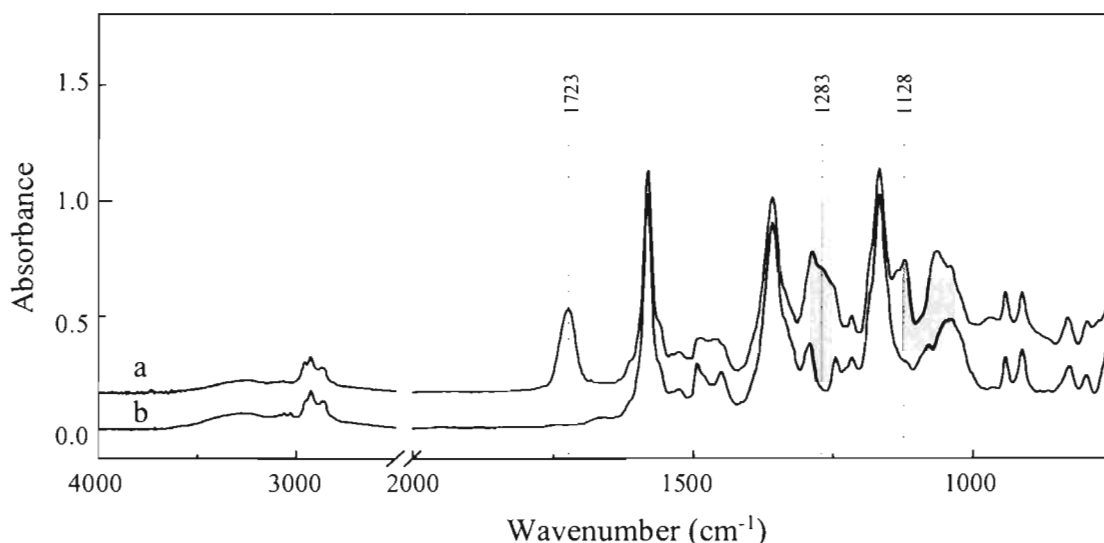


Figure 4.6 ATR FT-IR spectra of FABER-CASTEL (Grip Ball) blue ink at various manufactured date: (a) 08/ 09/ 2007 and (b) 31/ 05/ 2007.

#### 4.1.2 Spectral comparison of different brands of ballpoint pen inks

Two ballpoint pens with the same shade might be consisted of different chemical ingredients and compositions. ATR FT-IR spectra of both black and blue ballpoint pen inks with different brands are shown in Figure 4.7. Almost absorption bands of the ink spectra have corresponded to the dyes or pigments that manufacturer used. Although such spectra have the main absorption bands originated from the similar structure of dye, triarylmethane dye group, the kind of other components can be often identified as well. For example, the absorption bands in 1511-1422 cm<sup>-1</sup> and 1109-982 cm<sup>-1</sup> regions belonging to the C-H deformation vibrations that are assigned to non-colorant components are different in peak shape. Moreover, in fingerprint or low wavenumber region, there are complicated details that cause the non-superimposed spectra and show different components. This means that the inks from different brands consist of different compositions, such as binding components, and additives that can be distinguished from the observed spectra.

For additional information, both Pentel<sup>®</sup> and Pilot<sup>®</sup> manufacturer have their own ink or a company which produced ink specific to their company, some companies use common inks. For example, the Steadler<sup>®</sup> brand name imports ink

from other oversea companies [9]. They just change the barrel and assign different brand names.

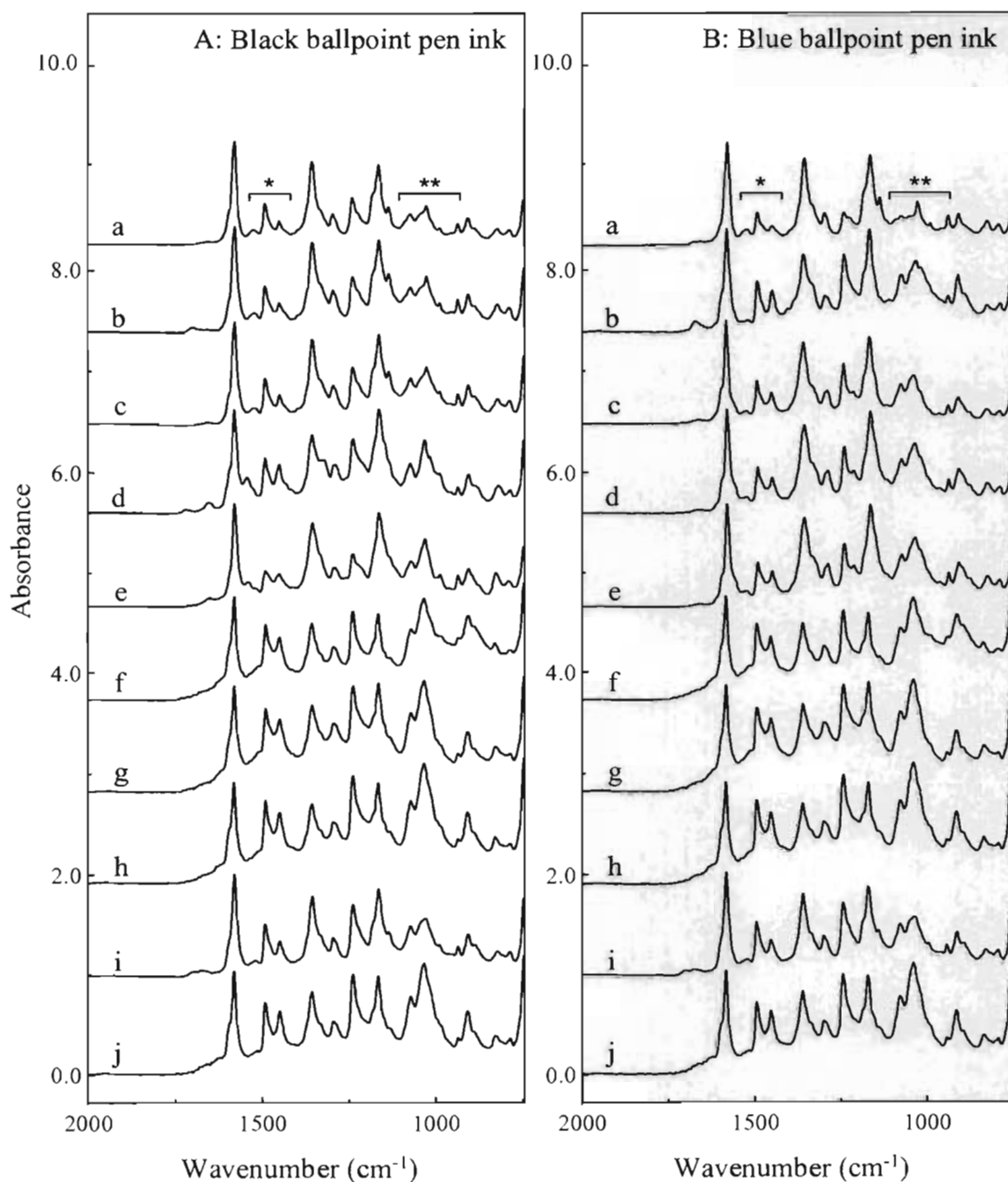


Figure 4.7 ATR FT-IR spectra of (A) black and (B) blue ballpoint pen inks: (a) Faber-Castel<sup>®</sup> (Grip Ball 1424), (b) Quantum<sup>®</sup> (GeloBal 007), (c) Lancer<sup>®</sup> (Spiral 0.5 825), (d) Standard<sup>®</sup> (g' soft), (e) Staedler<sup>®</sup> (Noris stick 434 F), (f) Horse<sup>®</sup> (Ball Pen H-402), (g) Reynolds<sup>®</sup> (Fine Carbure), (h) Pilot<sup>®</sup> (Super Grip), (i) Pentel<sup>®</sup> (Star V), and (j) The One<sup>®</sup> (GPB-3001).



#### 4.1.3 Spectral comparison of various models of the same brand ballpoint pen inks

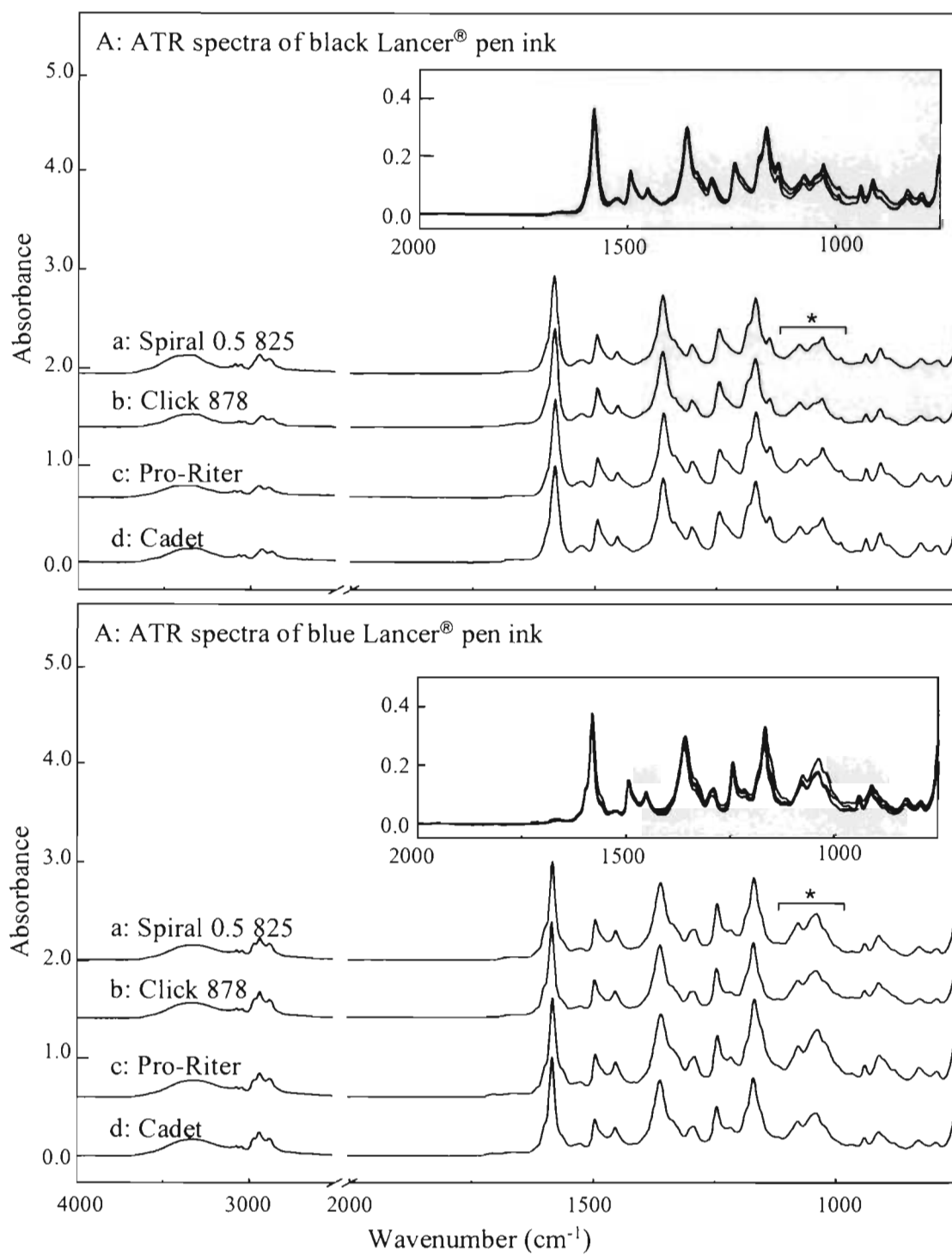


Figure 4.8 ATR FT-IR spectra of (A) black and (B) blue Faber-Castel® brand ballpoint pens ink.

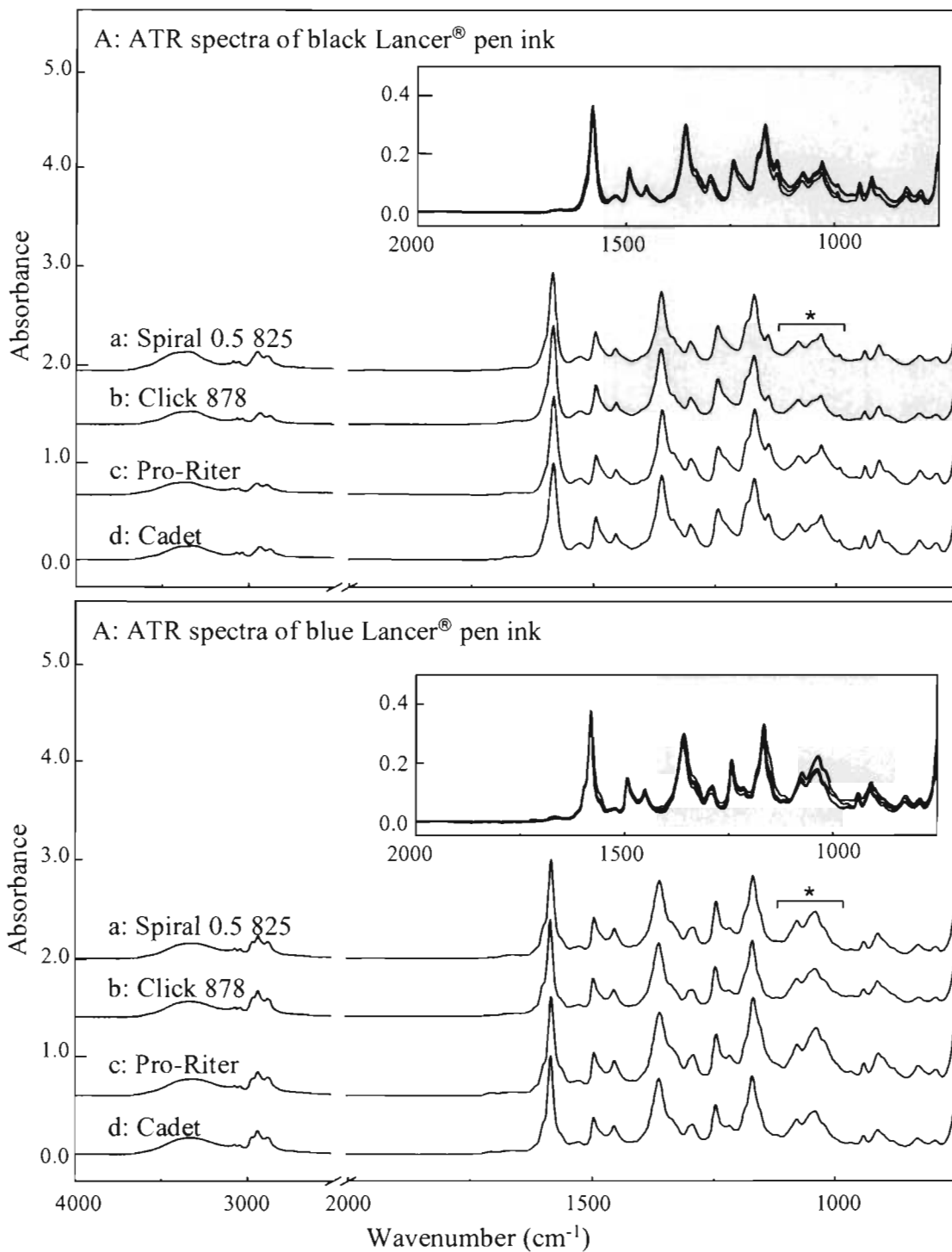


Figure 4.9 ATR FT-IR spectra of (A) black and (B) blue Lancer® brand ballpoint pens ink.

ATR FT-IR spectra of various models of black and blue Faber-Castel® brand ballpoint pen inks are shown in Figure 4.8. The observed spectra of black ink shown in Figure 4.8 (A) indicate the difference of spectral pattern, for example, the adsorption bands in 1120-980  $\text{cm}^{-1}$  region are assigned to C-OH stretching vibration. The alcohol C-O group is present in many classes, e.g. primary, secondary, and tertiary alcohols which absorb at different frequency in 1200-1000  $\text{cm}^{-1}$  region [46]. The frequency of C-O stretching vibration is dependent on various factors such as structural environment of the C-O group. Therefore, the ATR spectra show the different spectral feature of the C-O group that point out the different chemical compositions or ink formulas. Because of the variation in consumer demand and manufacturing cost constrain, the manufacturer has to design the properties and the appearance of ink for compatibility to such demanding. Both the marketing factors and the cost of product affect manufacturer towards selection of the basic material of ink.

Similarly, the blue ink spectra of Faber-Castel® brand shown in Figure 4.8 (B) display difference spectral pattern indicating the distinct components in each sample. Prior to the previous discussion, it is caused by the business aspects.

Spectra of Lancer® brand ballpoint pen inks are shown in Figure 4.9. ATR FT-IR spectra of black ink are shown in Figure 4.9 (A) display the spectral pattern to be exactly alike. All of the black ink spectra demonstrate unique characteristic as if such ink came from the identical source. In the same way, spectra of blue ink shown in Figure 4.9 (B), also illustrate the same spectral pattern. As this brand is locally made and retailed price is almost the same, the manufacturer may use the same ink to produce the various pen models in order to gain marketing benefit. They only change the ink barrel and/or brand name.

As a result, an ATR FT-IR spectroscopy technique can be utilized for a non-destructive spectral acquisition of ballpoint pen ink. Due to the non-destructive nature, short measurement time, simplicity, and spectral information directly related to chemical structures and composition, this technique can be employed for forensic analysis of pen ink.

## 4.2 Characterization of Paper

### 4.2.1 Spectral assignments of paper

The basic materials used in the production of papers are cellulose fibers mixed with inorganic extenders and organic binders [51-52]. ATR FT-IR spectra of the same paper measured at different positions are shown in Figure 4.10. The observed spectra show main molecular information that consists of cellulose fibers and calcium carbonates used as white pigment. The strong absorbance peaks in the range of 1200-850  $\text{cm}^{-1}$  belong to cellulose. The peak assignments of cellulose fiber are shown in Table 4.2. The spectrum of calcium carbonate is shown in Figure 4.10 (b). It is apparent that the sharp peak in low wavenumber region belongs to calcium carbonate. Peak assignments are shown in Table 4.3. The spectra of cellulose without calcium carbonate interference, shown in Figure 4.10 (a), do not show a sharp peak in low wavenumber region. At different positions of paper surface, mostly observed spectra show the characteristics of cellulose contained with calcium carbonate. Few spectra show only those of cellulose. Because of a very small contact area of the homemade Ge  $\mu\text{IRE}$  ( $50 \times 50 \mu\text{m}^2$ ), the sampling points may observe only cellulose fibers or together with some calcium carbonate.

The SEM image of the paper surface is shown in Figure 4.11. From the SEM image, it is obviously known that white particles deposited on the cellulose fibers are calcium carbonate. Some spectra from Figure 4.10 demonstrate only the characteristic of cellulose. This means the measured area do not have calcium carbonate. On the other hand, some spectra indicate the variation of different cellulose to calcium carbonate ratios in each position of paper.

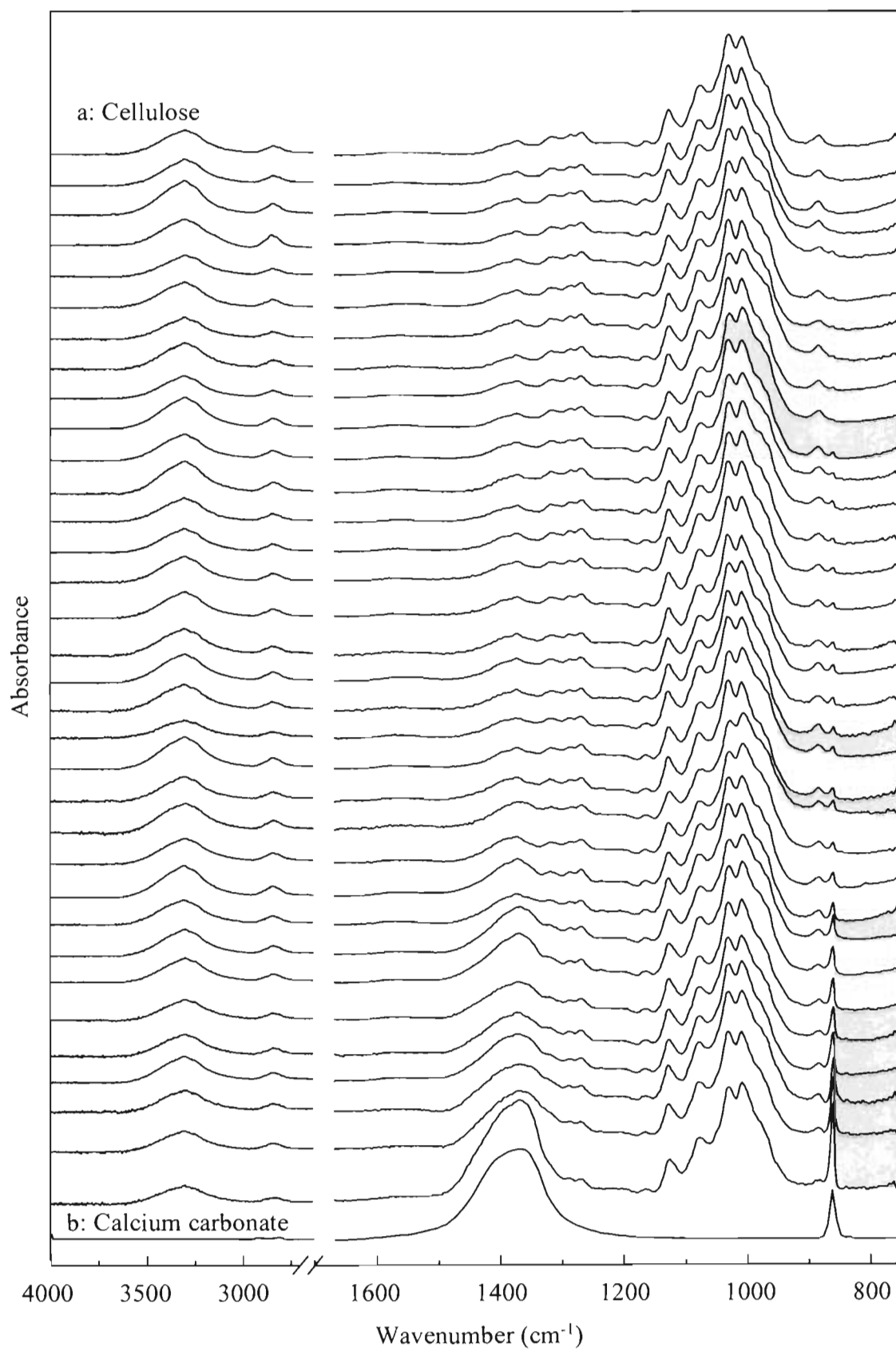


Figure 4.10 ATR FT-IR spectra of different points of the same paper sheet.

**Table 4.2** Peak assignments of cellulose fiber.

Wavenumber (cm <sup>-1</sup> )	Peak Assignments
3450-3160	O-H stretching vibration
2975-2840	C-H stretching vibration
1475-1460	C-H deformation vibration
1430-1370	In-plane O-H deformation vibration
1310-1000	Asymmetric C-O-C <b>stretching</b> vibration
1100	Symmetric C-O-C stretching vibration of cyclic ethers
1055-870	Conjugated -C=C- stretching vibration
1025	Symmetric C-O-C stretching vibration
815	Asymmetric C-O-C stretching vibration of cyclic ethers

**Table 4.3** Peak assignments of calcium carbonate.

Wavenumber (cm <sup>-1</sup> )	Peak Assignments
1650-1540	Asymmetric – CO <sub>2</sub> stretching vibration
1450-1360	Symmetric – CO <sub>2</sub> stretching vibration
890-800	Out-of-plane deformation of CO <sub>3</sub> <sup>2-</sup> ion

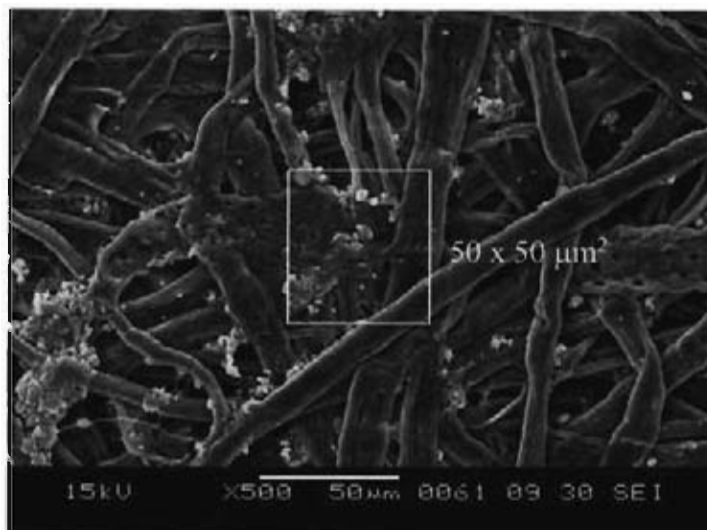


Figure 4.11 SEM image of the paper surface.

Since ATR FT-IR technique is a surface characterization technique, the contact between the sample and IRE had an influence on the chemical information of the observed spectra. ATR FT-IR spectra of paper measured at the same point with different degree of contact with the IRE are shown in Figure 4.12. The sample stage is gradually raised to increase the extent of contact. The spectra in Figure 4.12 indicate that the intensities are increased systematically when the contact between paper and the Ge  $\mu$ IRE are increased. Therefore, in each experiment, the perfect spectra are acquired from appropriate contact between the sample and IRE by observing that the spectral intensities have constant when the extent of contact is optimized.

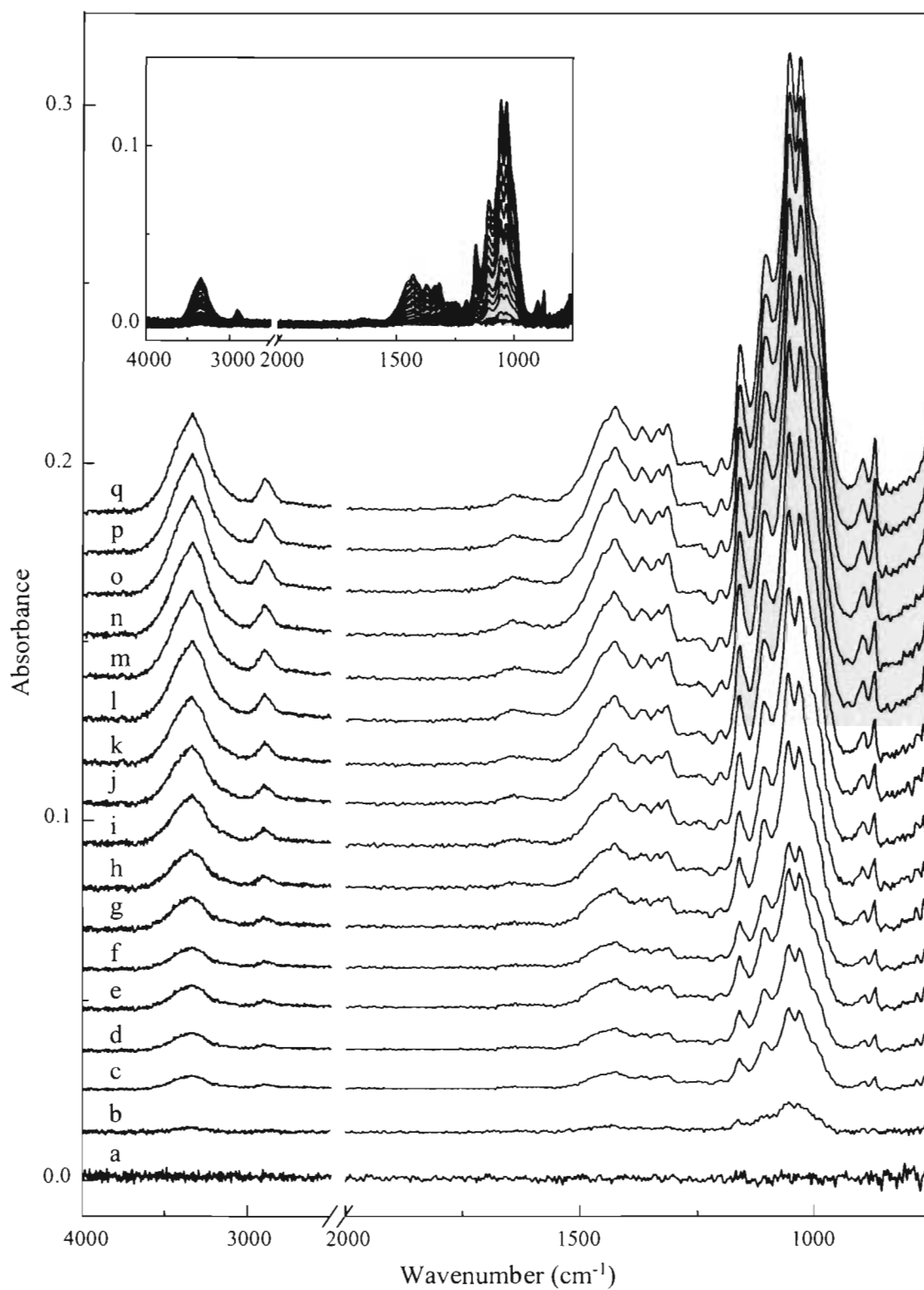


Figure 4.12 ATR FT-IR spectra of paper at the same point with different degree of contact with the slide-on homemade Germanium  $\mu$ IRE.



#### 4.2.2 Spectral comparison of different paper brands and weights

ATR FT-IR spectra of different paper brands that measured point by point at step size of 100  $\mu\text{m}$  are shown in Figure 4.13. According to the prior discussion, the spectra show the characteristics of main paper compositions that have variation of cellulose fibers to calcium carbonate ratios. As the spectra in each brand have the same spectral pattern, we cannot point out exactly about the source of the different paper. Because of such spectra, the different paper sheets have the same chemical compositions. Since the surface characterization of ATR FT-IR technique analyzed on the sample surface gives the chemical information of samples only at short distance from sample surface. Not only the ATR FT-IR technique cannot analyze the finished paper products, but also the other modes of FT-IR techniques cannot analyze them because the finished papers have the same ingredients [51].

The comparison of different weight (grams per square meter, gsm) of the same paper brand as shown in Figure 4.13 (E) and (F), indicate the same spectral pattern. By definition, one square meter is one A0 size sheet or 16 A4 size sheets. Thus, the different of gsm may be caused the different thickness of paper but have no influence on the compositions.

However, the information from paper spectra acquired by ATR FT-IR technique are serving purposes of the study of one or more inks deposited on the paper surface which are applied to the questioned document examination.

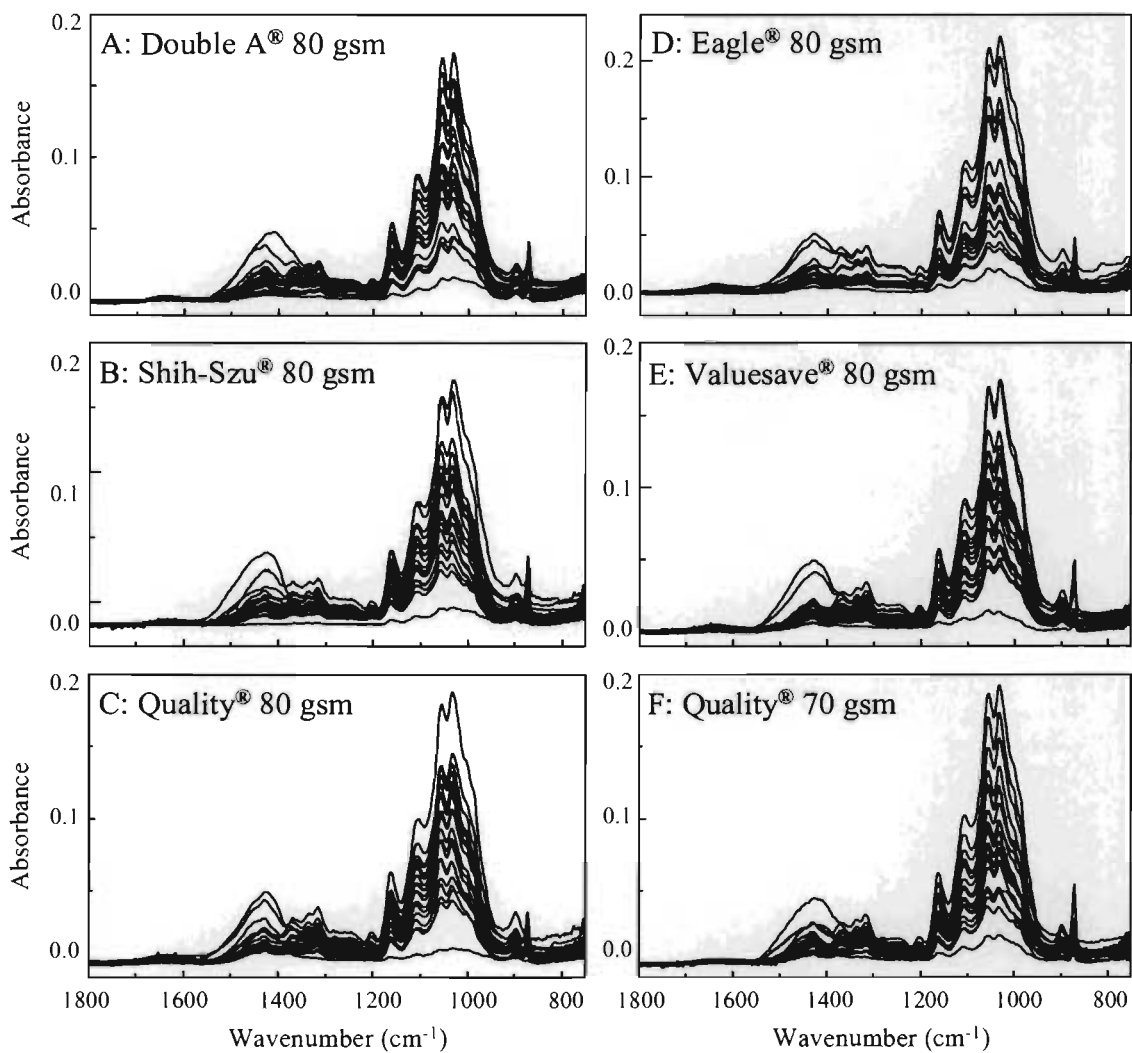


Figure 4.13 ATR FT-IR spectra of different paper brands and gsms: (A) Double A<sup>®</sup> (80 gsm), (B) Shih-Szu<sup>®</sup> (80 gsm), (C) Quality (80 gsm), (D) Eagle<sup>®</sup> (80 gsm), (E) Valuesave<sup>®</sup> (80 gsm), and (F) Quality<sup>®</sup> (70 gsm).

### 4.3 Characterization of ink written on paper

#### 4.3.1 Depth dependent of ink written on paper

Chemical information of ink written on paper is investigated by ATR FT-IR spectroscopy. Since the contact between sample and Ge  $\mu$ IRE has an influence on the peak intensities of the observed spectra, the ink written on paper at the same point are analyzed with various extents of contact with the IRE as shown in Figure 4.14. The peak intensities of those spectra are increased when the contact between paper and the Ge  $\mu$ IRE are systematically increased. Since the IRE does not contact with the sample at initiation, the observed spectrum does not show any absorption band. As the IRE contacts with the sample, the observed spectra show the characteristic absorption band with similar to cellulose. In general, if ink is written on paper, ink is coated on the cellulose fibers so that the first spectrum of ink written on paper that contact with Ge  $\mu$ IRE demonstrates the ink characteristic. This can imply that the ink is not coated on the cellulose fiber surface. Since cellulose is consisted of porous fiber, the ink can seep into such pores until the solvent diffuse and migrate away to reach equilibrium-like condition. For another reason, weight of ink in one stroke line is in ng/cm range [48]. The amount of ink is very minute comparable to the paper. The spectrum shows an outstanding characteristic of cellulose instead of ink itself.

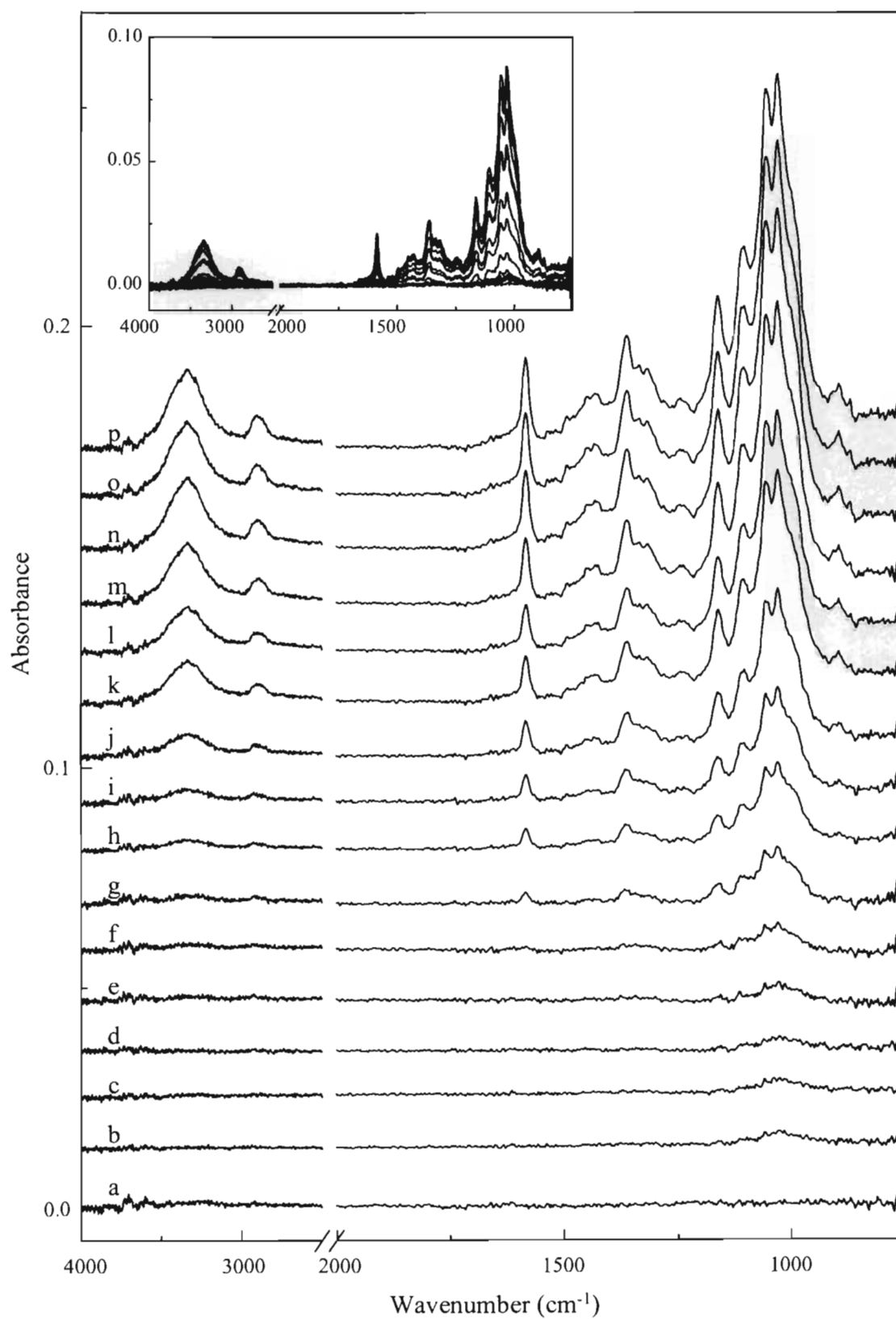


Figure 4.14 ATR FT-IR spectra of black Lancer<sup>®</sup> (Click 878) ink written on paper at the same point with various extent of contact with the homemade slide-on Ge  $\mu$ IRE.

### 4.3.2 Spectral assignment of ink written on paper

Since the ATR spectra of paper surface depending on the domination between cellulose fiber and calcium carbonate, it has the influence on the ATR spectra of ink written on paper at various points on the same continuous line as shown in Figure 4.15. Since the contact between the  $\mu$ IRE and sample in each point has variation, the spectra are normalized with the peak at  $1034\text{ cm}^{-1}$  corresponding to absorption band of cellulose. This could be beneficial for an easier comparison with other peak intensities corresponding to the quantity interpretation. The observed spectra show the absorption band of paper in range of  $1200\text{-}750\text{ cm}^{-1}$  and another bands are assigned to ink deposited on paper. The detail of absorption bands are shown in Table 4.4. One of all spectra in Figure 4.15 shows calcium carbonate-dominated with high intensity absorption band at  $875\text{ cm}^{-1}$  and the characteristic of ink is obscured. Therefore, the suitable ink written on paper spectra can be less of calcium carbonate interference. If the spectrum which high carbonate-dominated is ignored, all ATR spectra of ink from the same pen written on paper as shown in inset of Figure 4.15 demonstrate the same spectral pattern, peak shape and intensities especially in  $1600\text{-}1200\text{ cm}^{-1}$  relating to the unique characteristic of ink without interference of paper substrate.

From Figure 4.15, the spectra can be divided into two regions,  $3500\text{-}2845\text{ cm}^{-1}$  and  $1600\text{-}750\text{ cm}^{-1}$ . The later region is called fingerprint region. The absorption bands in  $3500\text{-}2845\text{ cm}^{-1}$  are assigned to O-H and C-H stretching vibration. The detailed peak assignments are shown in Table 4.1. It is very difficult to use such a region in order to separate the chemical information between ink and paper because the chemical information of both ink and paper show their characteristics in this region. On the other hand, the information of ink and paper can be distinguished in the fingerprint region.

**Table 4.4** Peak assignments of ink written on paper.

Wavenumber ( $\text{cm}^{-1}$ )	Peak Assignments	Characteristic	
		Ink	paper
3450-3160	O-H stretching vibration	√	√
2975-2840	C-H stretching vibration	√	√
1600-1580	Conjugated $\text{-C=C-}$ stretching vibration	√	
1470-1440	Asymmetric C-H deformation vibration	√	
1380-1350	Symmetric C-H deformation vibration	√	
1280-1220	Symmetric C-O stretching vibration	√	
1250-1150	Asymmetric C-O stretching vibration	√	√
1100	Symmetric C-O-C stretching vibration of cyclic ethers		√
1025	Symmetric C-O-C stretching vibration		√
890-800	Out-of-plane deformation of $\text{CO}_3^{2-}$ ion		√

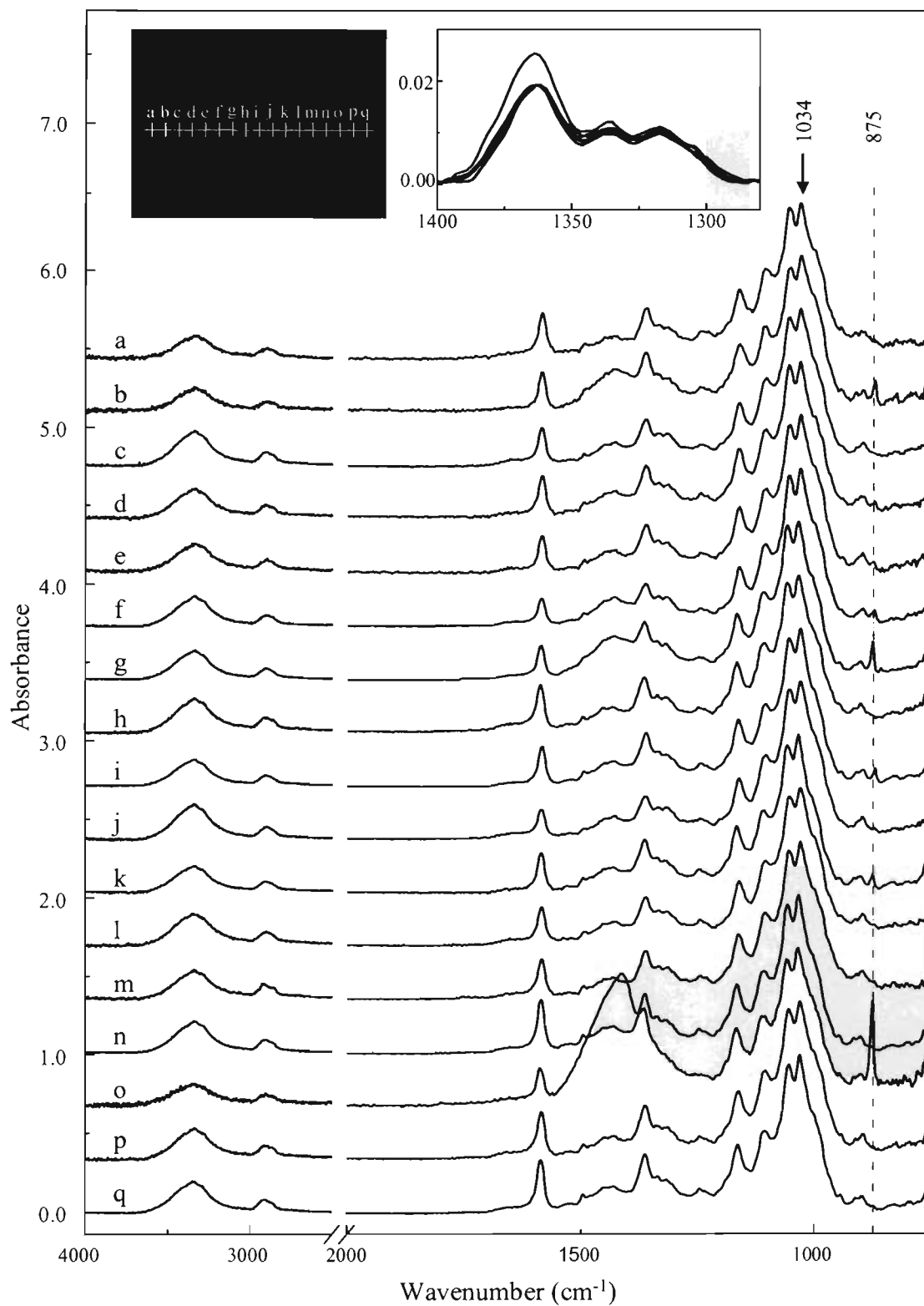


Figure 4.15 ATR FT-IR spectra of different points of Faber-Castel® (Grip Ball 1424) black ink of the same continuous line on paper. The interval of the sampling point is 50  $\mu\text{m}$  apart.

As shown in Figure 4.16, all spectra in Figure 4.15 can be divided into four groups by calcium carbonate interference. It is easy to see the sharp peak at  $875\text{ cm}^{-1}$  and broad peak in  $1550\text{-}1300\text{ cm}^{-1}$  region belonging to the calcium carbonate characteristic. The Figure 4.16 (A) shows spectral pattern combined with ink and paper characteristics without the contamination of calcium carbonate without the sharp peak in  $875\text{ cm}^{-1}$ . The observed spectra of ink on paper show the strong characteristic band of cellulose in  $1200\text{-}750\text{ cm}^{-1}$  region and ink trace characteristic in  $1500\text{-}1200\text{ cm}^{-1}$ . In Figure 4.16 (B), the paper spectrum shows that there is little interference of calcium carbonate but it does not effect on the interpretation of the spectrum of ink on paper. Both of spectra still show the clear character of ink written on paper with the peaks at  $1581$ ,  $1358$ , and  $1168\text{ cm}^{-1}$  assigned to the triarylmethane dye. From the spectra in Figure 4.16 (C), the paper spectrum shows more calcium carbonate characteristic with more interference to ink on paper in  $1600\text{-}1200\text{ cm}^{-1}$ . Finally, the spectra in Figure 4.16 (D), show high calcium carbonate interference with the loss information of ink trace written on paper. Therefore, the suitable ink on paper spectra could be less of calcium carbonate interference.

From Figure 4.15, the spectra in  $1600\text{-}1200\text{ cm}^{-1}$  region with less contamination of calcium carbonate characteristic are compared. According to the results of Section 4.1.2, the inks from the same pen have the same chemical compositions which are showed the same spectral pattern. Likewise, the spectra of ink from the same pen written on paper also show the same spectral pattern, peak shape and intensities, in such region. That can imply that such ink written on paper has the same chemical composition and are investigated by ATR FT-IR spectra.



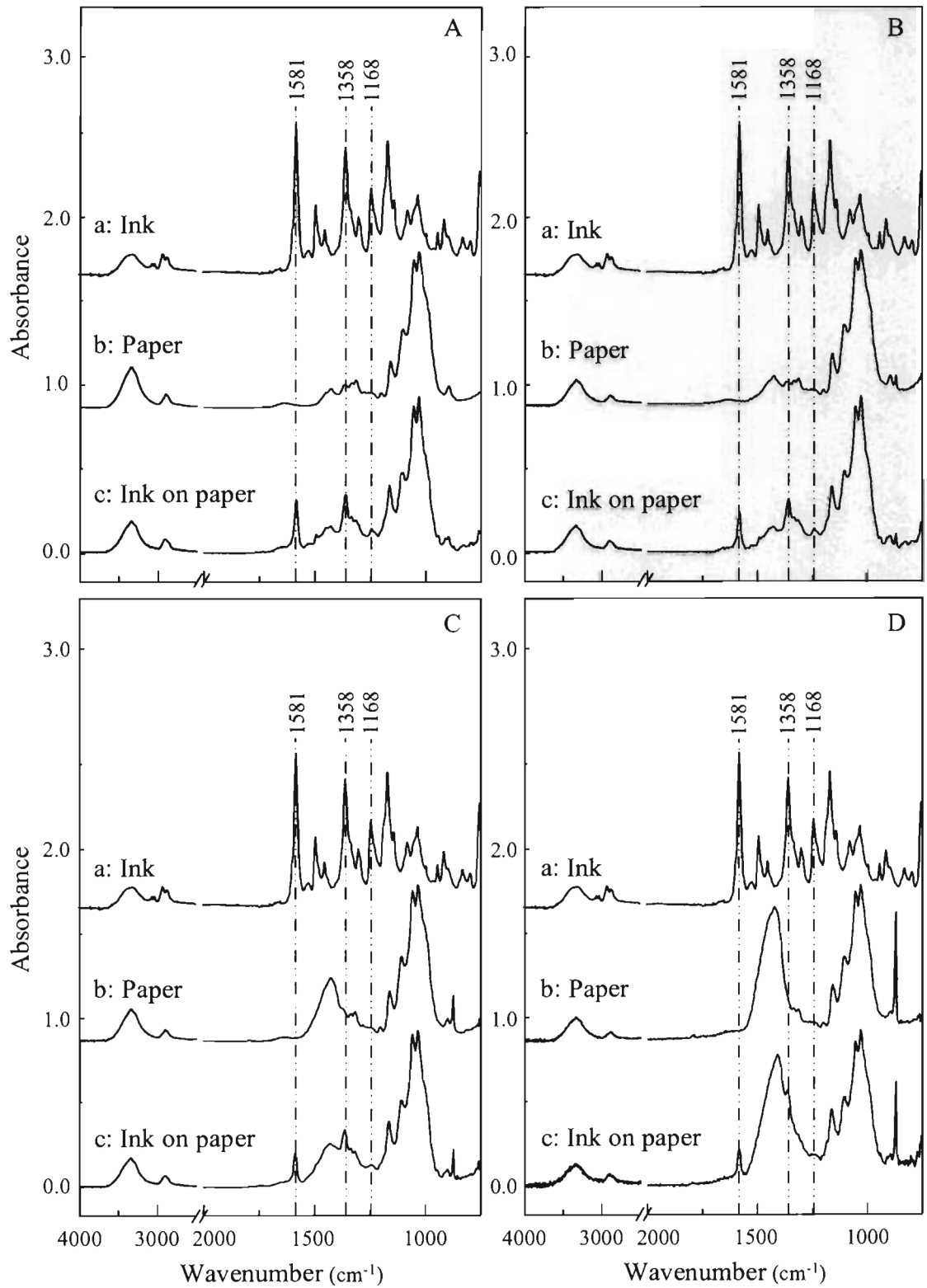


Figure 4.16 The ATR FT-IR spectra taken from Figure 4.16 classified by the highest peak intensity of calcium carbonate character (at 1498  $\text{cm}^{-1}$ ) can be divided into 4 groups (A, B, C, and D in order of increasing peak intensity).

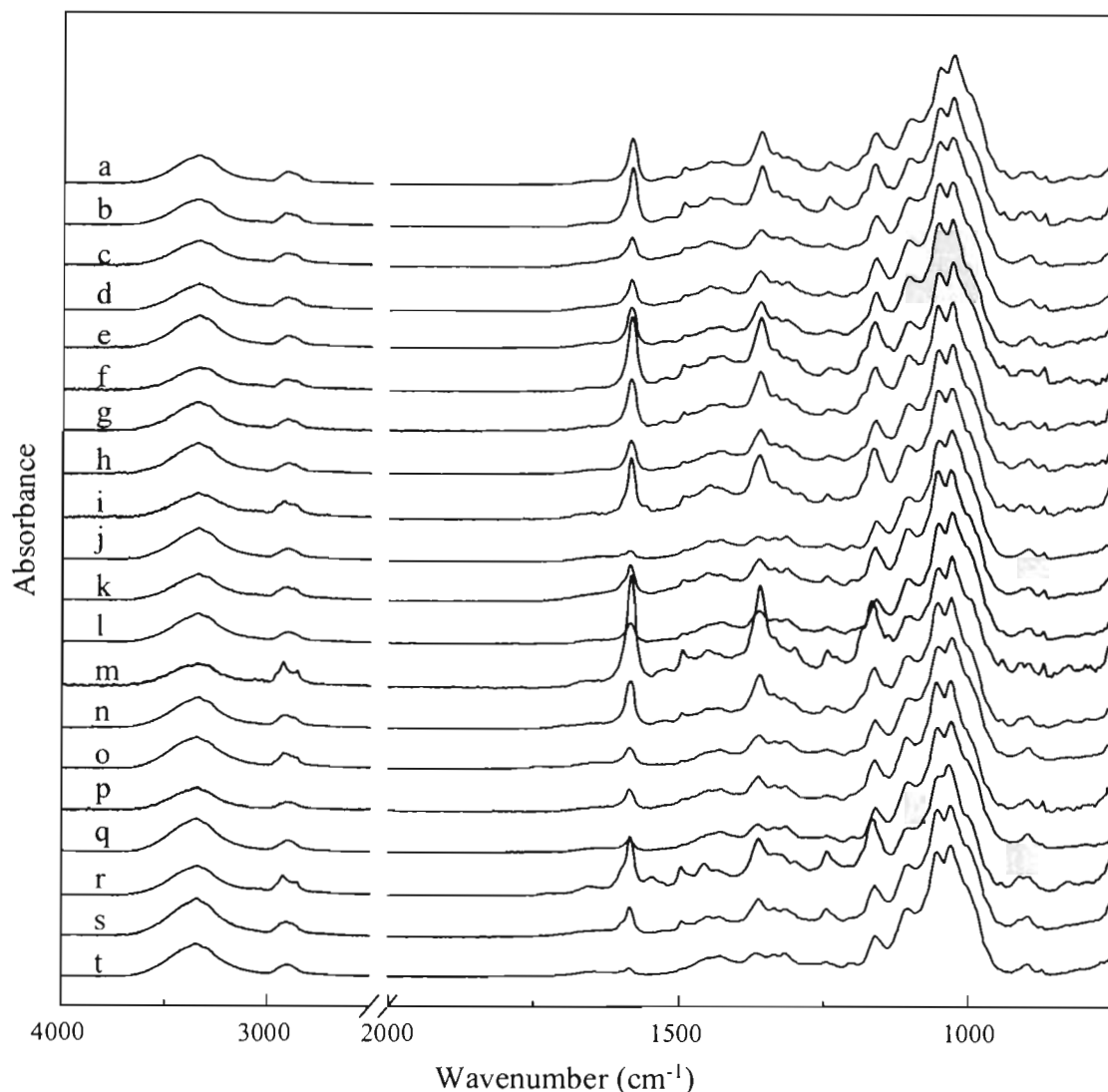


Figure 4.17 ATR FT-IR spectra of 20 commercial black ballpoint pen inks written on paper: (a) Faber-Castel<sup>®</sup> (Grip Ball 1424), (b) Faber-Castel<sup>®</sup> (Click Ball 1422), (c) Faber-Castel<sup>®</sup> (Super Tech Point 1420), (d) Faber-Castel<sup>®</sup> (Ball Pen 1423), (e) Lancer<sup>®</sup> (Spiral 825), (f) Lancer<sup>®</sup> (Click 878), (g) Lancer<sup>®</sup> (Pro-Riter), (h) Lancer<sup>®</sup> (Cadet), (i) Horse<sup>®</sup> (Ball Pen H-402), (j) Reynolds<sup>®</sup> (Fine Carbure), (k) Reynolds<sup>®</sup> (800), (l) Standard<sup>®</sup> (g'Soft), (m) Standard<sup>®</sup> (Fizz Hi Grip), (n) Stabilo<sup>®</sup> (Marathon 318), (o) Stabilo<sup>®</sup> (F), (p) Quantum<sup>®</sup> (GeloBal 007), (q) Quantum<sup>®</sup> (GeloBal QCGB 1230), (r) Pilot<sup>®</sup> (Super Grip), (s) Pentel<sup>®</sup> (Star V), and (t) Staedler<sup>®</sup> (Noris Stick 434 F).

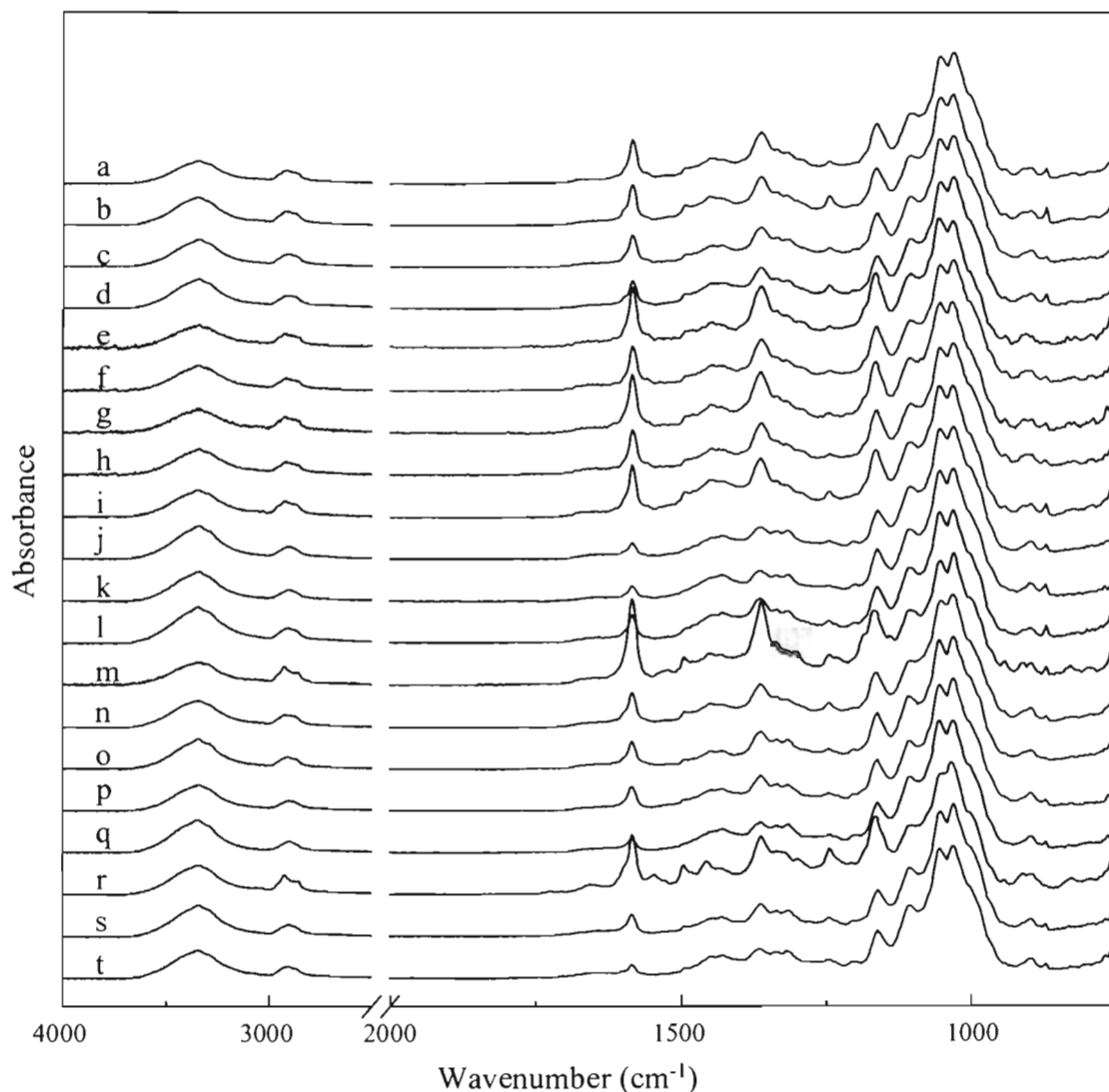


Figure 4.18 ATR FT-IR spectra of 20 commercial black ballpoint pen inks written on paper: (a) Faber-Castel® (Grip Ball 1424), (b) Faber-Castel® (Click Ball 1422), (c) Faber-Castel® (Super Tech Point 1420), (d) Faber-Castel® (Ball Pen 1423), (e) Lancer® (Spiral 825), (f) Lancer® (Click 878), (g) Lancer® (Pro-Riter), (h) Lancer® (Cadet), (i) Horse® (Ball Pen H-402), (j) Reynolds® (Fine Carbure), (k) Reynolds® (800), (l) Standard® (g'Soft), (m) Standard® (Fizz Hi Grip), (n) Stabilo® (Marathon 318), (o) Stabilo® (F), (p) Quantum® (GeloBal 007), (q) Quantum® (GeloBal QCGB 1230), (r) Pilot® (Super Grip), (s) Pentel® (Star V), and (t) Staedler® (Noris Stick 434 F).

ATR FT-IR spectra of some black and blue ballpoint pen inks written on paper from various manufacturers are shown in Figure 4.17 and 4.18, respectively. The observed ATR spectra show the distinction of spectral pattern in  $1600\text{-}1200\text{ cm}^{-1}$  due to pure ink deposited on paper has different chemical composition as are reported in Section 4.1.2.

### **4.3.3 Spectral comparison of various brands of ballpoint pen inks on paper**

Due to the region between  $4000\text{-}2000\text{ cm}^{-1}$  contains few absorption bands attributable to ink and are excluded from data analysis, so that further analysis are concentrated on the  $2000\text{-}750\text{ cm}^{-1}$ . The ATR spectra of various brand inks deposited on paper are shown in Figure 4.19. For black ink spectra shown in Figure 4.19 (A), the spectral pattern of such ink are distinctly different so the absorption bands in  $1600\text{-}1200\text{ cm}^{-1}$  region can be often identified as well. Similarly, the blue ink spectra from various brands shown in Figure 4.19 (B) have distinctly different spectral pattern. According to the previous discussion, the distinction of spectral patterns displayed that there is the different chemical composition.

As a result, the spectral pattern of each ink deposited on paper, especially in  $1600\text{-}1200\text{ cm}^{-1}$  are different due to the difference of ink chemical components and the information can be distinguished by ATR spectra.

Comparison of black and blue ink spectra with the same both model and brand deposited on paper is observed. From the observed spectra, most of the black and blue ink spectra with the same model and brand reveal the same spectral pattern. According to the results in Section 4.1.4, the black and blue inks with same model have some difference of pigment structure but they have similarity of other components (such as binder, solvent, and additive) of which the spectra show the difference in details near  $1200\text{ cm}^{-1}$  and the lower wavenumber region. Due to the spectra of ink deposited on paper show the strong band absorption of cellulose in  $1200\text{-}750\text{ cm}^{-1}$  region, the complicated details of ink in such region are obscured. The ATR spectra of pure ink can be distinguished in  $1200\text{-}750\text{ cm}^{-1}$ . However, the ATR

spectra of ink deposited on paper do not show the difference of ink information due to intense cellulose characteristic in the region.

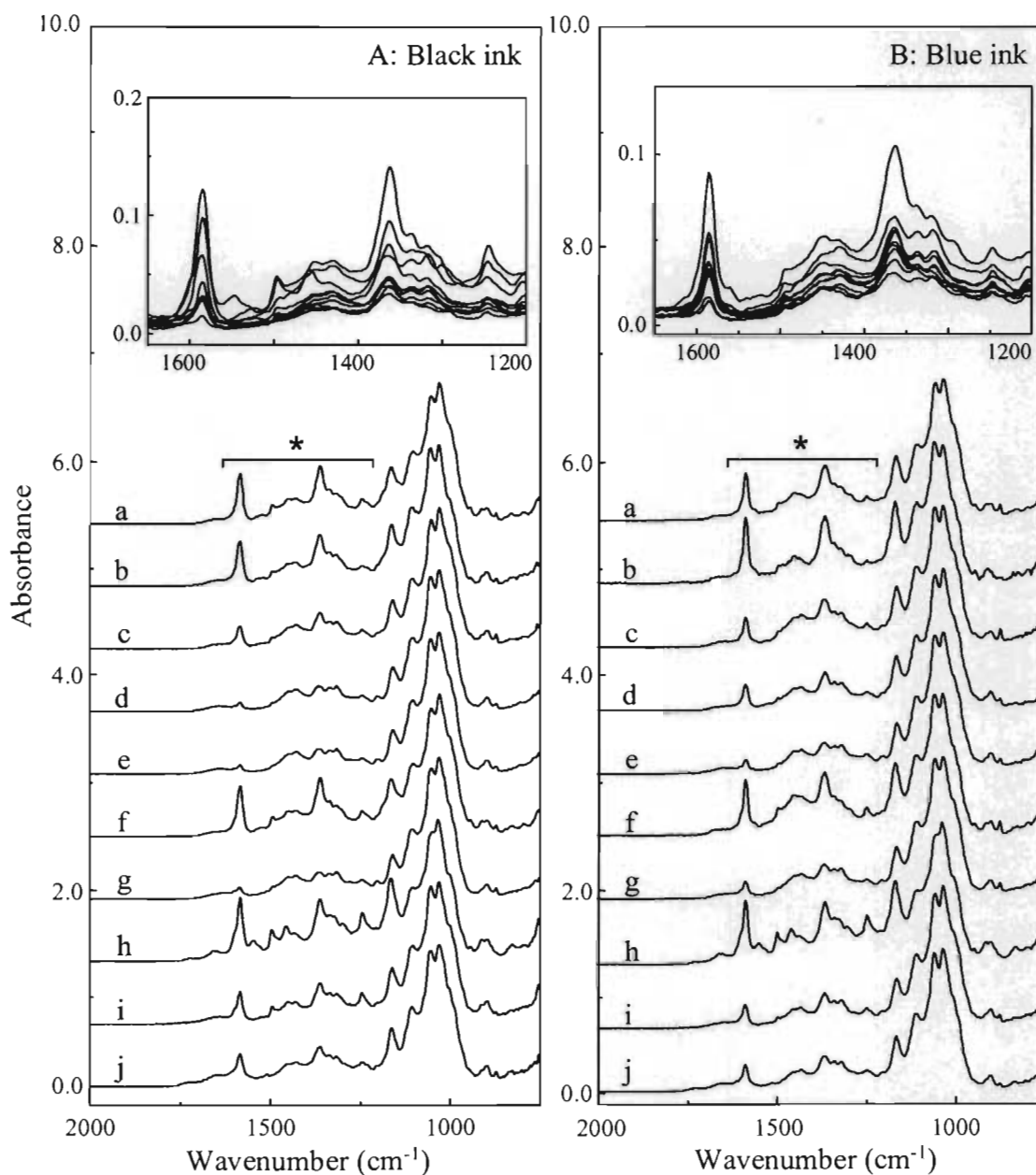


Figure 4.19 ATR FT-IR spectra of (A) black and (B) blue ballpoint pen inks: (a) Faber-Castel<sup>®</sup> (Grip Ball 1424), (b) Quantum<sup>®</sup> (GeloBal 007), (c) Lancer<sup>®</sup> (Spiral 0.5 825), (d) Standard<sup>®</sup> (g' soft), (e) Staedler<sup>®</sup> (Noris stick 434 F), (f) Horse<sup>®</sup> (Ball Pen H-402), (g) Reynolds<sup>®</sup> (Fine Carbure), (h) Pilot<sup>®</sup> (Super Grip), (i) Pentel<sup>®</sup> (Star V), and (j) The One<sup>®</sup> (GPB-3001).

#### 4.3.4 Spectral comparison of various models of the same brand ballpoint pen ink on paper

In Section 4.1.3, the ATR spectra of various models of Faber-Castel<sup>®</sup> and Lancer<sup>®</sup> inks are compared. They show the contrary results. In this section, the spectra of such brand ink written on paper are observed.

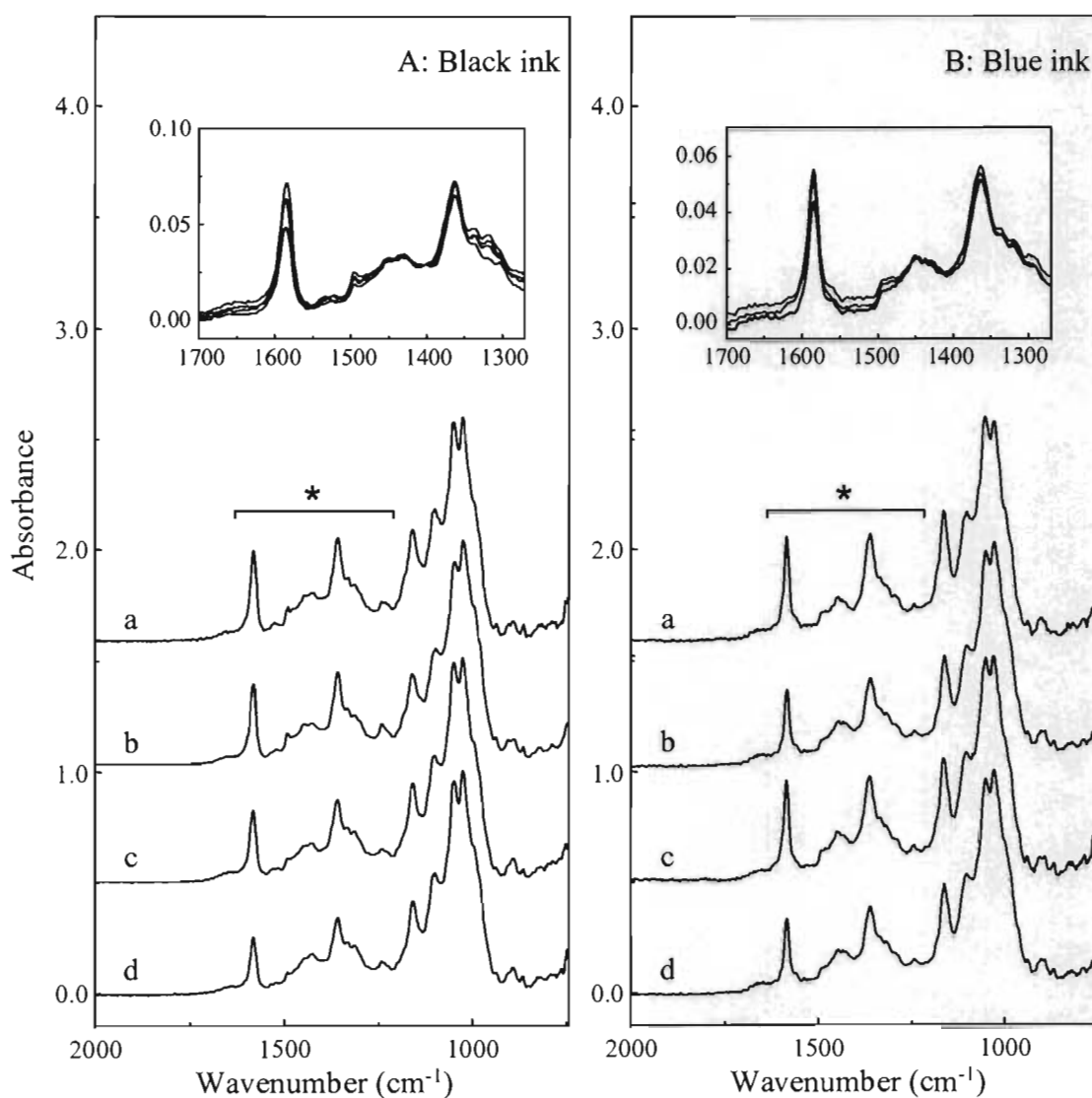


Figure 4.20 ATR FT-IR spectra of Faber-Castel<sup>®</sup> ballpoint pen inks: (A) black, (B) blue ballpoint pen ink on paper: (a) Faber-Castel<sup>®</sup> (Grip Ball 1424), (b) Faber-Castel<sup>®</sup> (Click Ball 1422), (c) Faber-Castel<sup>®</sup> (Super Tech Point 1420), and (d) Faber-Castel<sup>®</sup> (Ball Pen 1423).

The ATR spectra of black Faber-Castel® ink with various models are compared as showed in Figure 4.20 (A). They show the different spectral pattern, peak shapes and intensities in 1700-1250  $\text{cm}^{-1}$  region. It implies that they have the different chemical compositions in each model of pen ink. Likewise, the ATR spectra of blue ink as shown in Figure 4.20 (B) also show the different spectral pattern in such region.

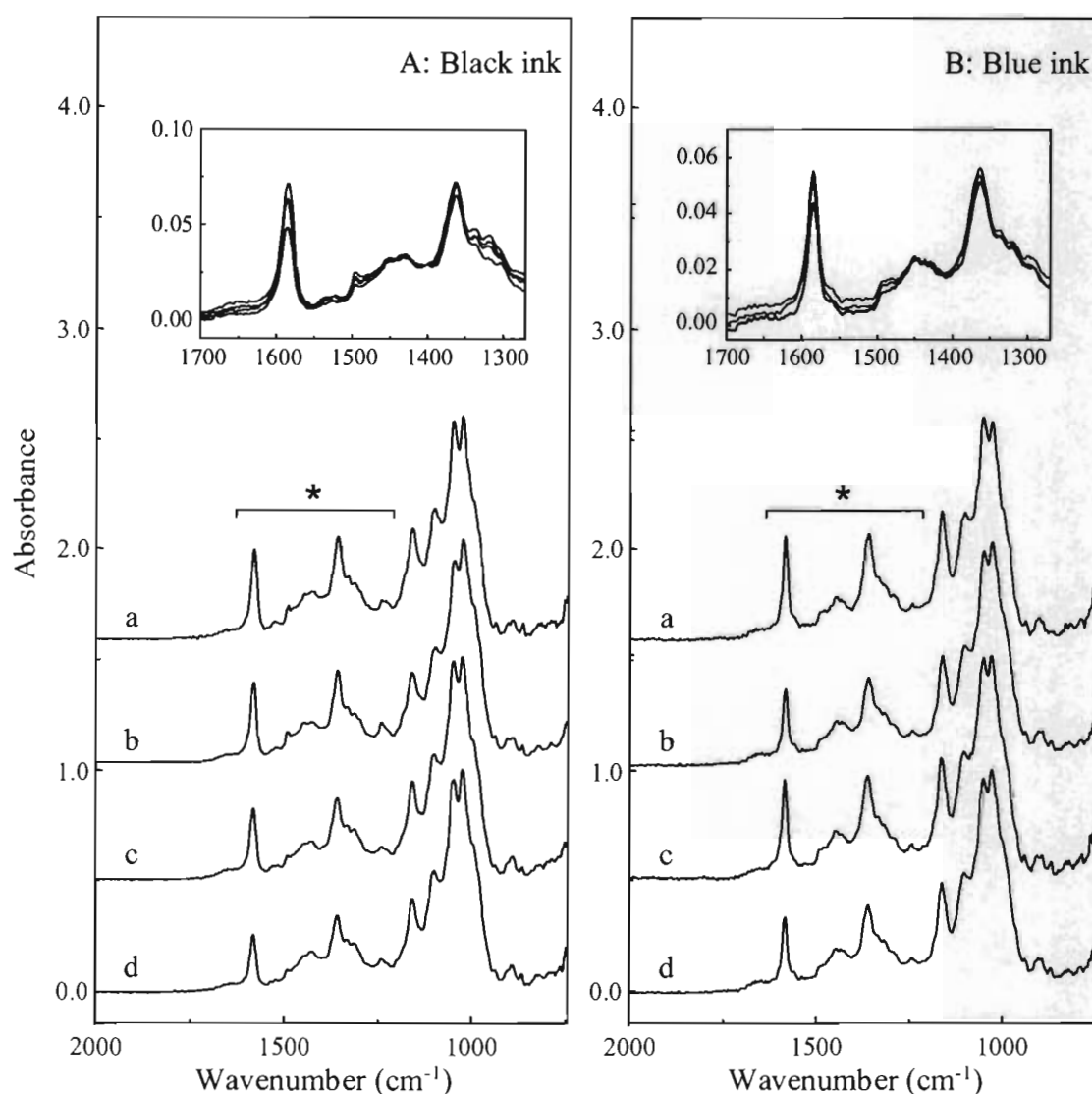


Figure 4.21 ATR FT-IR spectra of Lancer® ballpoint pen inks: (A) black, (B) blue ballpoint pen ink on paper: (a) Lancer® (Spiral 825), (b) Lancer® (Click 878), (c) Lancer® (Pro-Riter), and (d) Lancer® (Cadet).

According to the discussion in Section 4.1.3, the pure ink from various models of Faber-Castel<sup>®</sup> brand inks show the different chemical compositions observed from their spectra. Since the compositions of such pure ink are difference, the ink deposited on paper has also the different composition. Those make their spectra differ and can be distinguished by used their spectral pattern.

Black and blue Lancer<sup>®</sup> inks with the different models are compared as shown in Figure 4.21 (A) and (B), respectively. In the black ink, all spectra of different model pen inks show the same spectral pattern. They are also superimposed perfectly in 1700-1250  $\text{cm}^{-1}$  region. From the results in section 4.1.3 of black Lancer<sup>®</sup> pure ink with same model show the same spectral pattern, they also display the same spectral pattern of ink written on paper. Likewise, the blue ink spectra also show the same spectral pattern. These mean that they have the same chemical components deposited on cellulose fiber as discussed in Section 4.1.3.



#### 4.3.5 Spectral comparison of ageing of ink written on paper

Ageing of ink written on paper is studied since the ink composition can change with the time. All samples were kept in the same condition to avoid the factors of different storage condition that have influent on composition changing [15]. ATR spectra of various ballpoint pen inks written on paper which are collected every three days are shown in Figure 4.22. The observed spectra of each ink show the changing of composition that investigated by decreasing of the peaks intensity in range of 1400-1300  $\text{cm}^{-1}$  assigned to C-H deformation of triarymethane dye. ATR spectra of such ink written on paper kept for 21 days represent in Figure 4.23. The characteristic which makes the initial ink difference becomes the same as shown in the inset of Figure 4.23.

Although, there are various components in ink, inks after application on a paper appear colorant and trace of some additives. Such additives are negligent due to there are minute in ink compositions when compare to the dyes or colorants. In this sample, the dye used as colorant is crystal violet. The crystal violet can decompose into methyl violet which subsequently decomposes into tetramethyl para-rosaniline and further into other by loss of methyl groups [48]. The C-H deformation vibration of methyl group provide two bands, asymmetric (1465-1440  $\text{cm}^{-1}$ ) and symmetric (1390-1370  $\text{cm}^{-1}$ ), which may use to indicate the relative number of methyl group. It may be the crystal violet degrades over the time on paper following a demethylation mechanism [25].

Although the some absorption peaks of ink are obscured by paper characteristic, the region which show clearly ink character, 1600-1200  $\text{cm}^{-1}$ , can be identified. Ink written on paper with different brands and models has unique characteristic showing distinction of ATR spectra which related to their compositions. Furthermore, such ink is characterized with simple and nondestructive technique can apply the result to forensic document examination.

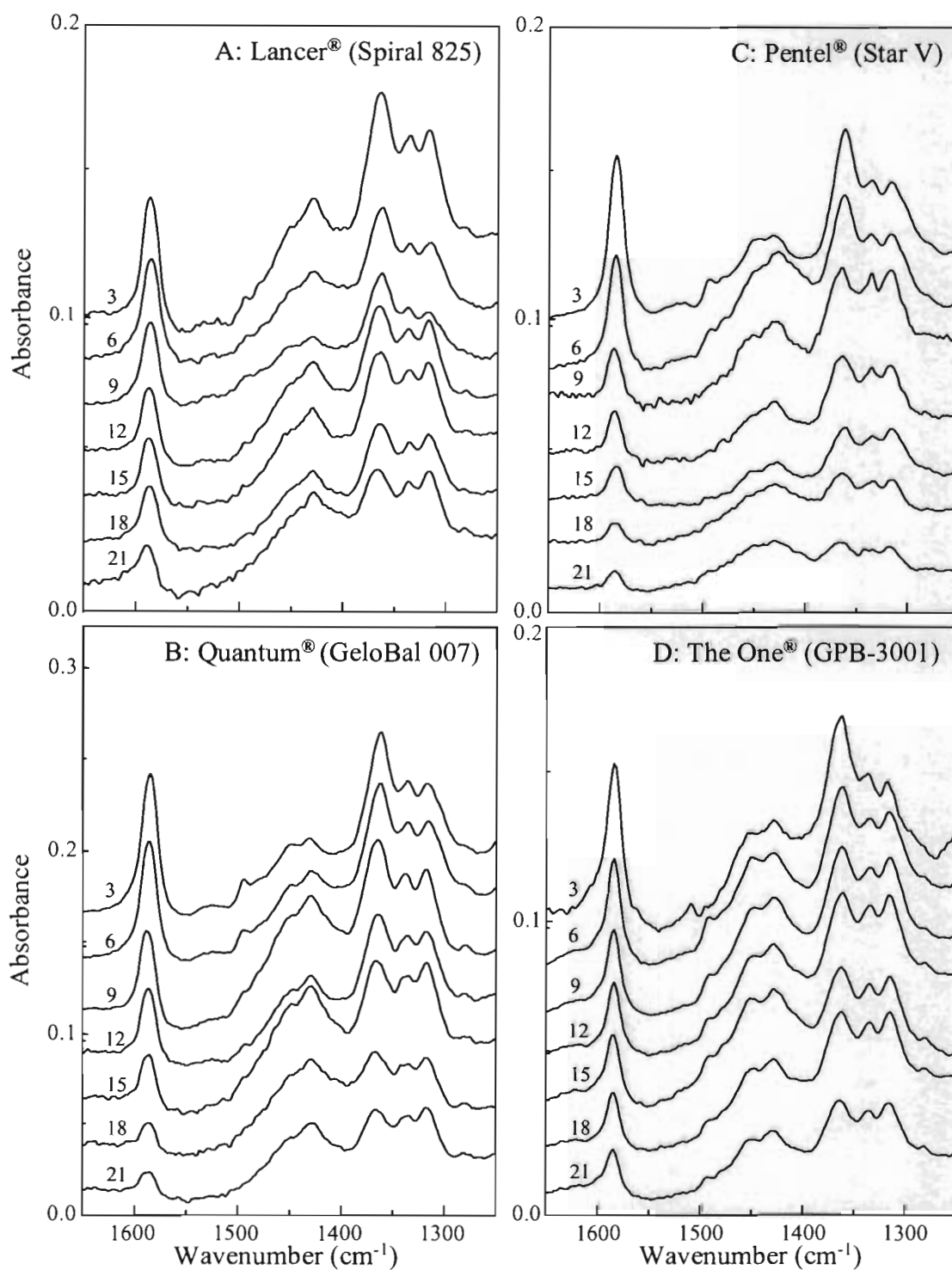


Figure 4.22 ATR FT-IR spectra of ink on paper: (A) Lancer® (Spiral 825), (B) Quantum® (GeloBal 007), (C) Pentel® (Star V), and (D) The One® (GPB-3001) detected every 3 days.

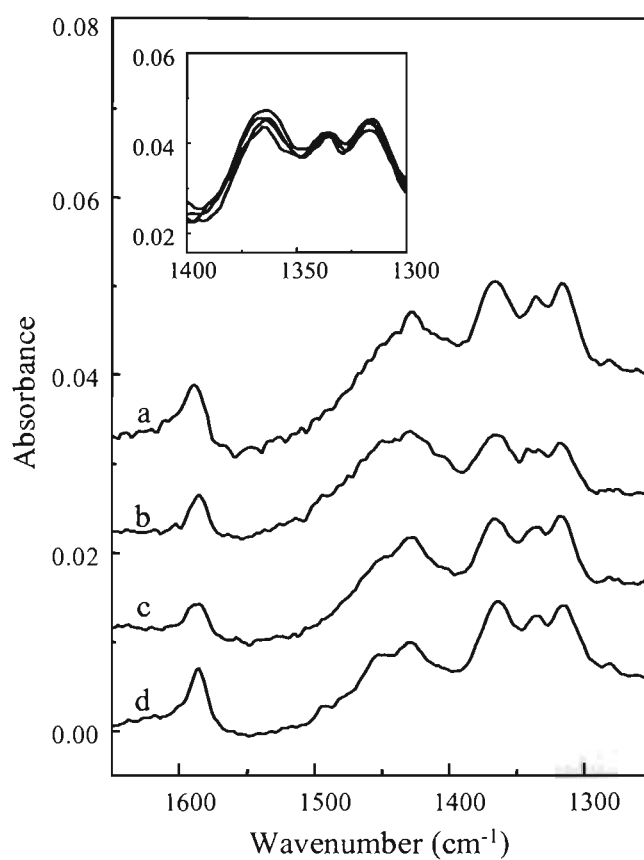


Figure 4.23 ATR FT-IR spectra of ink on paper: (a) Lancer<sup>®</sup> (Spiral 825), (B) Quantum<sup>®</sup> (GeloBal 007), (C) Pentel<sup>®</sup> (Star V), and (D) The One<sup>®</sup> (GPB-3001) after kept for 21 days.

#### 4.4 Characterization of line-crossing ink on paper

Information obtained from ATR FT-IR spectra provides the chemical signatures of component in ink. The different chemical ingredients of ink lead to the different spectral pattern. In this section, the situations of forging with various ballpoint pen inks are imitated. All results from previous sections are applied to prove that the ATR FT-IR technique can solve the problem of questioned document examination.

When the document is forged, two or more inks are written on the same document. In case of the questioned document, if they are not written at the same position, this will be easy to match or compare by ATR FT-IR spectra. Due to the limitation of ATR FT-IR microspectroscopic technique, if they are written at different position but having similar ink characteristic, it will be very difficult to differentiate. There are challenging task of forensic examination to characterize the crossing ink. In this section, the two ballpoint pen inks which have the clearly different spectral patterns are selected. It is easy to follow the changing of the chemical composition.

As the ink can soak into the cellulose fibers, ordered permeation of crossing-line inks is studied. The two blue ballpoint pen inks which have unique spectral pattern are selected, blue Faber-Castel® (Grip Ball 1424), and Pentel® (Star V) ink, to make the simulated situation. Both inks have clearly difference in spectral pattern because the Faber-Castel® brand ink characteristic shows the peak at  $1723\text{ cm}^{-1}$  assigned to carbonyl stretching vibration but not present in Pentel® characteristic.

The ATR FT-IR spectra of crossing of both inks written on paper at the same point are analyzed with various extent of contact with the IRE as shown in Figure 4.24 with difference in time to top up the second ink. The Pentel® ink is added to Faber-Castel® ink written on paper immediately and observed spectra at crossing point are shown in 4.24 (A). They show the characteristic role of bottom ink by observing from the absorption band at  $1723\text{ cm}^{-1}$  belonging to the unique characteristic of Faber-Castel® ink.

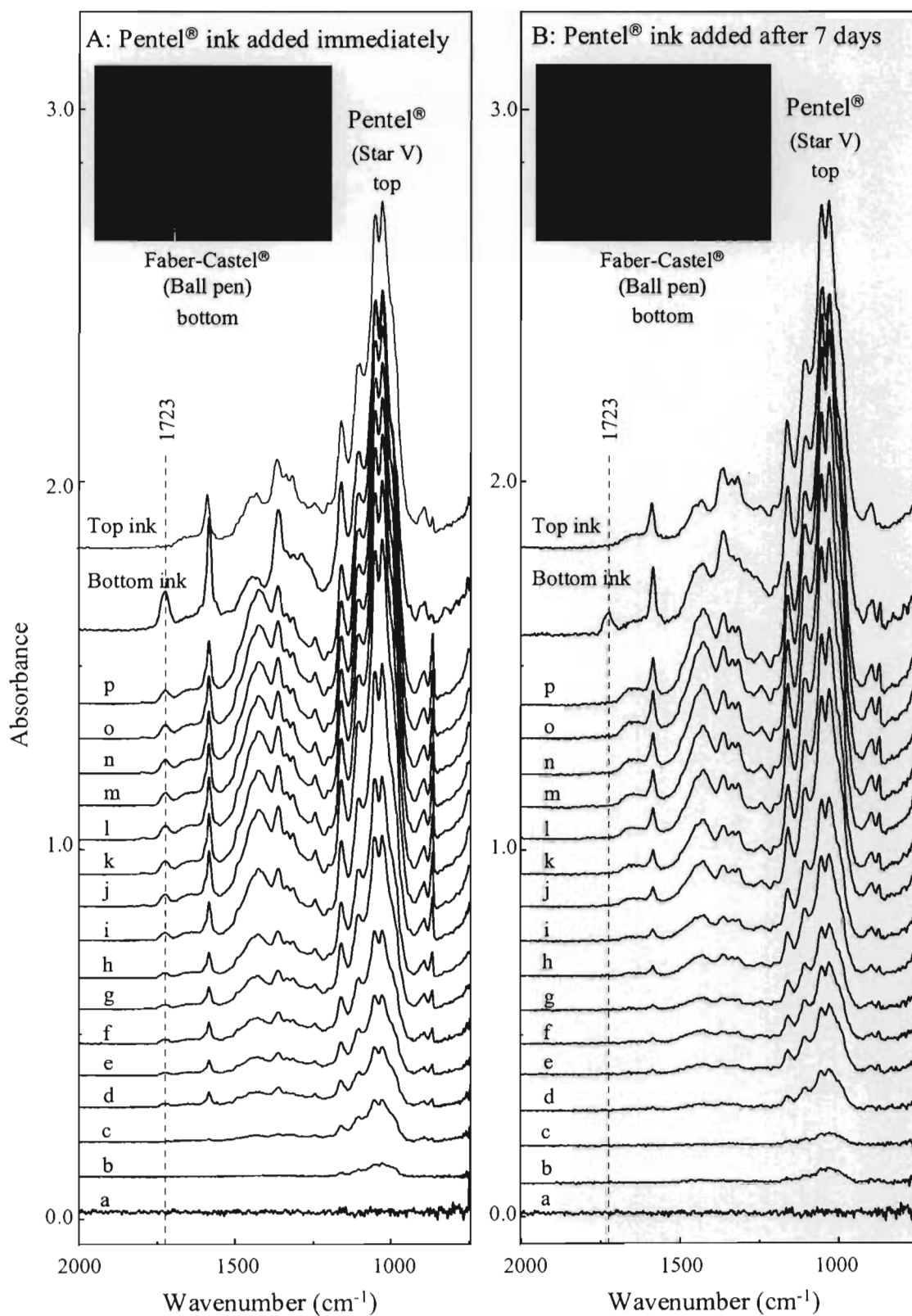


Figure 4.24 ATR FT-IR spectra of crossing ink between Faber-Castel® (Ball pen) ink top with Pentel® (Star V) on paper at the same point with various extent of contact with the homemade  $\mu$ IRE: (A) Pentel® ink added immediately and (B) added after 7 days.

According to ATR principle, penetration depth of electric field is the depth which electric field falls to  $1/e$  of original value at surface. This means that the electric field at surface has the strongest magnitude. It is impossible to show the characteristic of bottom ink bit does not present the top ink characteristic. Therefore, ATR spectra of the top of crossing inks provide the mixture of both inks characteristic.

In case of Pentel<sup>®</sup> ink is written for 7 days over the line of Faber-Castel<sup>®</sup> ink, all spectra of crossing point as shown in Figure 4.25 (B) do not show the absorption band at  $1723\text{ cm}^{-1}$ . This means that the first ink seeps into the cellulose fibers and dries. When the second ink added, such ink seeps to top on the first ink that causes the spectra showing only top ink characteristic.

ATR spectra of crossing of inks are collected with point by point measurement dragging pass the center of crossing area to monitor the trace of forging and are shown in Figure 4.25. ATR spectra of crossing ink of Faber-Castel<sup>®</sup> and Horse<sup>®</sup> top on the Reynolds<sup>®</sup> ink are shown in Figure 4.25 (A) and (B), respectively. The observed spectra of three initially points as shown in Figure 4.25 (A) demonstrate the characteristic of Reynolds<sup>®</sup> ink (a-c spectra). AT the center of crossing (d-h spectra), the spectral pattern show the absorption band at  $1723\text{ cm}^{-1}$  which is unique characteristic of Faber-Castel<sup>®</sup> ink. After such area, the observed spectra play the characteristic of Reynolds<sup>®</sup> ink again because the spectra disappear of the peak at  $1723\text{ cm}^{-1}$ .

According to the discussion above, the spectra in Figure 4.23 (B) also show the same result. Due to both of inks do not have the unique characteristic, the changing of spectral pattern which relate to the chemical composition in ink is not clear. The spectra at the center of crossing (d-h spectra) have the different in spectral pattern in  $1600\text{-}1200\text{ cm}^{-1}$  region when compare to other spectra.

This means that each of the spectra has the characteristic changing with the composition of ink on paper due to the ink coming from the different ink source. By

observing the absorption bands in the range of  $1600\text{--}1200\text{ cm}^{-1}$ , it elucidates the ink characteristic which is not dominated by cellulose characteristic.

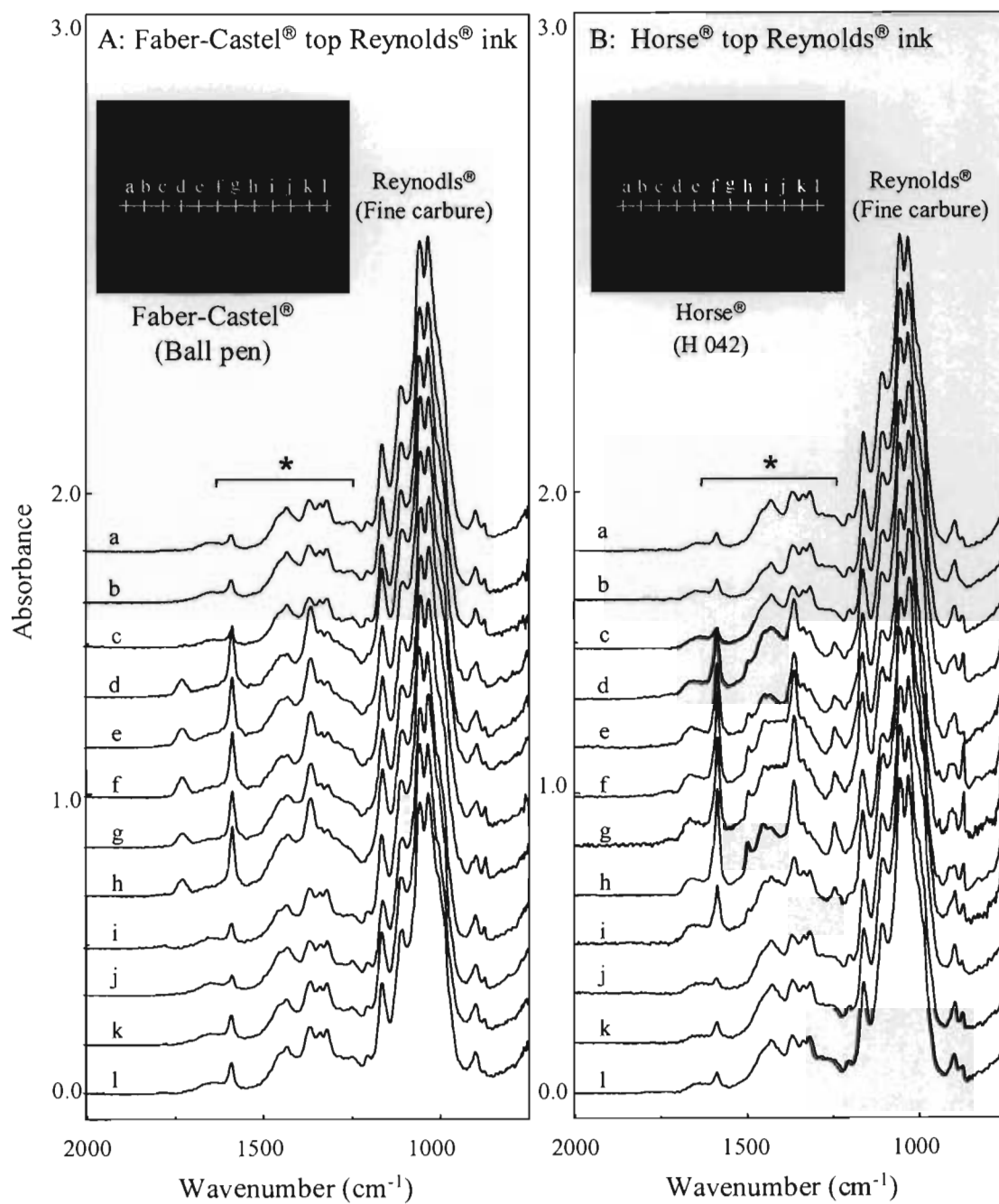


Figure 4.25 ATR spectra of (A) blue Faber-Castel® (Ball pen) and (B) blue Horse® (H 042) ink top on Reynolds® (Fine carbure).

On account of a real situation, it is not known that which method is suitable for analysis. The ATR FT-IR spectra of line crossing ink obtained from linear point by point measurement with dragging pass the center of the crossing in vertical and horizontal direction are shown in Figure 4.26. From the observed spectra, vertical analysis shows the change of spectral pattern evidently depending on the characteristic of top ink as shown in Figure 4.26 (A).

On the other hand, the horizontal analysis does not observe the alternation as shown in Figure 4.26 (B) but the spectra of crossing area show only higher peak intensities of ink characteristic, 1600-1200  $\text{cm}^{-1}$  region, than others. Due to the Standard<sup>®</sup> ink characteristic is suppressed by characteristic of top ink (Faber-castel).

To prove the discussion above, line crossing of ink coming from the same pen is studied. The spectra of linear point by point dragging pass the center of crossing ink are shown in Figure 4.27. Owing to ink coming from the same pen has the same spectral pattern, shielding of another ink characteristic as discussed in previous results are neglected.

All spectra in Figure 4.27 show the same spectral pattern but the cure of forging can be observed. At the crossing area, its show higher peak intensities of ink characteristic and unique absorption band of ink at 1723  $\text{cm}^{-1}$  which relates to quantitative meaning. Due to ink written with double stokes on paper have a mount of ink deposited on paper more than single stoke.



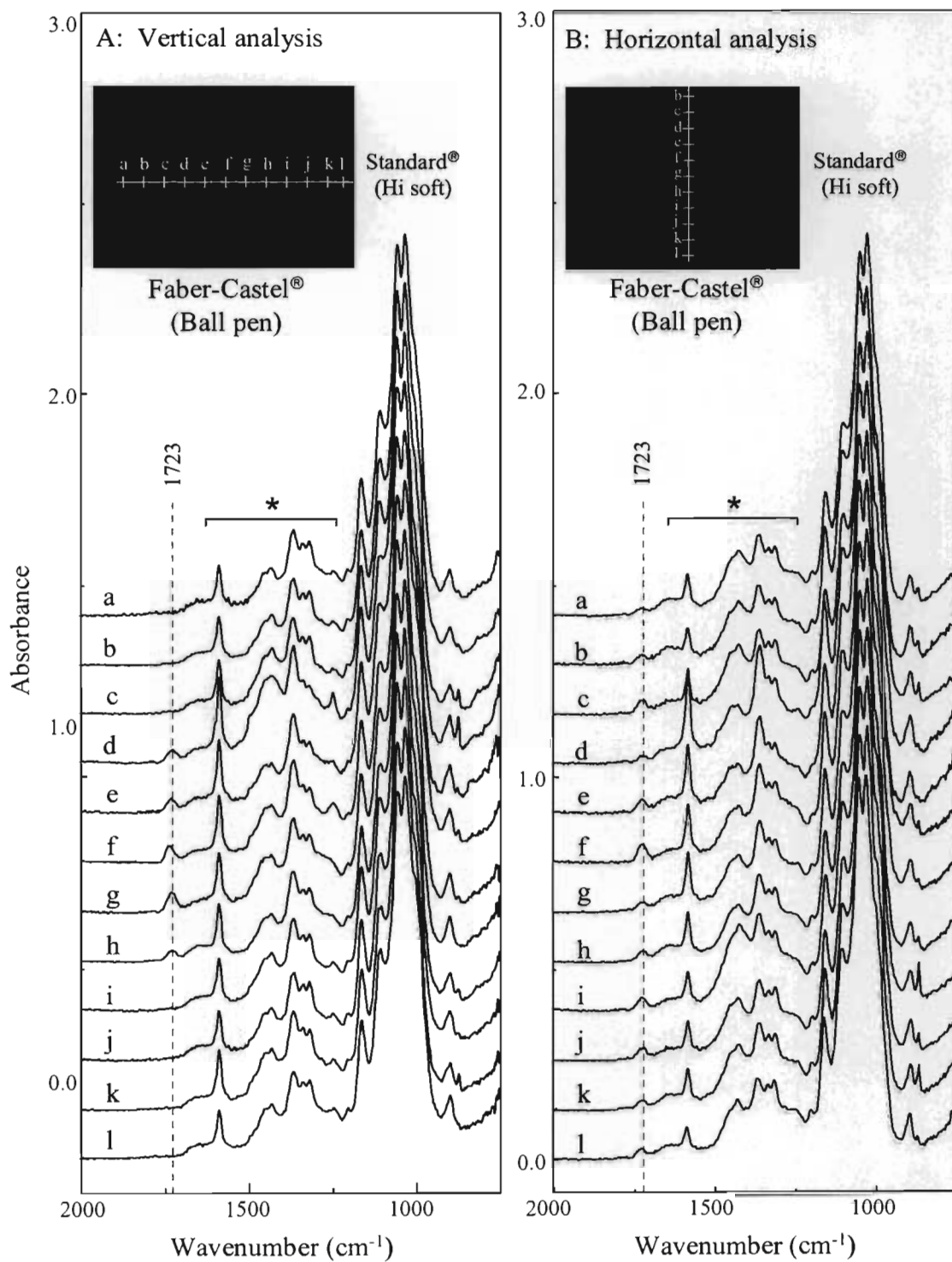


Figure 4.26 ATR spectra of blue Faber-Castel® (Ball pen) ink top with Standard® (Hi soft) ink: (A) horizontal and (B) vertical analysis.

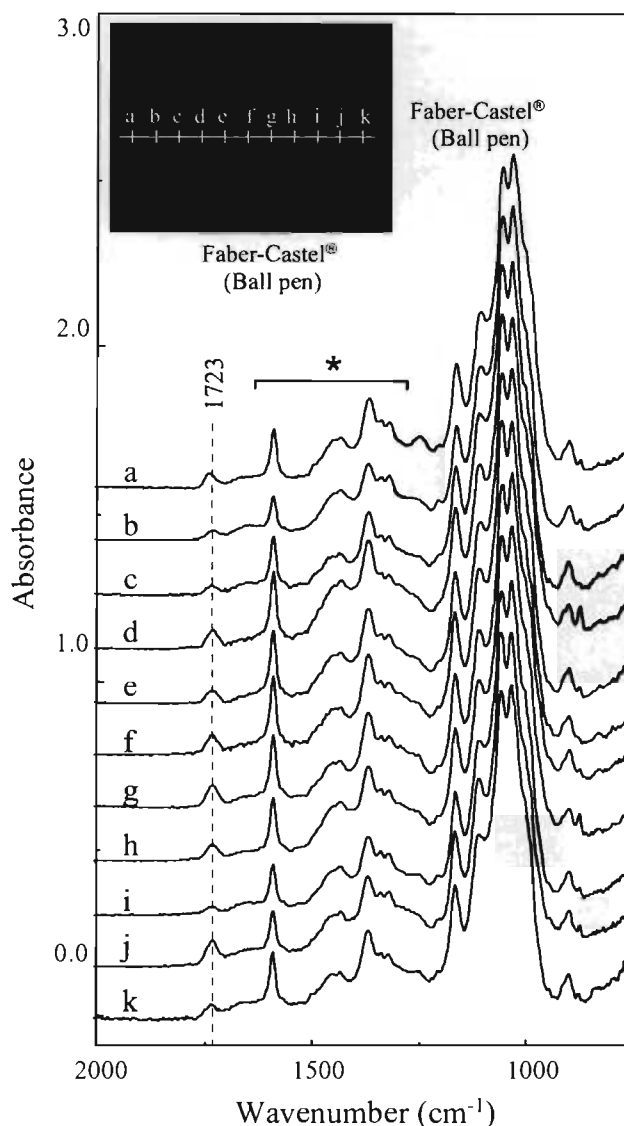


Figure 4.27 ATR spectra of crossing ink of blue Faber-Castel® (Ball pen) ink.

In real case, document evidence may be kept for a long time at various conditions after forging. Since the time has an influence on the ink composition changing, the crossing ink with Faber-Castel® topped by Reynolds® ink and kept for 45 days are studied. Spectra of crossing ink kept for a day which are measured by point by point are shown in Figure 4.28 (A). Since both inks have unique spectral patterns, they show a trace of alteration. Analysis with the same method of the sample kept for 45 days also demonstrates that trace as shown in Figure 4.28 (B). If the absorption band at  $1723\text{ cm}^{-1}$  is ignored, all spectra of crossing ink kept for 45 days have the same spectral pattern. This means that inks which have the similar characteristic may be hard to follow the trace of forging when it leaved for a long time

due to the composition changing with time and environmental condition as discussed in Section 4.3.4.

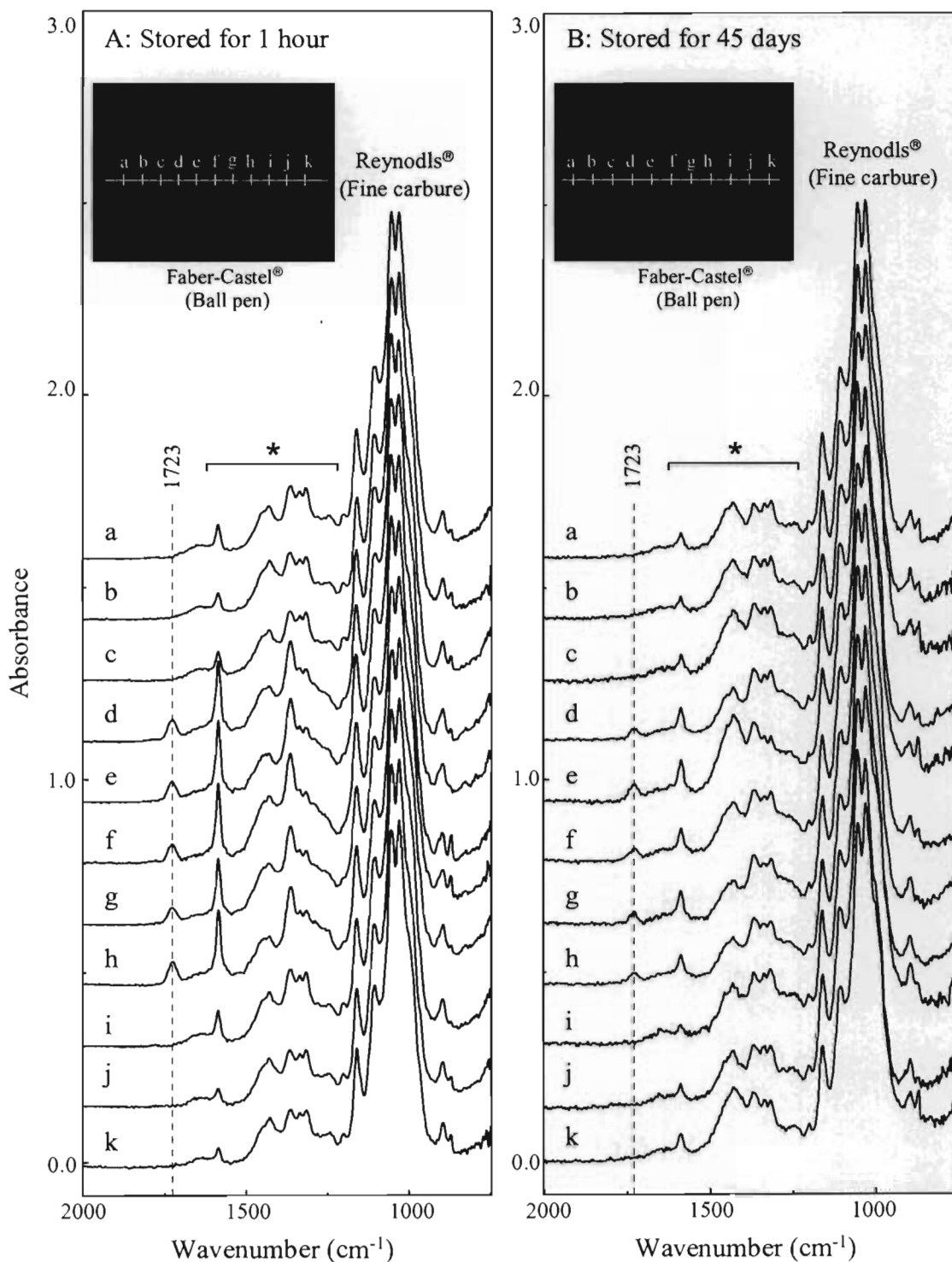


Figure 4.28 ATR spectra of blue Reynolds® (Fine carbure) ink top with Faber-Castel® (Ball pen) ink: (A) stored for 1 hour and (B) stored for 45 days.

The problem of identification of the alternation is the characteristic of ink which does not clearly differ. If inks forging onto document have unique characteristic, the ATR FT-IR technique with homemade Ge  $\mu$ IRE accessory is suitable to detect the trace of alternation. It is also quantitative analysis to investigate the trace of forging with the same pen by following the quantitatively ink which deposit on paper due to writing with double or more strokes. Therefore, this technique is one of the alternative techniques for forensic document examination.

ต้นฉบับไม่มีหน้านี้  
NO THIS PAGE IN ORIGINAL

## REFERENCES

- [1] Kasprisin, Ron. Pens and Inks. New York: John Wiley & Sons, 1999.
- [2] Pepper, Ian K. Crime Scene Investigation: Methods and Procedures. Berkshire: Open University Press, 2005.
- [3] Kunjappu, J.T. Essays in Ink Chemistry. Lancaster: Gazelle, 2002.
- [4] Tracton, A. Coatings Technology Handbook. 2<sup>nd</sup> ed. New York: Marcel Dekker, 2001.
- [5] Kunjappu, J.T. Polymer in Ink Chemistry. Ramsey: Rodman Publications, Inc., 2001.
- [6] Zlotnick, J.A.; Smith, F.P. Chromatographic and Electrophoretic Approaches in Ink Analysis. J. Chromatogr. B. 733 (1999) 265-272.
- [7] Langford, A.; Dean, J.; Reed, R.; Homes, D.; Weyers, J. and Jones, A. Practical Skills in Forensic Science. Essex: Pearson Prentice Hall, 2005.
- [8] Rendel, D.F. Advances in Chemistry Applied to Forensic Science. Chem. Soc. Rev. 34 (2005): 1021-1030.
- [9] Roux, C.; Novotny, M.; Evans, I.; Lennard, C. A Study to Investigate the Evidential Value of Blue and Black Ballpoint Pen Ink in Australia. Forensic Sci. Int. 101 (1999) 167-176.
- [10] Brown, S.; Sin-David, L. Diary of an astronaut: Examination of the Remains of the late Israeli astronaut Colonel Ilan Romon's Crew Notebook Recovered after the Loss of NASA's Space Shuttle Columbia. J. Forensic Sci. 52 (2007) 731-737.
- [11] Payne, G; Wallace, C. Reedy, B.; Lennare, C.; Schuler, R.; Exline, D. Roux, C. Visible and Near-Infrared Chemical Imaging Methods for the Analysis of Selected Forensic Samples. Talanta 67 (2005) 334-344.
- [12] Hammond, L. D. Validation of LAB Color Mode as a Nondestructive Method to Differentiate Black Ballpoint Pen Ink. J. Forensic Sci. 52 (2007) 967-973.
- [13] Ramotowski, R.S. Effect of Electron Beam Irradiation on Forensic Evidence. 2. Analysis of Writing Inks on Porous Surface. J. Forensic Sci. 49 (2004) 604-609.

- [14] Tsutsumi, K; Ohga, K. Analysis of Writing Ink Dyestuffs by TLC and FT-IR and Its Application to Forensic Science. Anal. Sci. 14 (1998) 269-274.
- [15] Weyermann, C.; Marquis, R.; Mazzella, W.; Spengler, B. Differentiation of Blue Ballpoint Pen Inks by Laser desorption Ionization Mass Spectroscopy and High-Performance Thin-Layer Chromatography. J. Forensic Sci. 51 (2006) 915-918.
- [16] Andrasko, J. HPLC Analysis of Ballpoint Pen Inks Stored at Different Light Conditions. J. forensic Sci. 46 (2001) 21-30.
- [17] Kher, A.; Mullolland, M.; Green, E.; Reedy, B. Forensic Classification of Ballpoint Pen Inks Using High Performance Liquid Chromatography and Infrared Spectroscopy with Principle Components Analysis and Linear Discriminant Analysis. Vib. Spectrosc. 40 (2006) 270-277.
- [18] Gibbs, P.J. Analysis of Ancient Dyed Chinese Paper by High-Performance Liquid Chromatography. Anal. Chem. 14 (1997) 1965-1969.
- [19] Branzeun, B.; Chem, C.; Gaudreau, M. Ballpoint Pen Inks: the Quantitative Analysis of Ink Solvents on Paper by Solid-phase Microextraction. J. Forensic Sci. 532 (2007) 209-215.
- [20] Andrasko, J. A Simple Microthermal Desorption Device. J. Forensic Sci. 51 (2006) 925-928.
- [21] Locicero, S.; Dujourdy, L.; Mazzella, W.; Margot, P. Dynamic of Ageing of Ballpoint Pen Inks: Quantification of Phenoxyethanol by GC-MS. Science&Justice, 44 (2006) 165-171.
- [22] Grim, D.M. Siegel, J.; Allison, J. Does Ink Age Inside of a Pen Cartridge? J. Forensic Sci. 47 (2002) 1294-1997.
- [23] Siegel, J; Allison, J.; Mohr, D.; Dunn, J. The Use of Desorption/Ionization Mass Spectrometry in the Analysis of Inks in Questioned Documents. Talanta 67 (2006) 425-429.
- [24] Weyermann, C.; Kirsch, D.; Costa-Vera, C. Photofading of Ballpoint Dyes Studied on Paper by LDI and MALDI MS. J. Am. Mass Spectrom. 17 (2006) 297-306.
- [25] Jones, R.W.; Cody R.B. Differentiation Writing Ink Using Direct Analysis in Real Time Mass Spectroscopy J. Forensic Sci. 51 (2006) 915-918.
- [26] Waeschle P.A. Examination of Line Crossing by Scanning Electron Microscopy. J. Forensic Sci. 24 (1979) 569-578.

- [27] Watson, G.S. Potential Application of Scanning Probe Microscopy in Forensic Science. J. Phys. 61 (2007) 1251-1255.
- [28] Kasas, S.; Khanmy-Vital, A. Examination of Line Crossing by Atomic Force Microscopy. Forensic Sci. Int. 119 (2001) 290-298.
- [29] Wang, J.; Luo, G.; Sun, S.; Wang, Z.; Wang, Y. Systematic Analysis of Bulk Blue Ballpoint Pen Ink by FTIR Spectrometry. J. Forensic Sci. 46 (2001) 1093-1097.
- [30] Zieba-Palus, J.; Kunicki, M. Application of the Micro-FTIR Spectroscopy, Raman Spectroscopy and XRF Method Examination of Inks. Forensic Sci. Int. 158 (2006) 164-172.
- [31] Wilkinson, T.J. Use of Synchrotron Reflectance Infrared Spectroscopy as a Rapid Direct, Non-destructive Method for Study of Ink on Paper. Appl. Spectros. 56 (2002) 800-803.
- [32] Wilkinson, T.J. Physics and Forensic. Physics World 15 (2003) 43-46.
- [33] Kher A. Forensic Classification of Ballpoint Pen Inks Using High Performance Liquid Chromatography and Infrared Spectroscopy with Principal Components Analysis and Linear Discriminant Analysis. Vib. Spectosc. 40 (2006) 270-277.
- [34] Ingel, J.D.; Crouch, S. Spectrochemical Analysis. New Jersey: Prentice-Hall Inc, 1998.
- [35] Urban, M.W. Attenuated Total Reflectance Spectroscopy of Polymer: Theory and Practice. Washington DC: American Chemical Society, 1996.
- [36] Stuart, B. Infrared Spectroscopy: Fundamentals and Application. New York: Harrick Scientific Corporation, 1979.
- [37] Chalmers, J.M. Handbook of Vibrational Spectroscopy. Vol 2. UK: John Wiley & Sons Ltd, 2002.
- [38] Harrick, N. J.: Internal Reflection Spectroscopy. New York: John Wiley & Sons Inc, 1967.
- [39] Ishida, H.; Ekgasit, S. New Quantitative Optical Depth Profiling Methods by Attenuated Total Reflectance Fourier Transform Infrared Spectroscopy: Multiple Angle/ Single Frequency and Single Angle/ Multiple Frequency Approaches Fourier Transform Spectroscopy: 11<sup>th</sup> International conference (1998) 40-59.



- [40] Ekgasit, S.; Padermshoke, A. Optical Contact in ATR/FT-IR Spectroscopy. Appl. Spectrosc. 55 (2001): 1352-1359.
- [41] Ekgasit, S. Ishida, H. New Optical Depth-profiling Technique by Use of the Multiple-Frequency Approach with Single ATR FT-IR Spectrum; Theoretical Development. Appl. Spectrosc. 51 (2007): 1488-1495.
- [42] Gunzler, H; Gremlich, H. U. IR Spectroscopy: An Introduction. Weinheim: WILEY-VCH, 2002.
- [43] Ekgasit, S.; Patayagorn, N.; Tongsakul, D.; Thammacharoen, C.; Kongyou, T. A Novel ATR FT-IR Microspectroscopy Technique for Surface Contamination Analysis without Interference of the Substrate. Anal. Sci. 23 (2007) 1-8.
- [44] Laporte, G.M.; Arredondo, M.D.; McConnell, T.S.; Joseph, C.S., Cantu, A.A., Shaffer, A.K. An Evaluation of Matching Unknown Writing Inks with the United States International Ink Library. J. forensic Sci. 51 (2006) 689-692.
- [45] Gunzler, H.; Gremlich H. IR Spectroscopy. Basel: Federal Republic of Germany, 2002.
- [46] Socrates, G. Infrared and Raman Characteristic Group Frequencies. 3rd ed. West Sussex: John Wiley & Sons Ltd, 2001.
- [47] Pretsch, E.; Buhlmann, P.; Affolter, C.: Structure Determination of Organic compounds. 1st ed. Heidelberg: Springer, 2000.
- [48] Weyermann, C.: A GC/MS study of drying of ballpoint pen ink on paper. Forensic Sci. Int. 168 (2006) 119-127.
- [49] Andrasko, J. Changes in Composition of Ballpoint Pen Inks on Aging in Darkness. J. Forensic Sci. 47 (2002) 324-327.
- [50] Hofer, R. Dating of ballpoint pen ink. J. Forensic Sci. 49 (2004) 1-5.
- [51] Spence, L.D.; Francis R.B.; Tinggi U. Comparison of the Elemental Composition of Office Document Paper: Evidence in a Homicide Case. J. Forensic Sci. 47 (2002) 648-651.
- [52] Andrasko, J. Changes in Composition of Ballpoint pen inks on Aging in darkness. J. Forensic Sci. 47 (2002) 324-327.

## CURRICULUM VITAE

**Name:** Miss Piyawan Canyouk

**Date of Birth:** December 15, 1983

**Address:** 125/145 Techawanich Rd. Bangsue Bangkok 10800, Thailand

**Education:**

2001 High School (Pibulwittayalai School, Lopburi)

2005 Bachelor of Engineering (Petrochemicals and Polymeric Materials), Silpakorn University, Nakornpathom, Thailand

2008 Master of Science (Petrochemistry and Polymer Science), Chulalongkorn University, Bangkok, Thailand

**Awards:** First runner-up Award of Oral Presentation in Polymer Graduate Conference, Mahidol University, Salaya, Nakornpathom, May 2007

First runner-up Award of Poster Presentation in 2<sup>nd</sup> International Conference on Forensic Science and Medical Science, Naresuan University, Phitsanulok, July 2007

First runner-up Award of Oral Presentation in 2<sup>nd</sup> CIFS Academic Day Conference, Central Institute of Forensic Science, Ministry of Justice, September 2007

First runner-up Award of Oral Presentation in the Science Forum 2008, Chulalongkorn University, March 2008